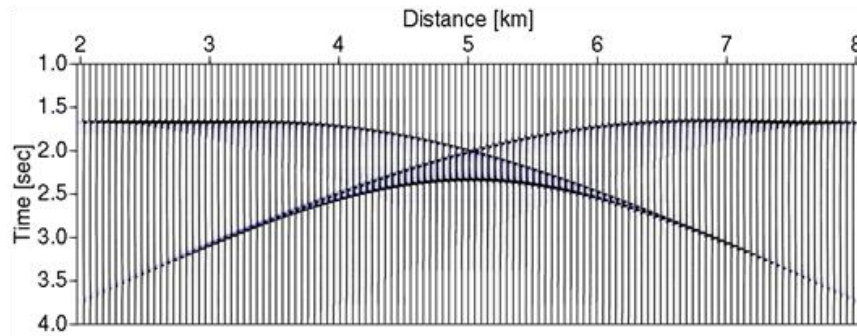
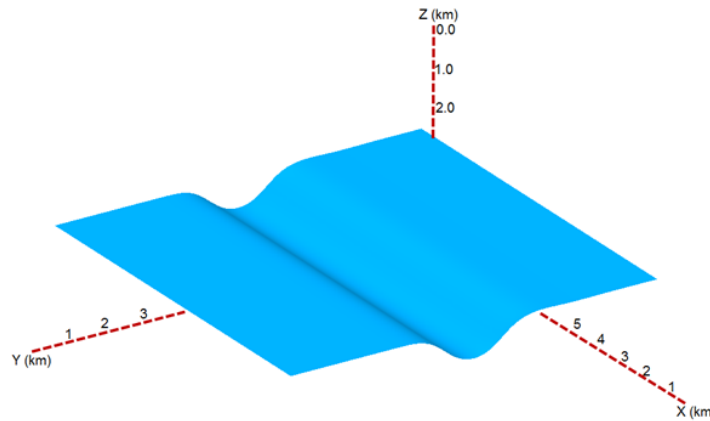


Master Thesis in Geosciences

Modeling by demigration

A feasibility study

Muhammad Junaid Yaqoob



UNIVERSITY OF OSLO

FACULTY OF MATHEMATICS AND NATURAL SCIENCES

Modeling by demigration

A feasibility study

By

Muhammad Junaid Yaqoob



Master Thesis in Geosciences
Discipline: Petroleum Geology and Geophysics
Department of Geosciences
Faculty of Mathematics and Natural Sciences

UNIVERSITY OF OSLO

[Spring 2009]

© Muhammad Junaid Yaqoob, 2009

Tutor(s): Professor Leiv-J. Gelius (UiO), Dr. Tina Kaschwich (NORSAR), and Dr. Isabelle Lecomte (NORSAR)

This work is published digitally through DUO – Digitale Utgivelser ved UiO

<http://www.duo.uio.no>

It is also catalogued in BIBSYS (<http://www.bibsys.no/english>)

All rights reserved. No part of this publication may be reproduced or transmitted, in any form or by any means, without permission.

*Dedicated to My Father, Brothers & especially
My Late Mother*

Acknowledgements

This thesis has been carried out in close collaboration with NORSAR and the Department of Geoscience, University of Oslo under the supervision of Professor Leiv Gelius, Dr. Tina Kaschwich and Dr. Isabelle Lecomte.

I pay my deepest gratitude to Professor Leiv Gelius from University of Oslo for his skilled guidance, full cooperation, insight critique and encouragement, which led me to the successful completion of this thesis.

I am especially indebted to Dr. Tina Kaschwich and Dr. Isabelle Lecomte from NORSAR for giving me an initiative to this study. Their inspiring guidance, dynamic supervision and constructive criticism helped to understand the seismic modeling methods.

Thanks also to Håvar Gjølystdal who has reviewed my work and made profitable comments on it. In general, I want to thank all NORSAR staff and particularly the Seismic Modeling team for their kind hospitality during my work in NORSAR.

I also feel much pleasure in acknowledging unforgettable company of my class fellows and friends in university during my studies and in excursions. I will always remember my association and affinities with all of them. I also acknowledge my friends in Kringsjø student village and especially Iftikhar Sultan for his help and support during my stay in Norway.

I also acknowledge the help, the encouragement, endless love, support and prayers of my family, which have always been a source of inspiration and guidance for me all the way.

Muhammad Junaid Yaqoob

Oslo, June 2009

Abstract

The aim of this thesis is to investigate and gain better understanding of a new modeling technique called modeling by demigration. Demigration itself can be defined as the inverse of true amplitude migration. This involves nothing more than the formulation of a reflection imaging process by which one can return from a true amplitude depth migrated section to the original common offset section. Modeling by demigration represents a special implementation of the demigration concept, where the input is no longer standard migrated data but artificially migrated target geological structure(s) defined by the user. In this thesis the artificially migrated inputs are computed by employing both a standard/classical approach and the PSDM simulator approach of NORSAR (SimPLI technology).

A feasibility study has been carried out where the modeling by demigration concept has been compared with more standard modeling techniques based on dynamic ray tracing and Kirchhoff Helmholtz integral.

Synthetic data were generated for three different geological structures; a syncline, an anticline, and a fault. The output from the various modeling methods were compared based on both visual inspection as well as quantitative measures of relative amplitude ratios. In addition, the synthetic datasets were migrated to see how well the original geological structures could be mapped back.

The conclusions from this study were as follows;

- The dynamic ray tracing method performed poor in the case of complex geology, as expected,
- Modeling by demigration proved to be a feasible concept when benchmarked with the standard Kirchhoff Helmholtz modeling technique,
- However, work needs to be carried out with respect to calibrations before direct (absolute) amplitude comparisons can be made, and
- The SimPLI approach can represent an alternative to the standard artificial migration proposed in the original version of modeling by demigration.

Table of Contents

Acknowledgements	i
Abstract	ii
Introduction	1
Chapter 1	
Theory & Methods	3
1.1 Green's functions	3
1.2 An introduction to the modeling methods studied	5
1.2.1 Standard ray tracing	5
1.2.2 Kirchhoff Helmholtz modeling	6
1.2.3 Seismic Modeling by Demigration	8
1.3 Modeling by demigration-implementation issues	10
Chapter 2	
Modeled seismic responses from simple geological structures	12
2.1 Syncline Model	14
2.1.1 Key Features	15
2.1.2 Seismic Modeling	16
2.2 Anticline Model	24
2.2.1 Key Features	25
2.2.2 Seismic Modeling	25
2.3 Fault Model	34
2.3.1 Key Features	34
2.3.2 Seismic Modeling	35
Chapter 3	
Conclusions	45
Appendix A	
Workflow & Tools	46
A.1 NORSAR-3D	46

A.1.1	Model Builder	46
A.1.2	Exporting and Importing a Model.....	47
A.1.3	Common Shot Survey.....	47
A.1.4	Common Shot Wavefront Tracer.....	49
A.1.5	Seismogram Generator.....	51
A.2	Kirchhoff Helmholtz Modeling.....	52
A.2.1	Interface Selection	52
A.2.2	Survey and event sets	53
A.2.3	Gather Selection	55
A.2.4	Seismograms	55
A.2.5	Kirchhoff Modeling	56
A.3	Modeling by demigration	58
A.3.1	Classical modeling by demigration	58
A.3.2	Modeling by demigration SimPLI approach.....	59
A.4	Kirchhoff PSDM migration	63
	References	70

Introduction

The aim of this thesis is to test and compare and different seismic modeling methods. The concepts of the various modeling techniques tested are first briefly discussed. To be able to rank and evaluate the methods, a set of different controlled models have been employed.

Modeling may involve comparison, simulation or representation of seismic data to define the limits of seismic resolution, assess the ambiguity of interpretation or make predictions. Generation of a synthetic seismogram from a well log and comparison of the synthetic or modeled trace, with seismic data is a common direct-modeling procedure. Generating a set of pseudologs from seismic data is the process known as seismic inversion, a type of indirect modeling. Models can be developed to address problems of structure and stratigraphy prior to acquisition of seismic data and during the interpretation of the data (Schlumberger, 2009). The agreement between data and a model does not prove that the model is correct, since there can be numerous models that agree with a given data set (Sheriff, 2002).

Historically ray-based modeling has been used extensively in seismology and seismic exploration to study propagation of seismic waves in layered media with varying elastic parameters. In early applications, the focus was mostly on calculating raypaths and traveltimes, referred to as kinematic ray tracing (Gjøystdal et al., 2007b). Throughout the 1970s and 1980s, numerical techniques were developed for dynamic ray tracing, which yields additional wavefront curvature and geometric spreading attributes. When combined with an approximate zero-order, high-frequency solution of the elastodynamic wave equation, reliable estimates of P-wave and S-wave amplitudes can be obtained (Červený & Hron, 1980). However, the classical ray tracing based method cannot handle complex wave phenomena like edge diffractions and caustics.

In this thesis, the NORSAR-3D software has been employed to trace rays. This software package is based on the wavefront construction (WFC) technique that represents the same robustness for smooth media as the more conventional grid methods, but with the additional power of computing multi arrivals. In addition, it is easy to modify the method to include reflection and transmission at discontinuous interfaces (Vinje et al., 1993).

Kirchhoff-Helmholtz (KH) modeling gives reflection seismograms that are more accurate and realistic than those obtained by classical ray tracing in case of complex geological structures. Ray theory is however still the basis of this modeling, and hence many ray advantages are inherited, such as the selection of specific events.

The Kirchhoff Helmholtz integral is a common used tool for modeling the reflected response from an acoustic or elastic interface due to a given incident field. For a dense distribution of source-receiver pairs on a fixed measurement surface, the Kirchhoff Helmholtz modeling integral provides, for a given interface, the reflection response as an amplitude distribution

along the corresponding traveltimes surface (Tygel et al., 1999) . In this thesis the Kirchhoff Helmholtz modeling will be considered as a reference method.

Demigration is a seismic forward modeling scheme based on seismic imaging. Demigration itself can be defined as the inverse of true amplitude migration. It can be shown that the familiar Kirchhoff migration integral has two inverse integrals in an approximate sense, i.e., the Kirchhoff Helmholtz modeling integral and the Kirchhoff demigration integral (Santos et al., 2000a).

In this thesis a special version of demigration denoted “modeling by demigration” has been considered. The input is not longer a complete depth migrated image but an artificially migrated geological structure defined by the user.

Two different versions of modeling by demigration were considered:

- Employing the standard implementation as described by Santos et al. (2000a),
- Replacing the artificial migration equation of Santos et al. (2000a), with the SimPLI approach.

Only the case of zero offset data output from demigration was considered in this thesis work.

This thesis has been organized in three main sections; first, a brief introduction to theory and methods is given, followed by a comprehensive test part where the various modeling methods are tested employing controlled and simple geological models. Finally, a discussion part is given a summary of the main observations together with some concluding remarks.

Chapter 1

Theory & Methods

The aim of this thesis is to compare different seismic modeling techniques, with special emphasis on modeling by demigration. This chapter gives an overview and brief introduction to all the modeling schemes tested. For all methods Green's functions are needed. In this thesis they are calculated using ray tracing.

1.1 Green's functions

The Green's functions (GF) represent the wave field propagation from a point at the acquisition surface (source or receiver) to any point in a given velocity model. One way of calculating Green's functions is by ray tracing, which is a high-frequency approach. Among the parameters calculated by ray-tracing, accurate traveltimes are important for a proper depth location in case of migration, but amplitudes and other parameters may be used as well, especially for an "amplitude-preserving" type of imaging (Yilmaz, 2001).

The Green's functions contain traveltimes and amplitude information and can be written formally as (source side) (Yilmaz, 2001):

$$G(\vec{r}, \vec{r}_s, t) = A_{\vec{r}_s \rightarrow \vec{r}} \delta(t - t_{\vec{r}_s \rightarrow \vec{r}}). \quad (1)$$

Where δ represents the initial impulse, A is the amplitude after propagation (including spherical divergence and absorption) from the source location \vec{r}_s to an arbitrary point \vec{r} and t represents the corresponding traveltimes.

In order to obtain the GF's needed for Kirchhoff Helmholtz modeling, first the one-way traveltimes from all source-receiver positions to the regular sampled interfaces are calculated. Afterwards the obtained results are added for each source and receiver pair.

Figure 1.1a shows schematically the wavefronts associated with a Green's function computation between a source point and a given image (diffraction) point. Figure 1.1b shows a similar sketch for receiver side Green's function. The circular wavefronts correspond to constant traveltimes. By adding the source and receiver GF (c.f. Figure 1.1c) scattering isochrones are formed, which are curves representing equal scattering traveltimes.

Scattering isochrones indicate the possible locations where the scattered energy may come from a given traveltimes. Therefore, the superposition of all isochrones generates the migrated image. In homogeneous media, the scattering isochrone is given by an ellipse with the source and receiver at the focal points: the elliptical shape is due to the summation of circular wavefronts (Guy, 2009).

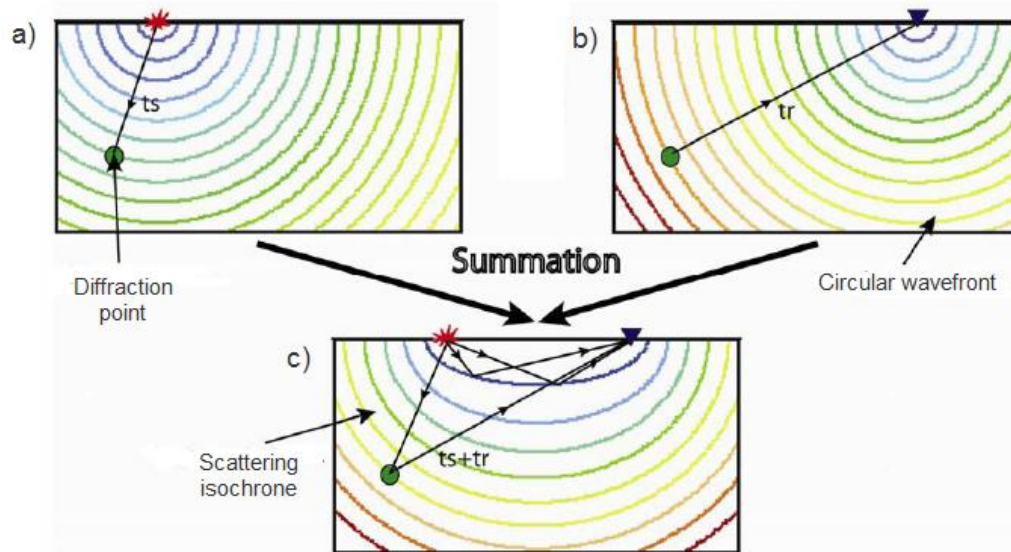


Figure 1.1: Scattering isochrones in a homogenous velocity model for a given source receiver pair (Guy, 2009).

Practical applications of Green's functions in both modeling and migration/inversion require repeated calculations for all possible image points. Hence, fast methods are essential, and a good candidate is ray tracing. However, a GF can be calculated using finite difference methods as well (Yilmaz, 2001).

In this thesis, the Green's functions will be calculated by employing an efficient implementation of dynamic ray tracing denoted "Wavefront Construction" (Vinje et al., 1993). This approach allows that one starts with a moderate ray density and then interpolates rays along wavefronts if necessary.

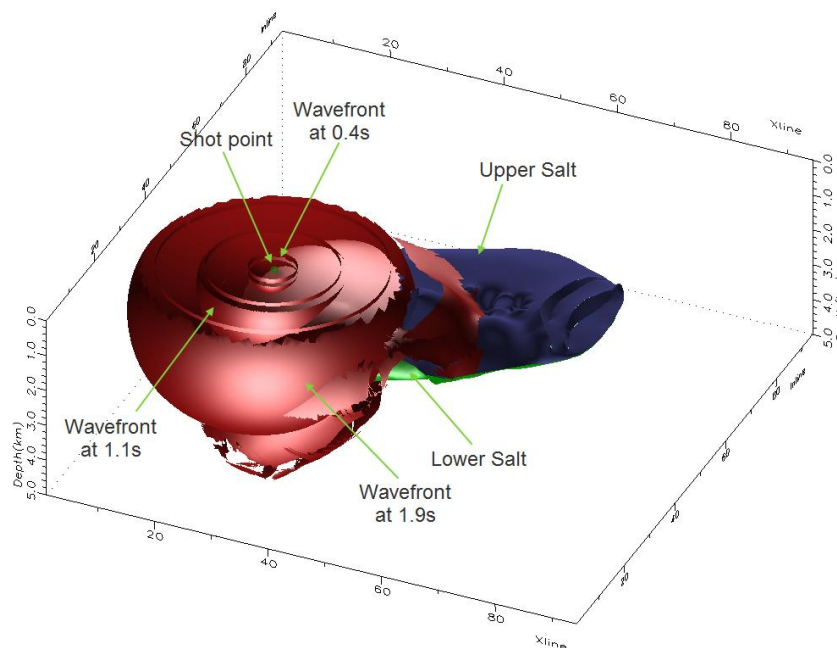


Figure 1.2: SEG/EAGE Salt model used to illustrate the wavefront concept. The wavefronts at different time steps are shown, along with the horizon of Top and Lower Salt

Figure 1.2 shows an example of this concept using the so-called SEG/EAGE Salt Model. Starting from a single shot the wavefronts at different time steps can be easily seen. The wavefront construction method mimics true wave propagation in the sense that entire wavefronts are propagated time-step by time-step to create a “moving surface” that passes through the model. A triangular mesh with a ray at each node is used to represent the wavefronts. Standard dynamic ray tracing is used in tracing rays from one wavefront to the next.

1.2 An introduction to the modeling methods studied

This section gives a brief discussion of each of the modeling methods studied in this thesis. To get an initial idea of how well they perform a simple dome model as shown in Figure 1.3a will be employed. All the computational results are taken from Santos et al., 2000b.

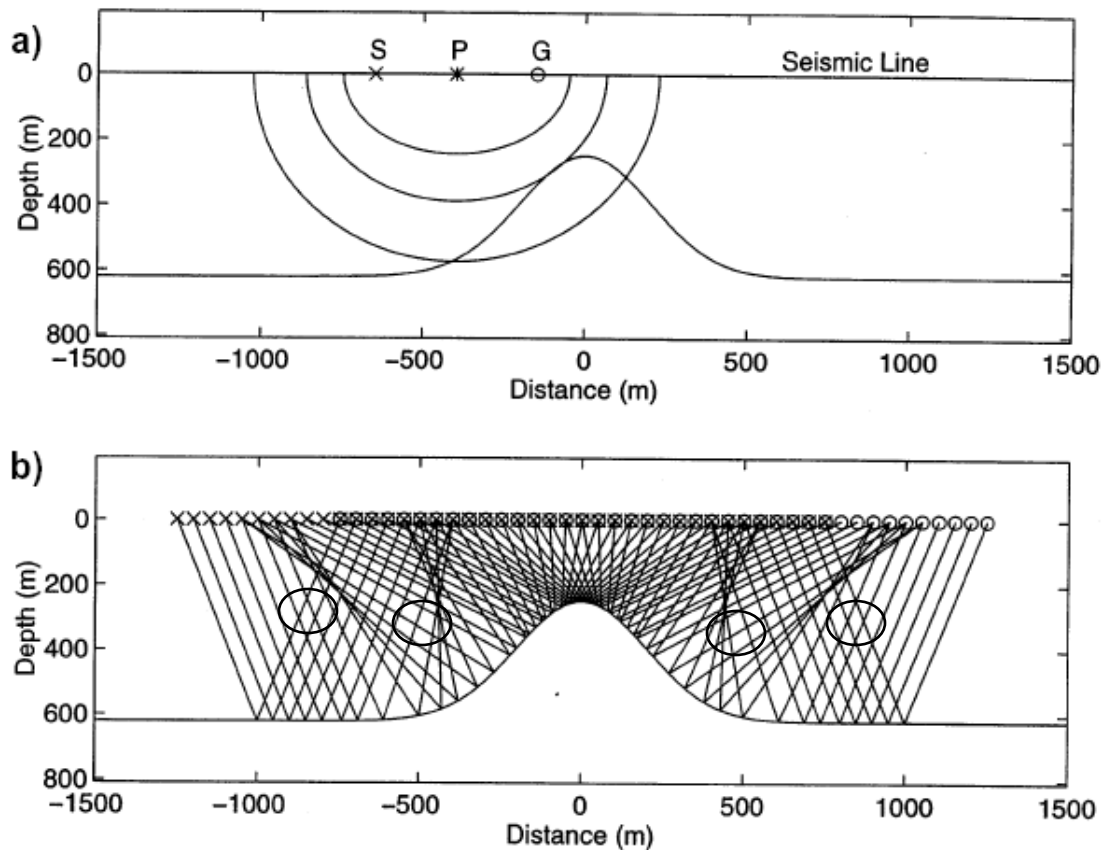


Figure 1.3:(a)Dome like reflector with wavefronts for a given source receiver pair (S) and (G) (b) represents the corresponding ray tracing of the structure, also the caustics produced are encircle (from Santos et al., 2000b).

1.2.1 Standard ray tracing

The ray tracing technique is based on an approximation to the general wave equation and is strictly valid for high frequency signals only. The standard zero order method cannot handle edge diffractions and caustics properly. Essentially, ray tracing follows the specular energy as predicated by Snell’s law. In isotropic media, the rays are orthogonal to the wavefronts. However, in the case of anisotropy this is no longer the case (c.f. Figure 1.4).

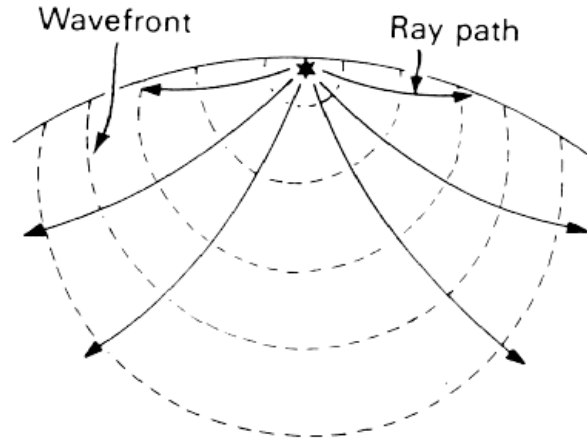


Figure 1.4: Rays and wavefronts in an anisotropic media.

When ray tracing is employed to model the dome structure in Figure 1.3a, the result obtained is shown in Figure 1.5 (as common offset data). The encircled areas represent caustics (focused) events that are not properly described by ray tracing as already mentioned.

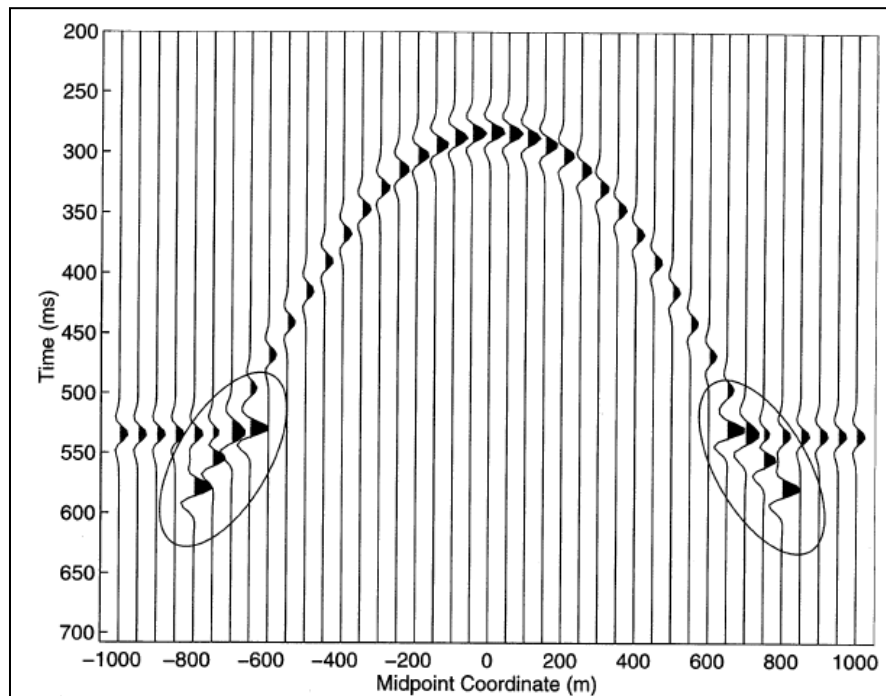


Figure 1.5: Synthetic common-offset seismic section obtained using standard ray tracing (Santos et al., 2000b).

The details of the workflow adopted to obtain the ray tracing seismic models are given in Appendix A, section A.1.

1.2.2 Kirchhoff Helmholtz modeling

Kirchhoff Helmholtz (KH) modeling is employed in areas which are geologically complex. Compared with standard ray tracing, the method has the potential of giving more accurate results on the expense of computational speed. Ray theory still forms the basis of the modeling, and hence many advantages are inherited, such as the selection of specific events (Santos et al.,

2000b). In order to model the reflection response of a chosen interface, rays are traced to that interface from the sources and receivers (i.e. Green's functions computations).

Consider now a fixed source–receiver pair S, G as shown in Figure 1.6. The Kirchhoff forward-modeling integral computes the reflected wavefield as a superposition of primary-reflected wave contributions along all reflecting interfaces under consideration. Since the superposition is a linear process, we restrict the present analysis to a single target reflector $z = \Sigma(\vec{x})$, where \vec{x} is a 2D vector describing the horizontal coordinates in a global Cartesian system. Moreover, it is assumed that the source and receiver are linked through a given measurement configuration described by a 2D parameter vector $\vec{\xi}$, i.e., $S = S(\vec{\xi})$ and $G = G(\vec{\xi})$. Moreover, assuming the so called Kirchhoff approximation where both source and receiver GF's are computed employing ray tracing the KH modeling integral takes the form (Santos et al., 2000a):

$$IK(\vec{\xi}, t) = \frac{1}{2\pi} \iint d^2\vec{x} W(\vec{\xi}, P_\Sigma) \partial_t F[t - \tau(\vec{\xi}, P)]|_{z=\Sigma(\vec{x})}. \quad (2)$$

Where $IK(\vec{\xi}, t)$ represents the Kirchhoff synthetic section, $W(\vec{\xi}, P_\Sigma)$ is a weight function that consists of an obliquity factor, the specular plane wave reflection coefficient of the incident wave at the reflector, and the source and receiver Green's function amplitudes. Also $P = (\vec{x}, z)$ is an arbitrary point in depth, P_Σ represents a point on the reflector with coordinates $(\vec{x}, \Sigma(\vec{x}))$, $F[t]$ is an analytical source pulse, and $\tau(\vec{\xi}, P)$ is the travel time from the source $S(\vec{\xi})$ via the reflection point P_Σ to the receiver $G(\vec{\xi})$.

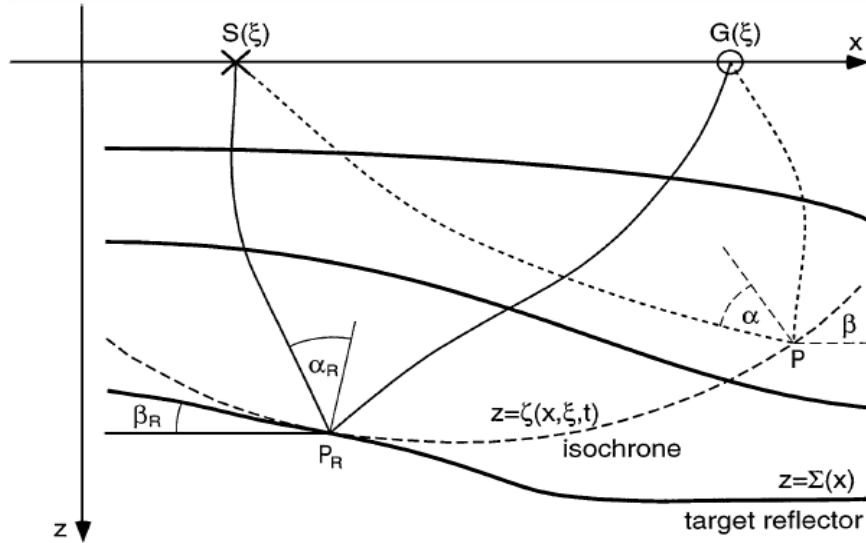


Figure 1.6: Inhomogeneous earth model with smooth interfaces. Also shown is one isochrone for the indicated source–receiver pair (Santos et al., 2000a).

Applying the KH method to model the dome structure in Figure 1.3a gives the result shown in Figure 1.7. A comparison with the ray tracing result in Figure 1.5 shows that:

- The caustic events have been more accurately modeled
- Some spurious events have been introduced (the encircled regions). These are due to discontinuities in the first-arrival field caused by ray tracing.

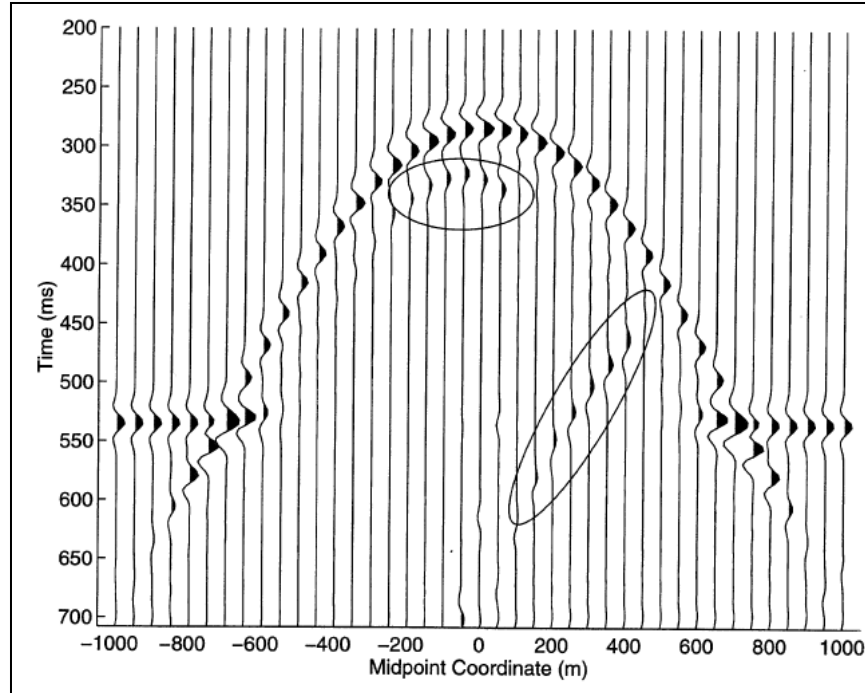


Figure 1.7 Synthetic common-offset section showing reflections as obtained from Kirchhoff Helmholtz modeling of the dome structure shown in Figure 1.3a (Santos et al., 2000b).

When employing the Kirchhoff approximation, possible caustics in the source and receiver field are not allowed. In case of the dome model, such caustics were present as can be seen from the ray paths in Figure 1.3b.

Note however, that Kirchhoff Helmholtz modeling is perfectly suited (and especially designed) to model caustics and diffractions caused by the shape of the reflector itself.

A detail workflow is given in Appendix A, section A.2 for the Kirchhoff Helmholtz modeling.

1.2.3 Seismic Modeling by Demigration

Demigration is a seismic forward modeling scheme based on seismic imaging. Demigration itself can be defined as the inverse of true amplitude migration. The true amplitude reflector image can directly be constructed from a given sharp reflector and a chosen source pulse. Then in a second step, the true-amplitude demigration can be performed, thus offering a new seismic modeling method, modeling by demigration.

The fact that the familiar Kirchhoff migration integral seems to have two inverse integrals in an approximate sense (i.e., the Kirchhoff Helmholtz modeling integral given in Eq.(2) and the Kirchhoff demigration integral given in Eq.(3) leads inevitably to the question whether the two processes described by these integrals are identical. The answer is that, although closely related, they are different processes. Their close relationship, however, leads to the conclusion that it should be possible to use Kirchhoff demigration to achieve the goals of Kirchhoff forward modeling (Santos et al., 2000a).

The basic operation of demigration is that in order to obtain the seismic data at a given time ' t ' for a fixed source-receiver position $\bar{\xi}$, the migrated events are stacked along an isochrone

corresponding to the reflection time 't'. This leads to the following expression for the Kirchhoff demigration integral (Santos et al., 2000a)

$$ID(\vec{\xi}, t) = \frac{1}{2\pi} \iint d^2\vec{x} W_D(\vec{x}, \vec{\xi}, t) \partial_z M(\vec{x}, z) \Big|_{z=\zeta(\vec{x}, \vec{\xi}, t)}. \quad (3)$$

Where $ID(\vec{\xi}, t)$ is the demigrated data; $W_D = (\vec{x}, \vec{\xi}, t)$ is a true amplitude weight factor; $z = \zeta(\vec{x}, \vec{\xi}, t)$ describes the isochrone, and $M(\vec{x}, Z)$ is the artificial true amplitude migrated section. The migrated section associated with a given reflector $\Sigma(\vec{x})$ can be mathematically approximated as (Santos et al., 2000a);

$$M(\vec{x}, Z) = A(\vec{x})F[S(\vec{x})(Z - \Sigma(\vec{x}))]. \quad (4)$$

In Eq. (4) A represents an amplitude factor which should resemble the correct (plane wave) reflection coefficient $R(\vec{\xi})$ at the stationary (specular) point $\vec{x}^* = \vec{x}^*(\vec{\xi})$.

Moreover the factor S should give the correct pulse stretch at the same point. Eq. (4) shows that the migrated section is obtained by placing the correctly scaled and stretched source pulse $F[t]$ along the reflector.

Application of the modeling by demigration technique to the dome structure in Figure 1.3a gave the result shown in Figure 1.8 (Santos et al., 2000b). When compared with the result from KH modeling (Figure 1.7) the caustics are equally well modeled and the artifacts are no longer present.

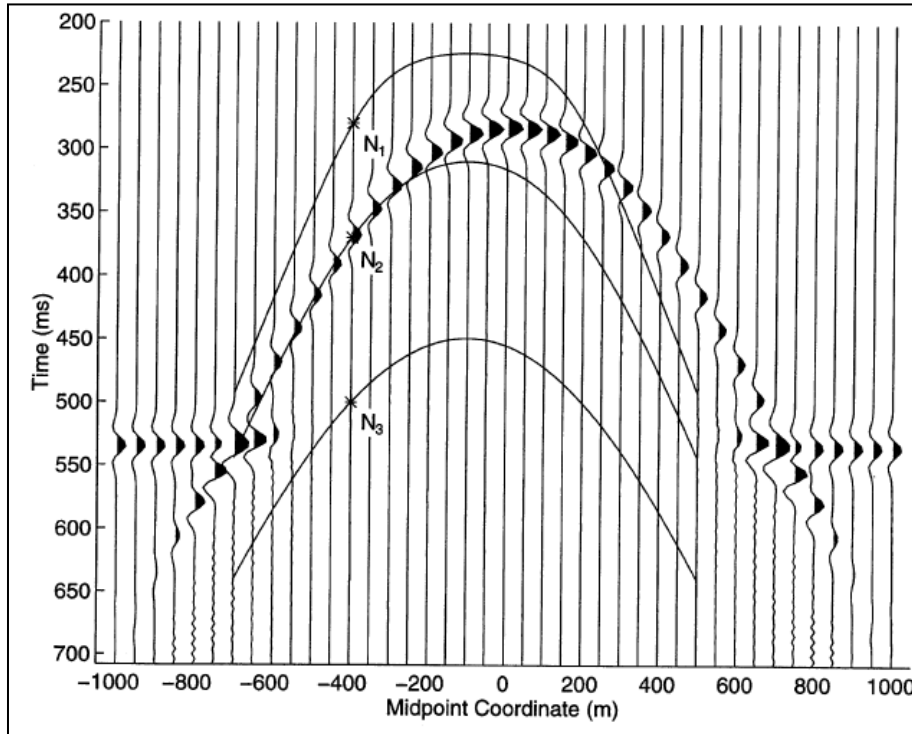


Figure 1.8: Synthetic common-offset section showing the modeled reflections as obtained from modeling by demigration. Also shown are three diffraction stack curves (Santos et al., 2000b).

1.3 Modeling by demigration-implementation issues

In this thesis, only a zero-offset acquisition was considered. For such a case, all quantities are available in order to compute the migrated image of a given reflector from Eq. (4). The explicit expression for the stretch factor at the stationary point is now (from Santos et al., 2000a).

$$S(\vec{x}^*) = \frac{2 \cos \beta_R}{v_R}. \quad (5)$$

Here β_R is the local reflector dip (c.f. Figure 1.7) and v_R being the local velocity. Moreover, the amplitude factor A is now given by the normal incidence reflector coefficient (from Santos et al., 2000a).

$$A(\vec{x}^*) \cong R(\vec{\xi}) = \frac{\tilde{\rho}_R \tilde{v}_R - \rho_R v_R}{\tilde{\rho}_R \tilde{v}_R + \rho_R v_R}. \quad (6)$$

Where $\tilde{\rho}_R$, ρ_R and \tilde{v}_R , v_R are the density and velocity above and below the considered target reflector at the reflection point. Combination of Eqs. (3)-(6) gives a feasible implementation of modeling by demigration.

In this thesis we will also study an alternative approach to calculate the artificial migrated section given by Eq.(3), based on the so called SimPLI technique (Lecomte, 2008). The SimPLI (Simulated Prestack Local Imaging) concept efficiently estimates a PSDM section without carrying out a complete migration.

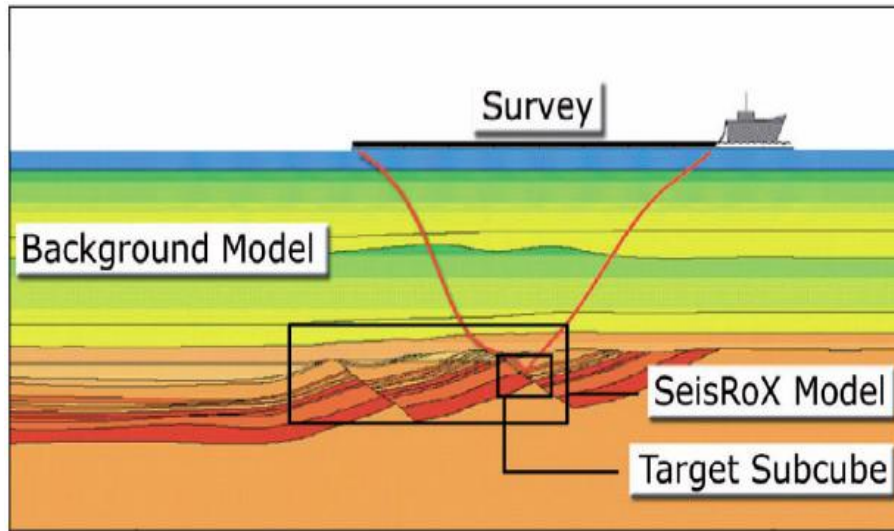


Figure 1.9 : The concept of local target oriented modeling (Gjøystdal et al., 2007a).

The SimPLI method is designed for local target oriented analyses. A detailed geomodel called the SeisRoX model, containing the structure (horizons) and available physical properties in the layers is generated for the entire zone of interest, that is, the zone where the seismic response is to be studied. Anywhere within the model a local target is defined, which is a sub-cube of the model that produce the seismic response (c.f. Figure 1.9).

An important assumption for producing a realistic seismic response of a deep target model is to take proper care of the propagation effects in the overburden. For this purpose, a background model is defined constituting a relatively smooth macro velocity model from the surface down to and including the target zone.

SimPLI is a ray-based method that provides a flexible, interactive and robust concept way of estimation Point Spread Functions (PSFs) associated with PSDM (Gelius et al., 2002). Once the PSFs are calculated, they are used to “blur” the actual reflectivity to reproduce the imaging effect of PSDM. A key element to calculate PSF using ray tracing is the illumination vector I_{SR} (Lecomte & Kaschwich, 2008).

The SimPLI concept is that a reflectivity cube is convolved by a 3D spatial wavelet or Point-Spread Function (PSF). The PSF is derived by FFT from wave number filters calculated with the illumination vectors I_{SR} , obtained via ray tracing or similar. The survey used in the thesis is a zero offset case. The result is a simulated PSDM image containing both 3D resolution and illumination effects (Lecomte & Kaschwich, 2008). This principle is illustrated in Figure 1.10.

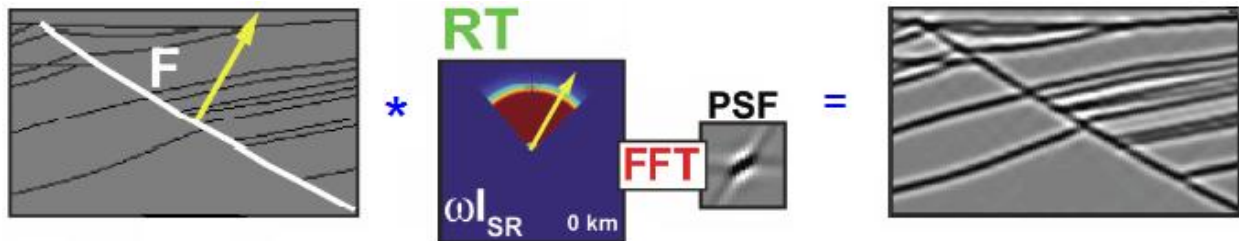


Figure 1.10: The principal of simulated PSDM (modified from Lecomte & Kaschwich, 2008).

The modeling by demigration workflow is discussed in Appendix A, section A.3.

Chapter 2

Modeled seismic responses from simple geological structures

In this thesis four different modeling approaches have been used to generate synthetic datasets for a variety of geological structures, these approaches are;

- Ray tracing (using wavefront construction approach, Vinje et al., 1993),
- Kirchhoff Helmholtz modeling (Kraaijpoel, 2003),
- Modeling by demigration,
 - Conventional implementation (Santos et al., 2000a),
 - SimPLI approach (Lecomte, 2008).

The workflows for all the modeling techniques considered are described in Appendix A.

To perform a feasibility study of the different modeling techniques, it is necessary to create a set of controlled data. Correspondingly, synthetic models have been created based on simple geological structures. In this chapter, a brief introduction of the different geological models is given followed by a detailed discussion of the results obtained from the different modeling techniques. For each layer the models were assigned constant properties; these include P-wave velocity (V_p), density (D), and Shear-wave velocity (V_s). The V_s has been calculated by the constant ratio $V_p/V_s=1.732$. The Table 2.1 shows the values for each layer in the models.

Property	Value	
	Layer 1	Layer 2
V_p (km/s)	2.4	2.8
V_s (km/s)	1.385	1.617
D (g/cm³)	2.0	2.4

Table 2.1: Different properties for layer 1 and layer 2.

Zero offset data were generated employing NORSAR-3D (c.f. Appendix A, section A.1.3). The survey geometry is shown in Figure 2.1 employing a source spacing of 50m. For demonstration purposes traced rays for the syncline model are shown in Figure 2.1b.

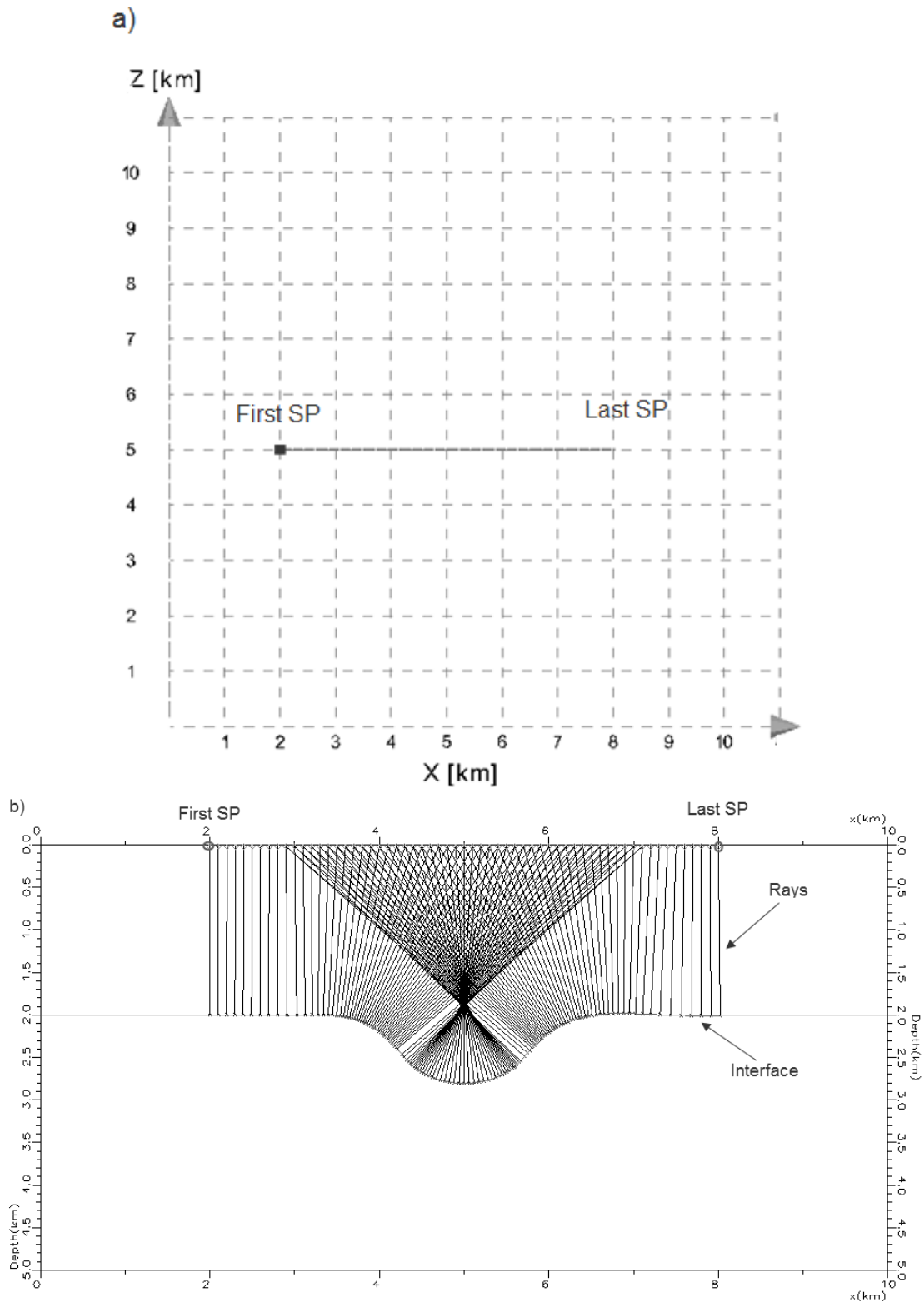


Figure 2.1: a) Layout of zero offset survey, b) 2D view of zero offset survey of syncline, showing the reflected rays along the interface.

2.1 Syncline Model

In structural geology, a syncline is a downward-curving fold, with layers that dip toward the center of the structure. A syncline can be regarded as one of the simplest geological structures. In principle the deeper the center of curvature, the broader the convex reflection forming the central portion of the syncline. The syncline signature on an unmigrated seismic section is much like an anticline.

In a reflector such as a syncline, the concave feature produces three ray paths to the receiver as shown in Figure 2.2a. They generally have different lengths (SP1, SP2, and SP3) and produce more than one arrival at the receiver. The vertical ray will not be the shortest or the first to arrive if the bottom of the syncline is further from the shot point than the shoulders (i.e. the center of the curvature of the reflector is below the surface). As in this experiment the shot point moves along, (covered by positions 1 to 10 in Figure 2.2b) the shortest path moves from one side of the syncline to the other. The three arrival times for each of the transmitter positions 1 to 10 together produce a 'bow tie' on the sections as shown in Figure 2.2c (Mussett et al., 2000).

A syncline with a center of curvature placed in the center of the model has been created in NORSAR-2D (c.f. Figure 2.3). This model was then transferred to NORSAR-3D using the work flow explained in Appendix A.

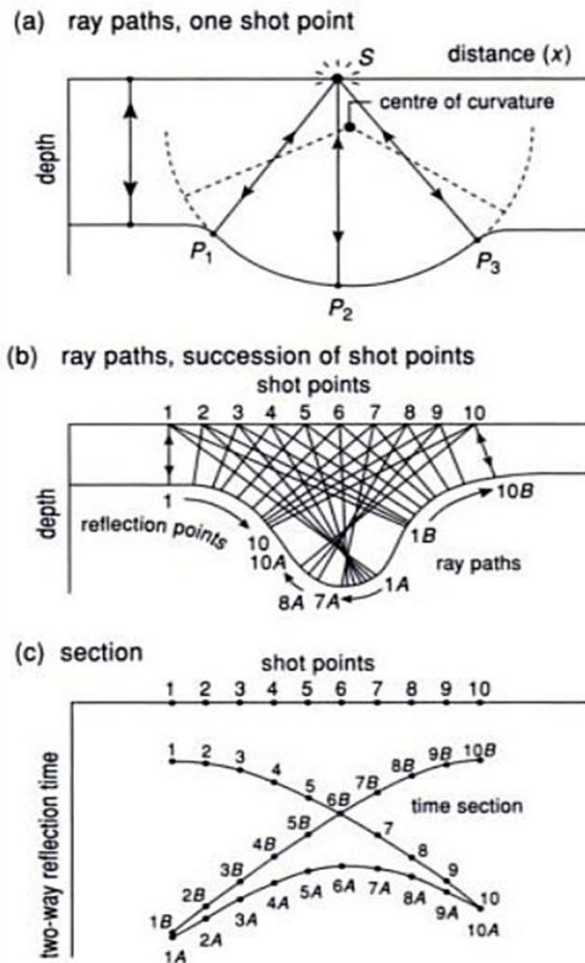


Figure 2.2: Distortions of syncline (Modified from Musset et al, 2000).

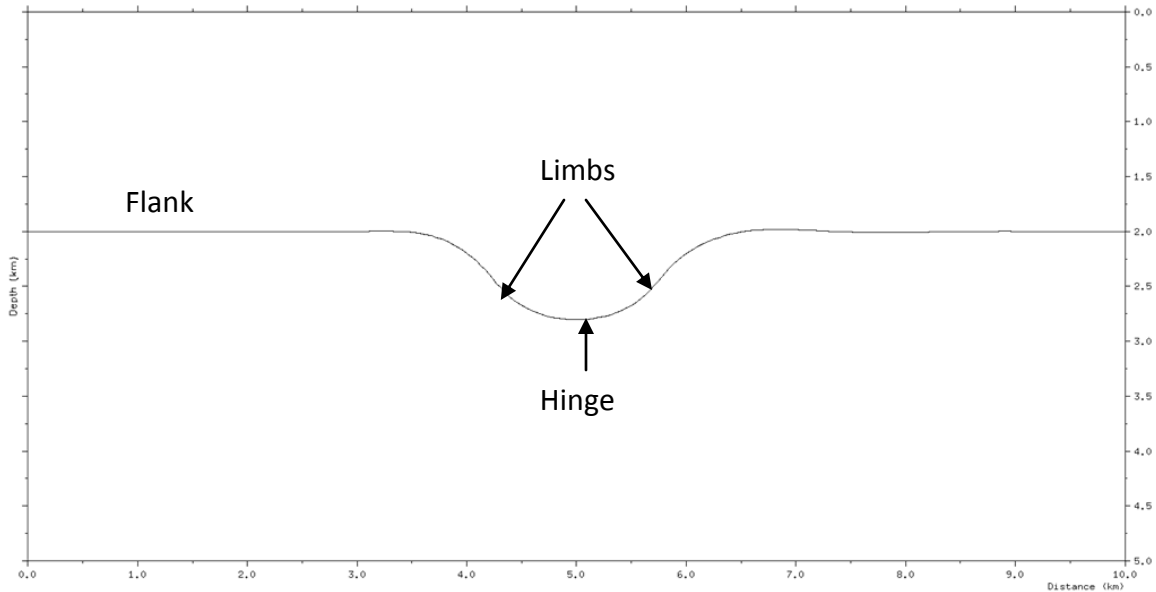


Figure 2.3: 2D view of the syncline model, different terminologies for the syncline structure are also indicated.

2.1.1 Key Features

The key feature of a syncline is the bow-tie effect (c.f. Figure 2.4). This is established as concave-upward events in the seismic data caused by a buried focus. These distortions can be corrected by proper migration of the data. Focusing of the seismic waves produces three reflected events for each surface (receiver) location. The name was coined for the appearance of the events in unmigrated seismic data (Schlumberger, 2009).

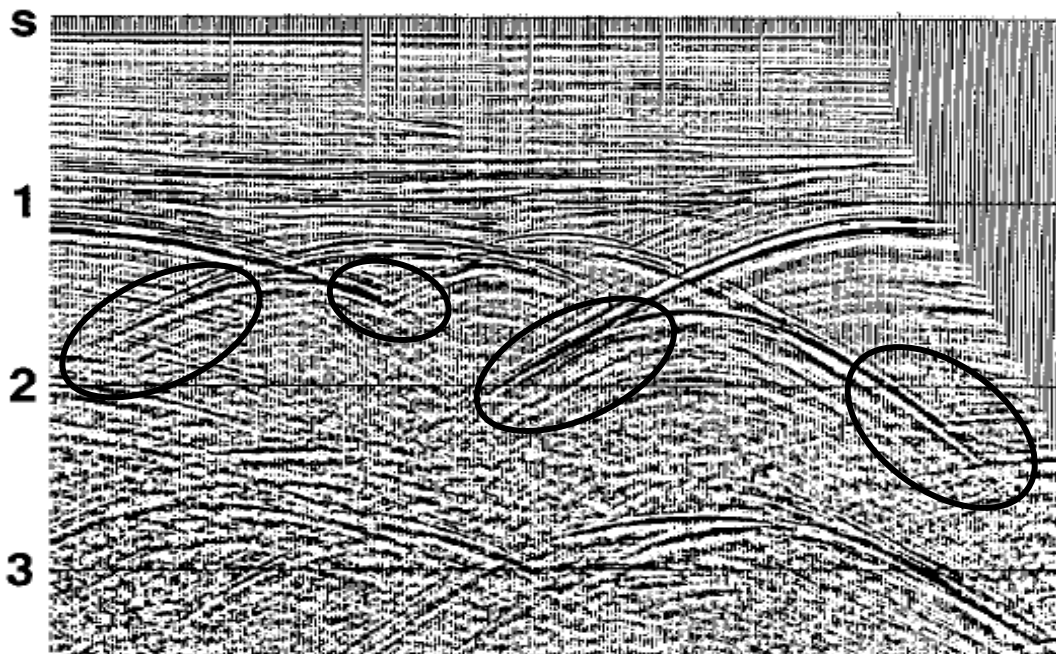
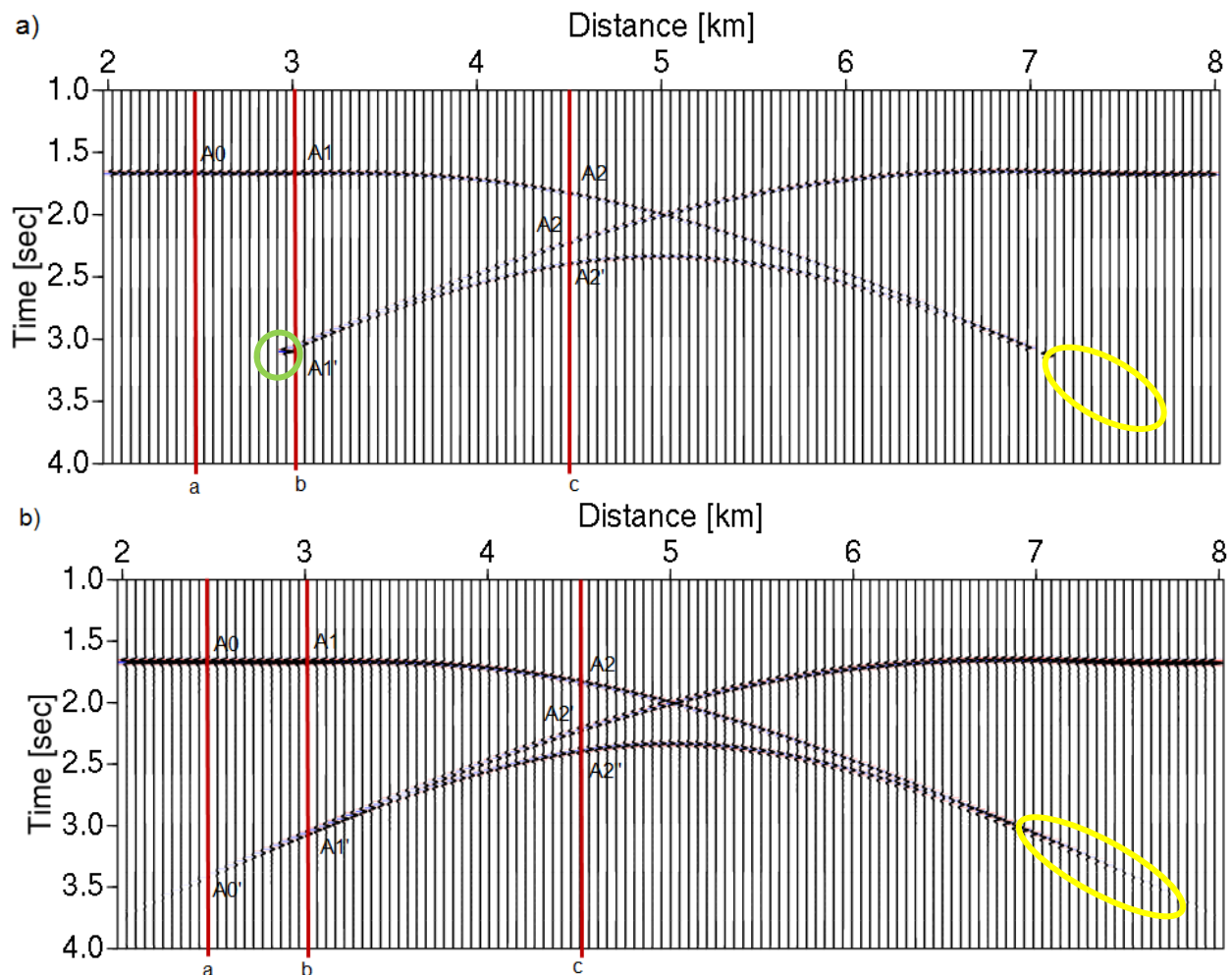


Figure 2.4: Key features in an unmigrated seismic section for a syncline (modified from Sheriff, 1981); the bow ties are of special interest and have been carefully studied employing the different modeling methods.

2.1.2 Seismic Modeling

Figure 2.5 shows the different modeling results for the syncline structure. Clearly, all seismic sections bear resemblance to each other, especially for the center part of the structure (c.f. Figure 2.5). However, the fish tail created by ray tracing in Figure 2.5a (e.g. indicated by yellow circle) is less prominent than the ones obtained by Kirchhoff Helmholtz modeling (Figure 2.5b) and modeling by demigration (Figures 2.5c and 2.5d). In addition, it can be observed that there are some unrealistic high amplitudes for the ray tracing data at the cusps which are indicated by the green circle in Figure 2.5a. When plotting the seismic section these high amplitude values cause dimming of amplitudes for the ray tracing in comparison to the Kirchhoff Helmholtz result.

The seismic data obtained by Kirchhoff Helmholtz modeling shows the entire fish tail feature. For both modeling by demigration results, the seismic sections contain residual noise due to the summation process (e.g., areas indicated by green arrows in Figures 2.5c and 2.5d). It can be observed that the noise for the classical modeling by demigration has mainly positive amplitudes. In comparison, for modeling by demigration using the SimPLI approach the residual noise shows mainly negative amplitudes. The fishtail still appears in both seismic sections for modeling by demigration.



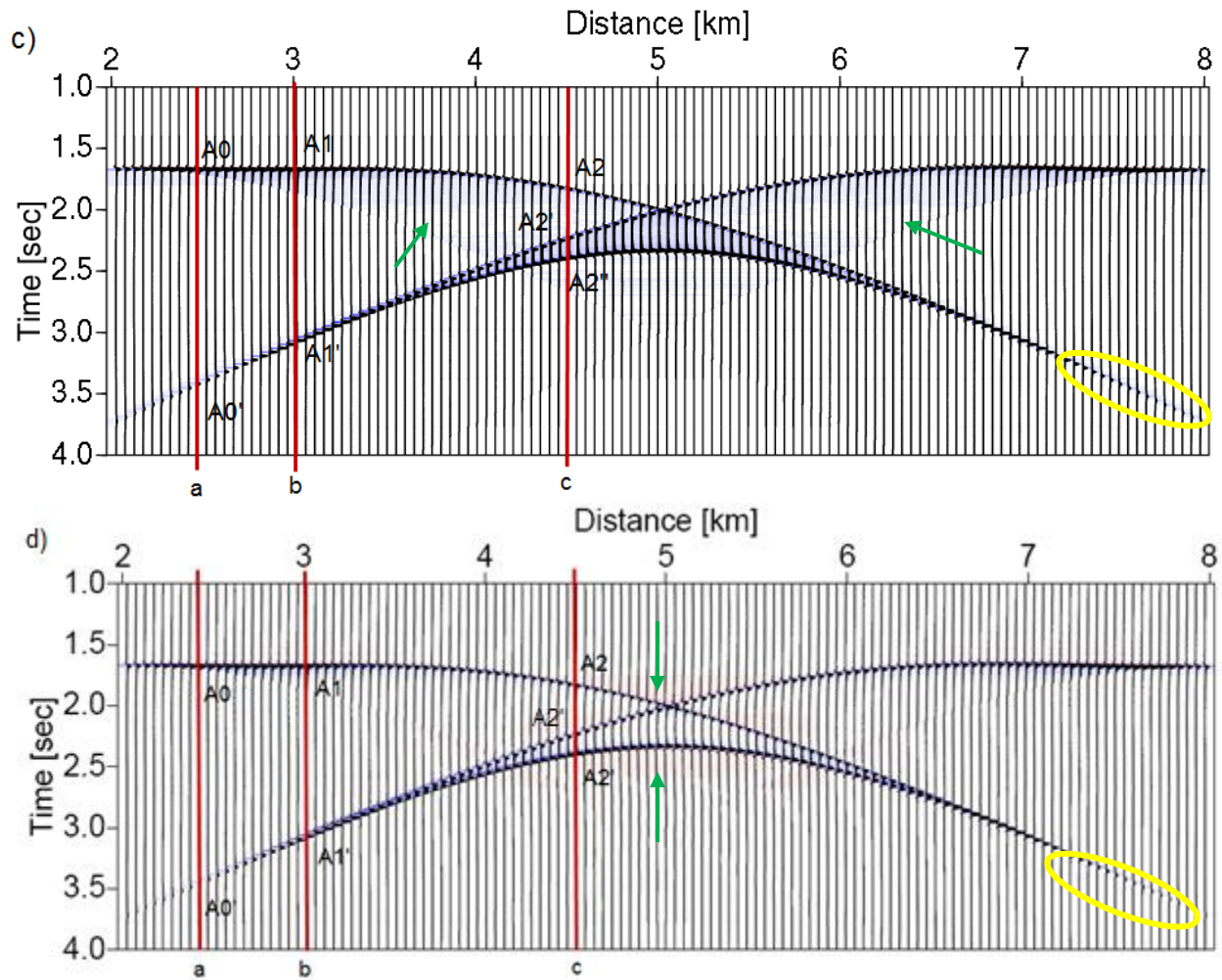


Figure 2.5: Synthetic data for the syncline obtained by using a) ray tracing b) Kirchhoff Helmholtz modeling c) standard modeling by demigration d) modeling by demigration (SimPLI approach). Also shown is the location of the traces for Figure 2.6.

For a detailed investigation on amplitude changes in the seismic data I concentrate on three different trace locations, marked by positions a, b, and c in Figure 2.5 (indicated by red lines).

The modeling results for all trace locations are displayed in Figures 2.6a to 2.6c. At these trace locations the maximum amplitude values were identified, respectively. These picked amplitude values are also listed in the respective figures. Since the implementation of the various theories are still under development additional calibrations are necessary in order to do direct amplitude comparisons. Therefore, in this thesis only relative amplitudes are considered. These are summarized in Table 2.2.

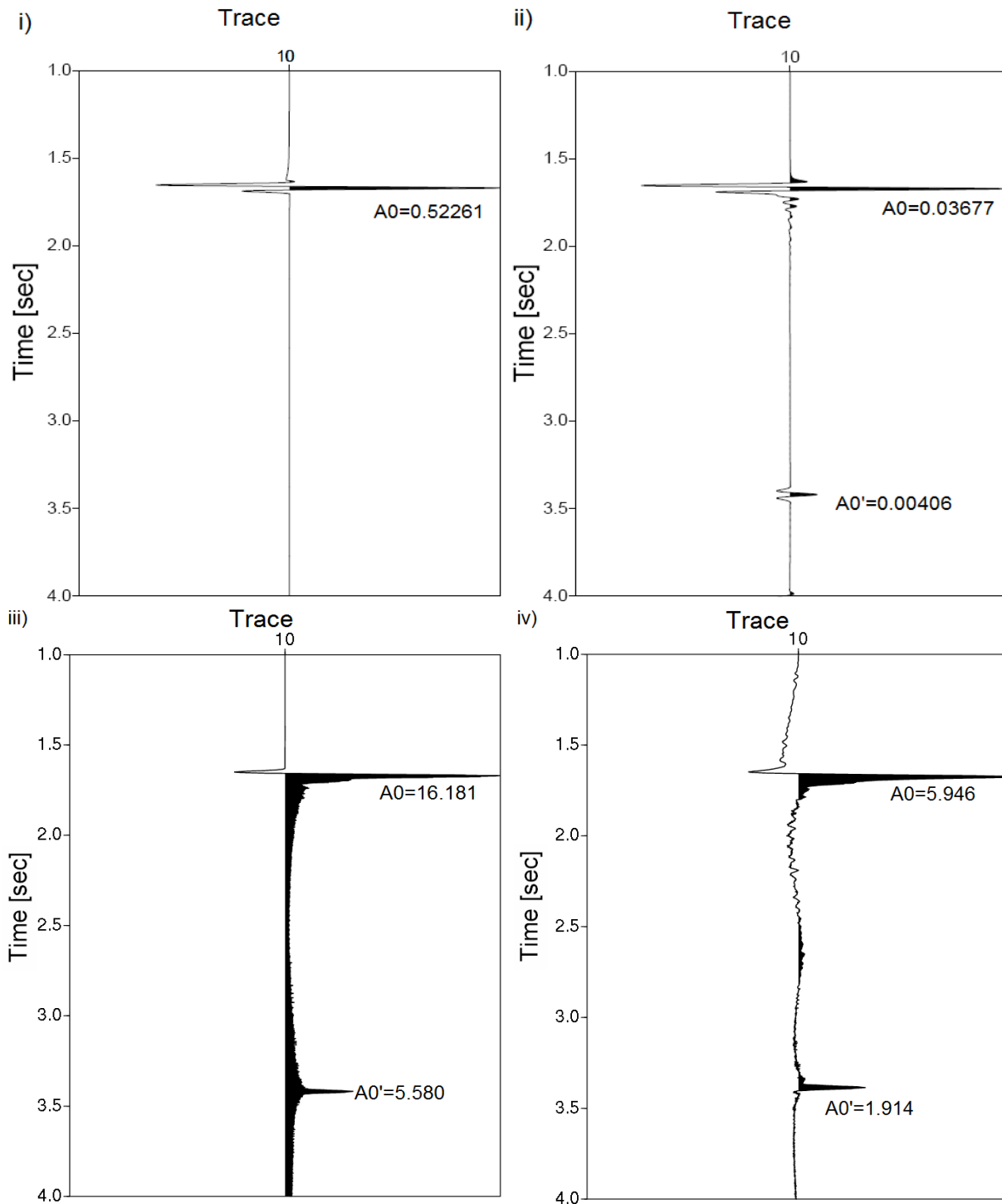


Figure 2.6a): Amplitude values for different modeling techniques at trace position 'a'; i) seismic trace ray tracing data, ii) seismic trace for Kirchhoff Helmholtz model, iii) seismic trace for modeling by demigration, and iv) seismic trace for modeling by demigration using SimPLI approach.

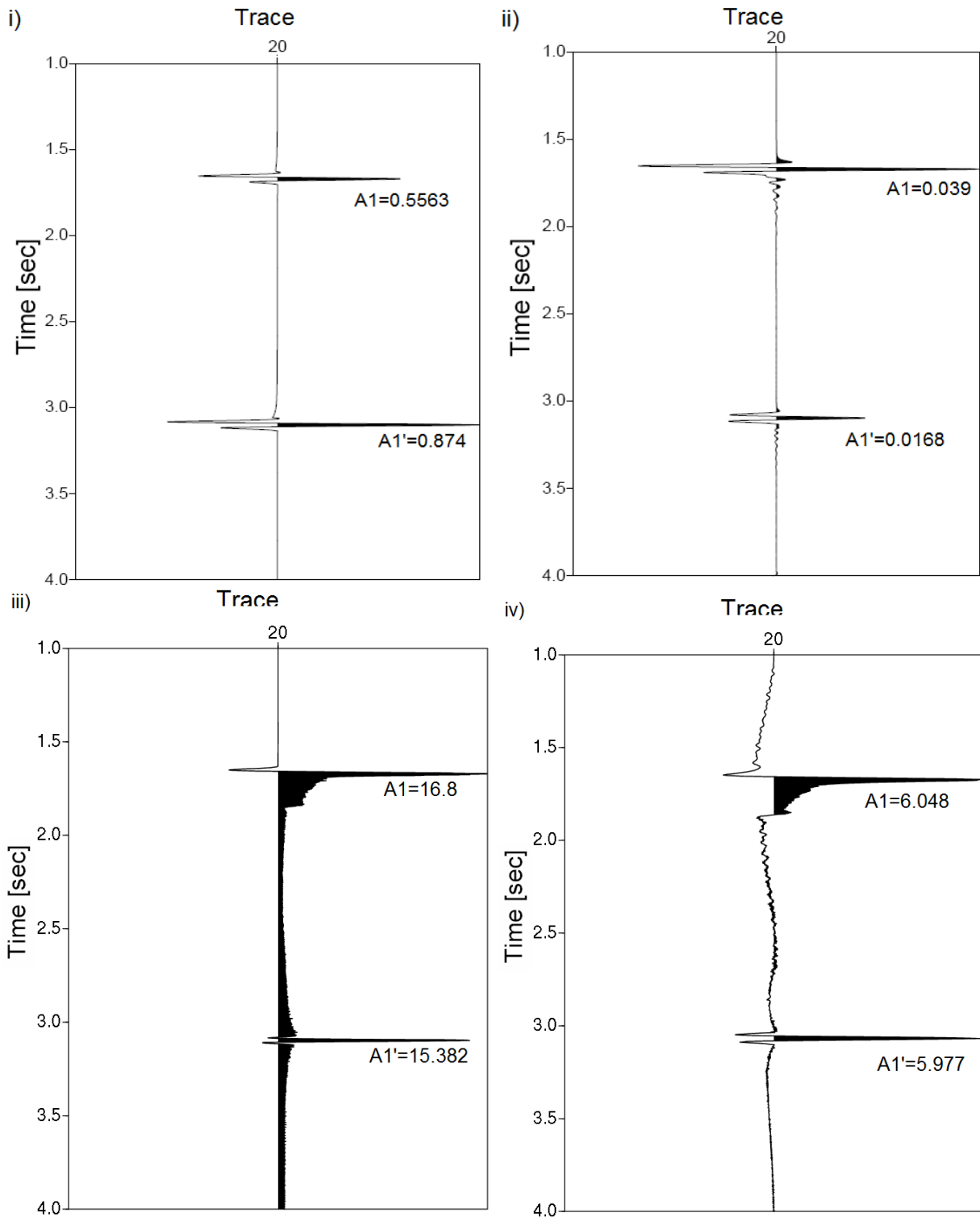


Figure 2.6b): Amplitude values for different modeling techniques at trace position 'b'; i) seismic trace ray tracing data, ii) seismic trace for Kirchhoff Helmholtz model, iii) seismic trace for modeling by demigration, and iv) seismic trace for modeling by demigration using SimPLI approach.

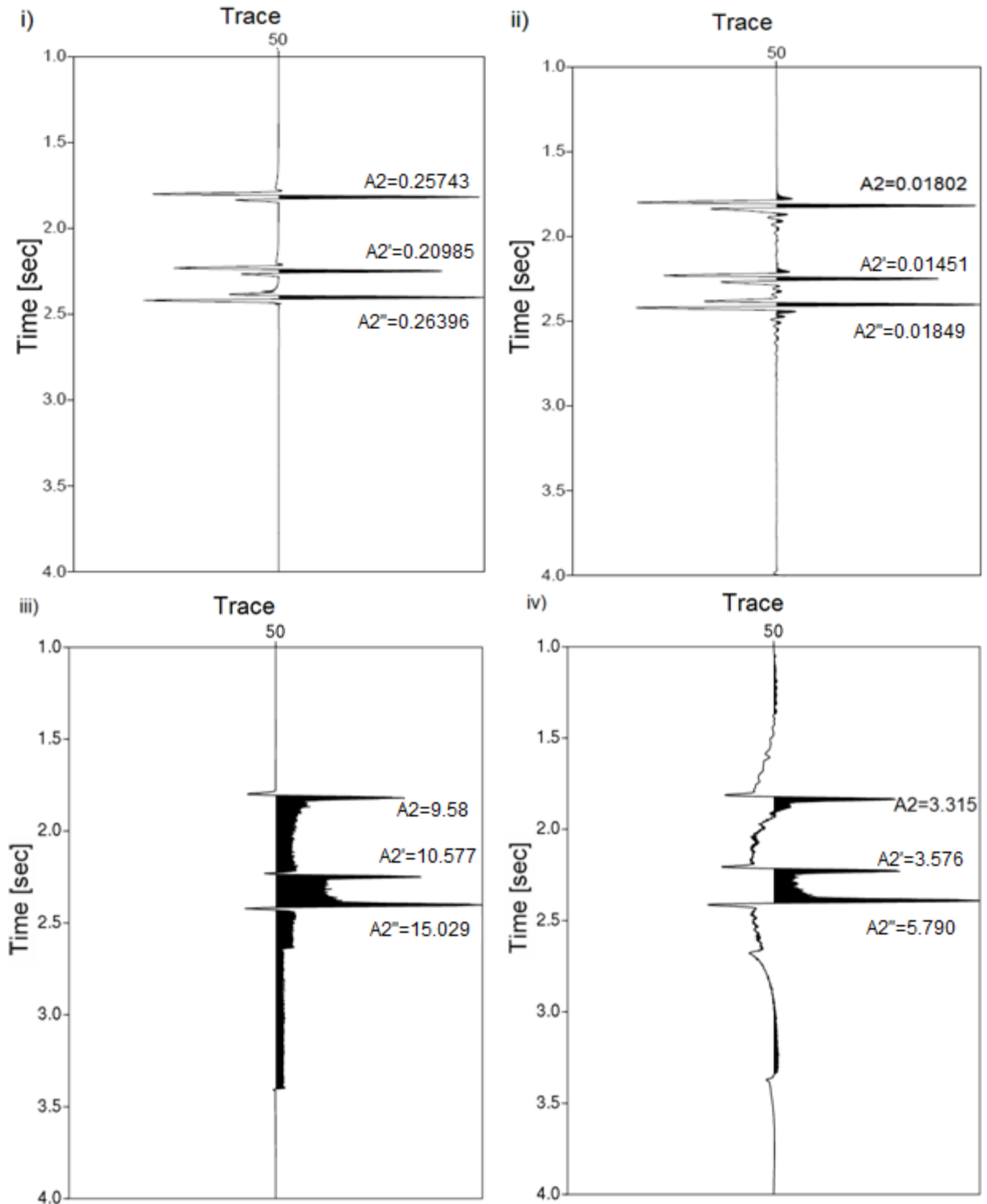


Figure 2.6c) Amplitude values for different modeling techniques at trace position 'c'; i) seismic trace ray tracing data, ii) seismic trace for Kirchhoff Helmholtz model, iii) seismic trace for modeling by demigration, and iv) seismic trace for modeling by demigration using SimPLI approach.

The trace location 'a' corresponds to the flank of the syncline (c.f. Figure 2. 3). Trace location 'a' (c.f. Figure 2.6a) contains multiple arrivals except for the ray tracing data. The Kirchhoff Helmholtz modeling data clearly shows a wavelet containing positive and negative amplitudes. This is not true for the modeling by demigration. Although, both modeling by demigration results (conventional and the SimPLI approach) show later arrivals, the later arrivals (A0') exhibit only positive amplitudes. This can be due to the fact that the negative amplitudes are so weak that when the summation operation is performed these are dominated by the larger positive amplitudes. However, for the other two trace locations there are slight negative amplitudes for the later arrivals.

Trace location 'b' corresponds to the upper limb side of the syncline structure (c.f. Figure 2.3). For this location (c.f. Figure 2.6b), amplitude picking is quite difficult due to the fact that different arrivals are merged together. Here, the amplitudes (A1') become larger due to the constructive superposition of the seismic response. It can also be seen that the later arrivals in modeling by demigration are not amalgamated with each other unlike the Kirchhoff Helmholtz modeling.

The trace location 'c' is at the center part of the limb of the syncline structure (c.f. Figure 2.3). For this trace location (c.f. Figure 2.6c) three distinct arrivals can be identified in all the modeling methods. The arrival at A2 corresponds to the limb of the syncline, whereas A2' and A2'' correspond to the hinge of the syncline structure.

Method	A1/A0	A2/A0	A1'/A0'	A2'/A0'	A2''/A0'
Ray Tracing	1,064465	0,492585	-	-	-
Kirchhoff Helmholtz Modeling	1,060647	0,490073	4,137931	3.573892	4,438424
Modeling by Demigration	1,038255	0,592052	2,756631	1.89552	1,716846
Modeling by Demigration (SimPLI)	1,017154	0,557518	3,12278	1.868339	1,731975

Table 2.2: Amplitude variations for different modeling methods at different time and trace location.

The ratio A1/A0 gives the correlation of amplitude variations from the trace location 'b' to 'a'. For all seismic sections, this ratio is approximately 1, which corresponds to small amplitude differences.

The ratio A2/A0 gives the correlation of amplitude variations from the trace location 'c' to 'a'. For all methods the ratio is approximately 0.5, which corresponds to a decrease in amplitudes from trace location 'a' to 'c'. For both modeling by demigration results, the amplitude difference is slightly smaller than for the ray tracing and the Kirchhoff Helmholtz results.

I also picked the amplitudes at the same trace location for the later arrivals and the same ratios were computed between the trace locations (see Table 2.2).

For the ray tracing there is no reference amplitude A0'. The ratios A1'/A0' for all remaining modeling techniques show stronger distinctions than for the first arrivals (A1/A0). Since the area for the later arrival is complex, amplitude picking is quite difficult. In general, the ratio is high for the later arrivals, in particular for Kirchhoff Helmholtz modeling. However, both

modeling by demigration results show strong similarities with respect to amplitude changes. This can be observed in the ratios of $A2'/A0'$ and $A2''/A0'$.

2.1.2.1 Migration

All the seismic modeling results were afterwards migrated, employing the NORSAR software IMAGING. This is done because the migrated sections will reveal weaknesses of the obtained seismic sections by different modeling techniques. Due to the fact that the geological model is known, the correct position and shape of the reflector is well defined and the obtained results can easily be judged. The complete workflow used in migration is described in Appendix A, section A.4.

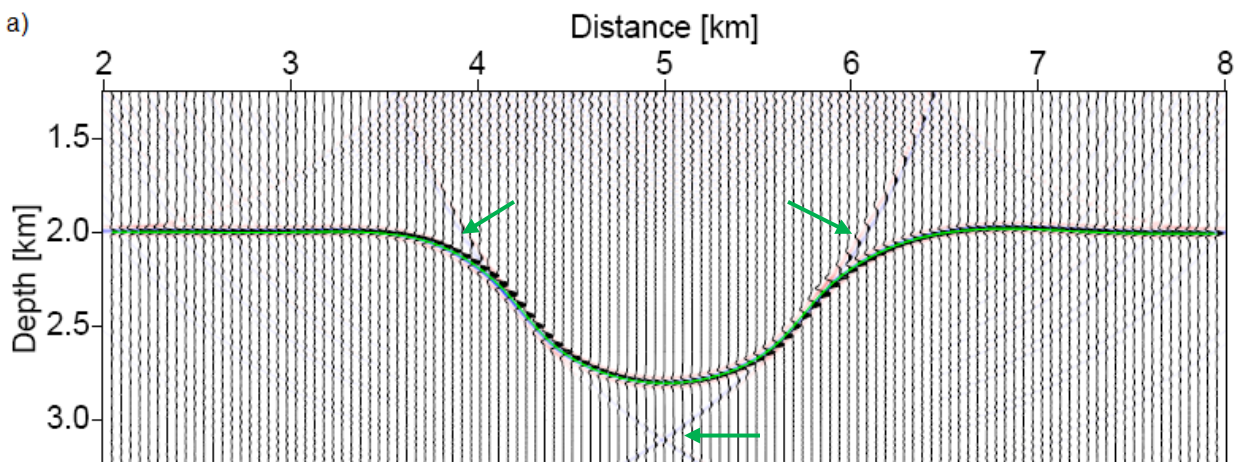
For the ray traced data strong residual noise near to the limb and hinge of the syncline (indicated by green arrows in Figure 2.7a) remains in the migrated section. Clearly, the lack of the completed seismic response at the cusps of the fish tail leads to these stronger artifacts. Consequently, for realistic high complex geological models the ray tracing modeling approaches its limit.

In comparison, the Kirchhoff Helmholtz seismic section contains only random residual noise, but small noise level (c.f. Figure 2.7b).

For modeling by demigration results the observed noise level is higher than for the Kirchhoff Helmholtz result (c.f. Figures 2.7c and 2.7d). However, for both demigration modeling techniques the seismic sections contains random noise, hence the obtained migrated images exhibit residual noise. Besides, for these cases the seismic traces show high frequency variation that influences the final image.

In the case of the classical modeling by demigration, more noise can be observed below the hinge of the syncline rather than the flanks, indicated by green arrows in Figure 2.7c.

For the case of modeling by demigration using the SimPLI approach, it is observed that the noise is smeared along the reflector. However, since the seismic model in Figure 2.5d contained noise with negative amplitude above the fish tail, migration causes this noise to be prominent on the top of the structure; this is indicated by the green arrows in Figure 2.7d.



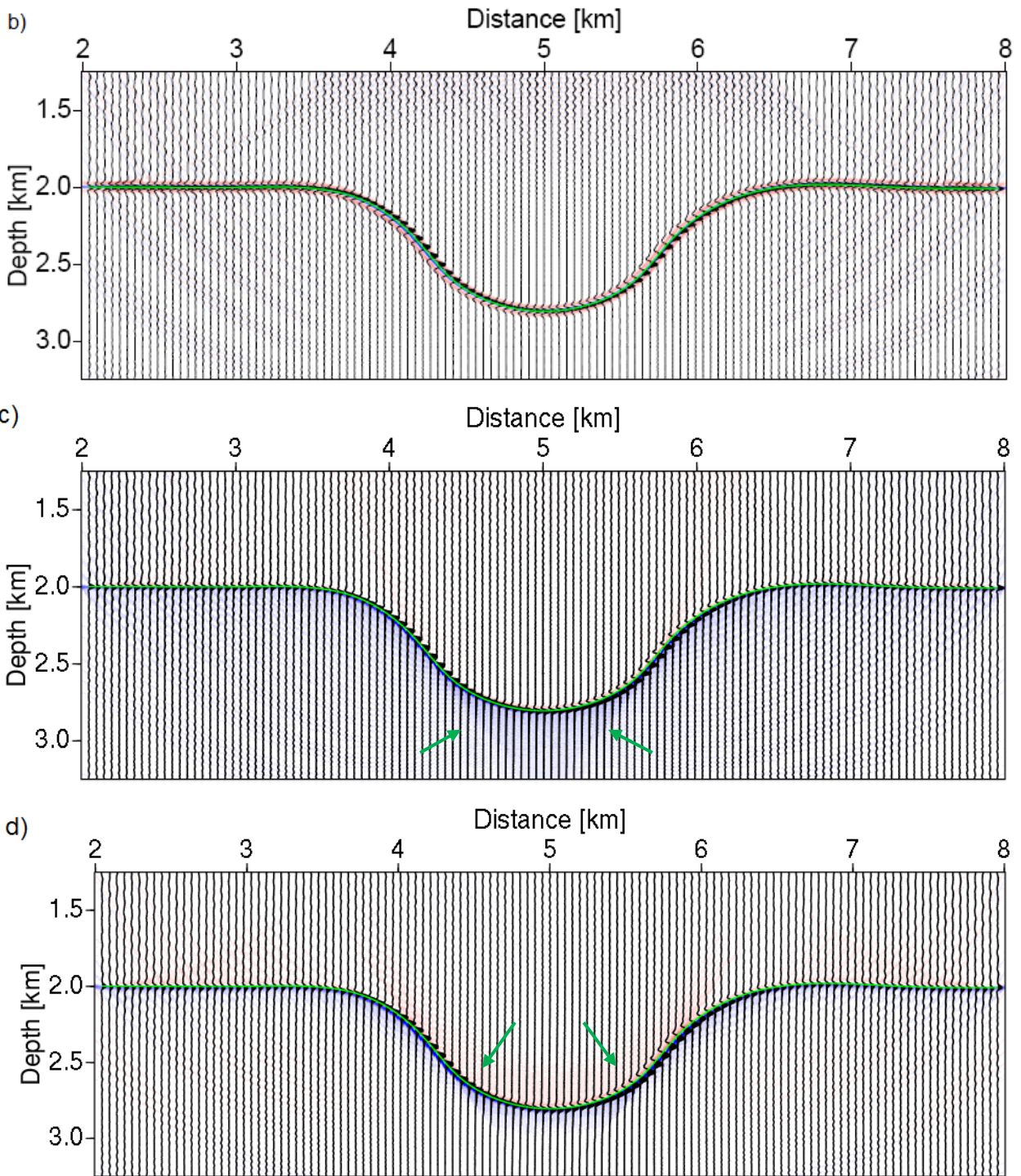


Figure 2.7: Migration result for different seismic modeling methods a) ray tracing, b) Kirchhoff Helmholtz model c) modeling by demigration, d) modeling by demigration using SimPLI approach. The green line represents the syncline structure.

2.2 Anticline Model

In structural geology, an anticline is a fold that is upward convex and has its oldest beds at its core. The anticline is regarded also as a simple structural trap for hydrocarbons.

The seismic expression of an anticline, like syncline, depends upon curvature, depth and position of the center of curvature of the folded strata. A gentle anticline is just a little widened in the seismic expression but otherwise scarcely changed, while a sharply folded, narrow one appears on the seismic section as a gently folded wide anticline (Mussett et al., 2000). Figure 2.8a shows the geometry of the geological model, superimposed by few rays and Figure 2.8b shows the unmigrated time section of the same model.

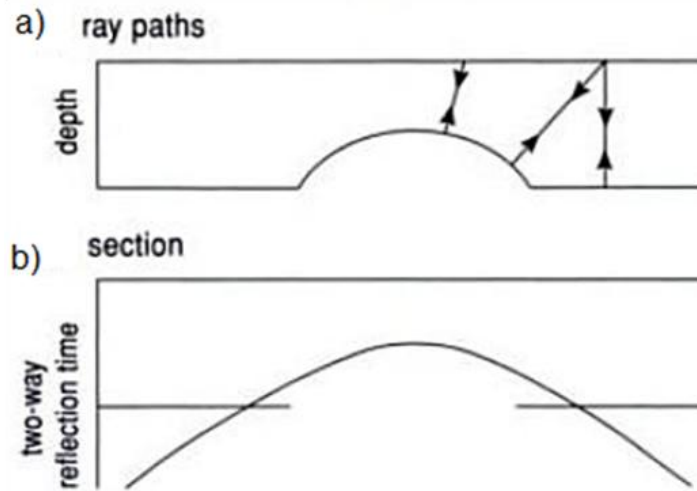


Figure 2.8: Distortions of anticline (Modified from Mussett et al., 2000).

An anticline with a center of curvature placed in the center of the model has been created in NORSAR-2D (c.f. Figure 2.9). This model was then transferred to NORSAR-3D using the work flow explained in Appendix A.

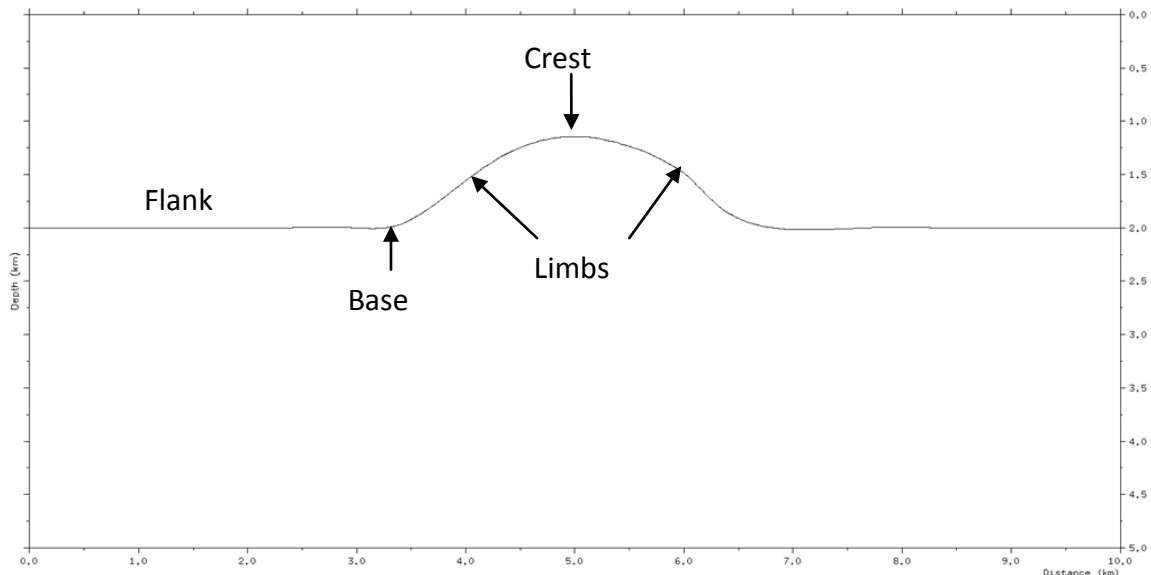


Figure 2.9: 2D view of the anticline model, different terminologies for the anticline structure are also indicated.

2.2.1 Key Features

The unmigrated seismic section shows a broader and wider structure as the original anticline as can be seen in Figure 2.10. The artifacts represented by diffracted waves from the edges at the base of the anticline are marked with circles (c.f. Figure 2.10); these features were studied carefully during this thesis employing different modeling techniques.

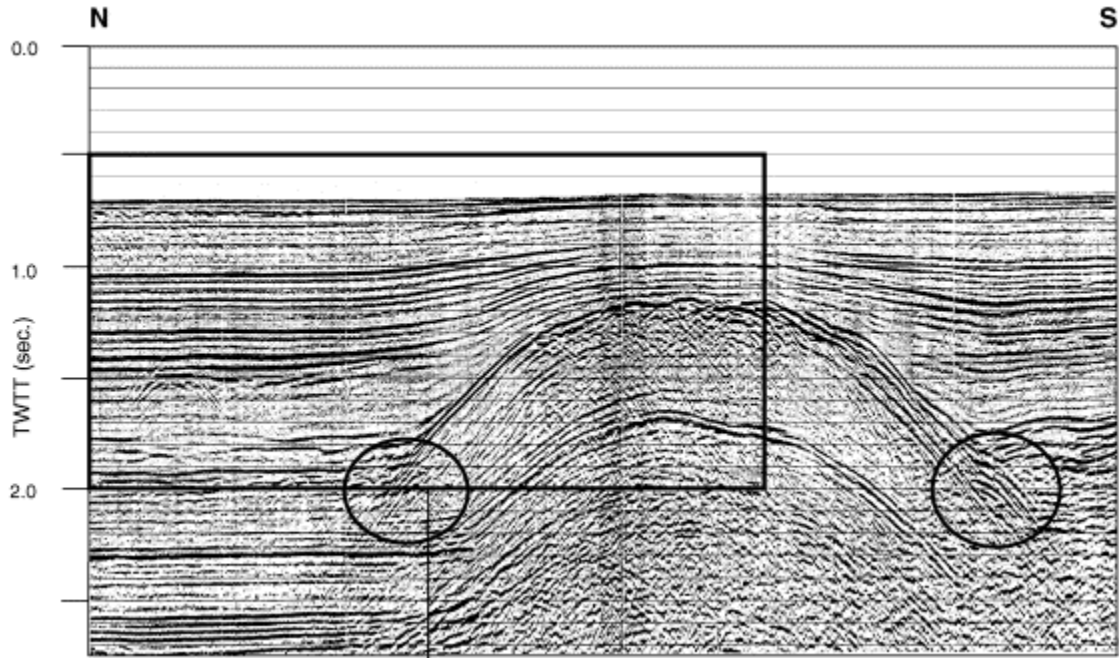


Figure 2.10: Unmigrated seismic section for anticline, key features studied in the thesis is circled (modified from Masferroa et al., 2001).

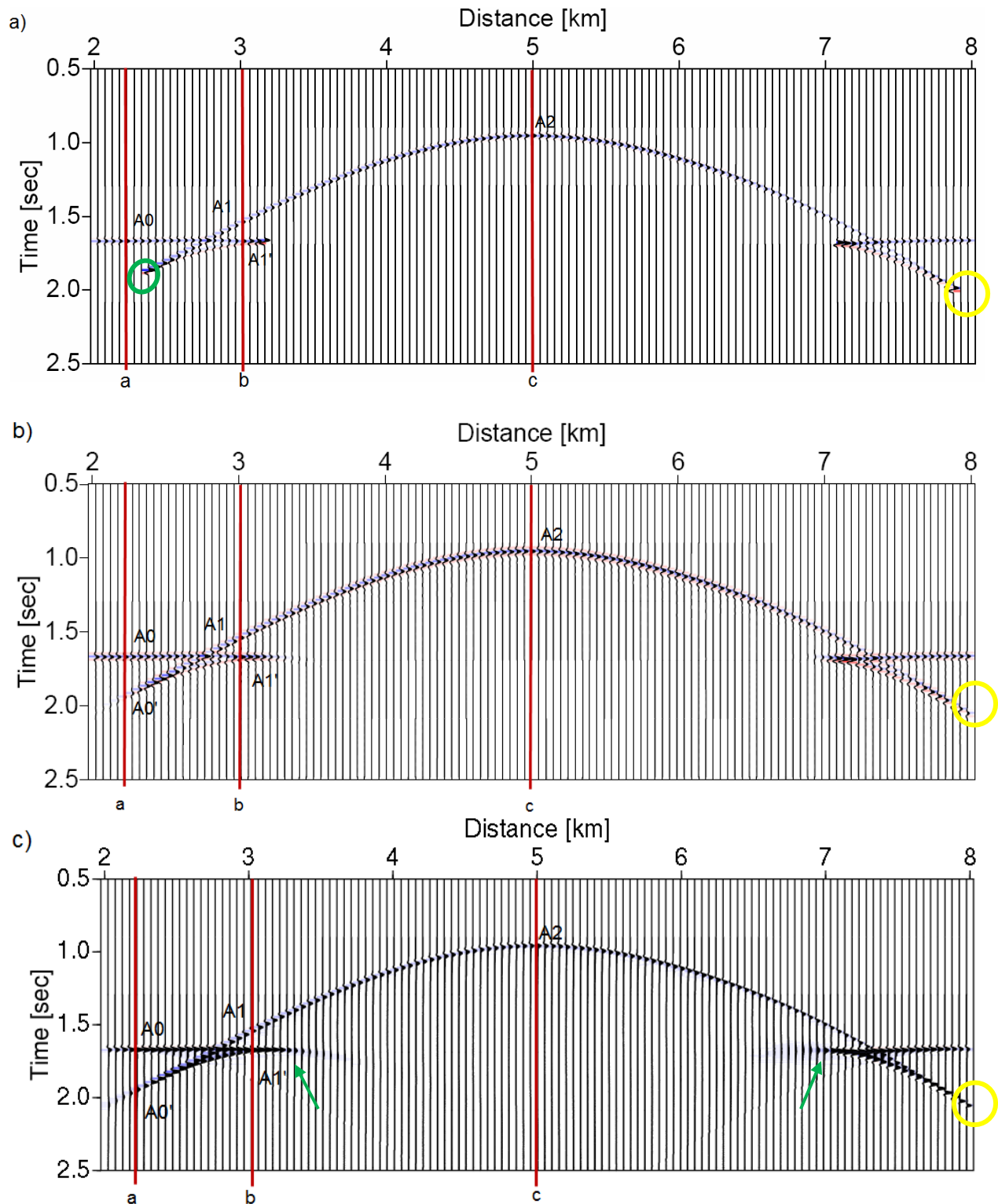
2.2.2 Seismic Modeling

For the anticline geological model the same modeling methods have been applied as for the syncline case. Figure 2.11 shows the different seismic data obtained by these methods. By visual examination of this data, it can be deduced that all show resemblance at the crest of the anticline.

However, the standard ray tracing methods again truncates the fish tail feature (indicated by the yellow circle in Figure 2.11a), whereas Kirchhoff Helmholtz modeling (Figure 2.11b) and modeling by demigration results contain the entire structure (Figures 2.11c and 2.11d).

At the tip of the tail, indicated by the green circle in Figure 2.11a, ray tracing exaggerates the amplitude values. These high amplitudes cause the overall amplitudes to be dimmed in comparison to the Kirchhoff Helmholtz modeling result.

For both modeling by demigration results, the seismic sections contain residual noise due to the summation process (e.g., areas indicated by green arrows in Figures 2.11c and 2.11d). The noise for the classical modeling by demigration has mostly positive amplitudes compared to modeling by demigration using the SimPLI approach, which has mostly negative amplitudes.



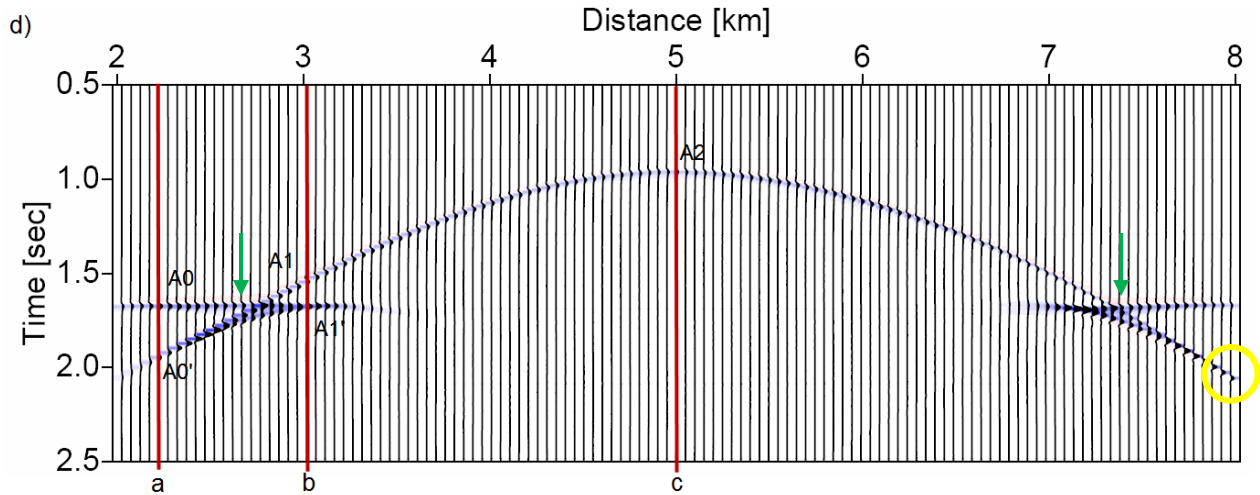


Figure 2.11: Synthetic data for anticline model obtained by a) ray tracing b) Kirchhoff Helmholtz modeling c) standard modeling by demigration, and d) modeling by demigration with SimPLI approach. Also shown are the locations of traces used to pick amplitudes for Figure 2.12.

For a detailed investigation of the amplitude variations in the seismic data, I concentrate on three different trace locations, marked by 'a', 'b', and 'c' in Figure 2.11 (indicated by red lines).

The largest positive peak amplitudes for each trace have been identified. All traces are displayed in Figures 2.12a to 2.12c with picked amplitudes values.

Due to lacking of proper calibrations for the modeling methods, again relative amplitudes will be compared to each other, rather than the direct picked amplitudes. To compute the relative amplitudes trace location 'a' is taken as the bases. These ratios are shown in Table 2.3.

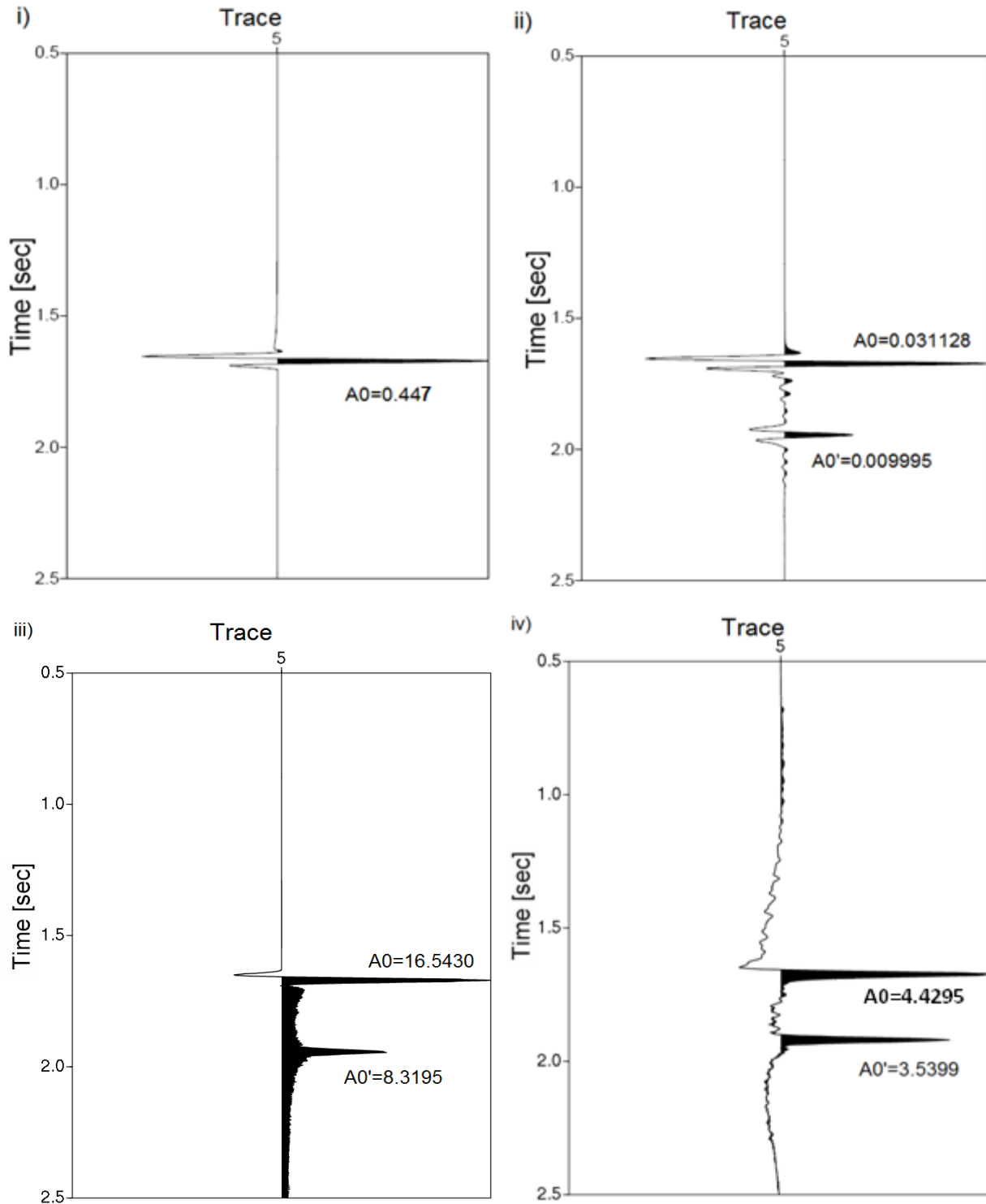


Figure 2.12a: Amplitude values for different modeling techniques at trace position 'a' for anticline. i) seismic trace ray tracing data, ii) seismic trace for Kirchhoff Helmholtz model, iii) seismic trace for modeling by demigration, and iv) seismic trace for modeling by demigration using SimPLI approach.

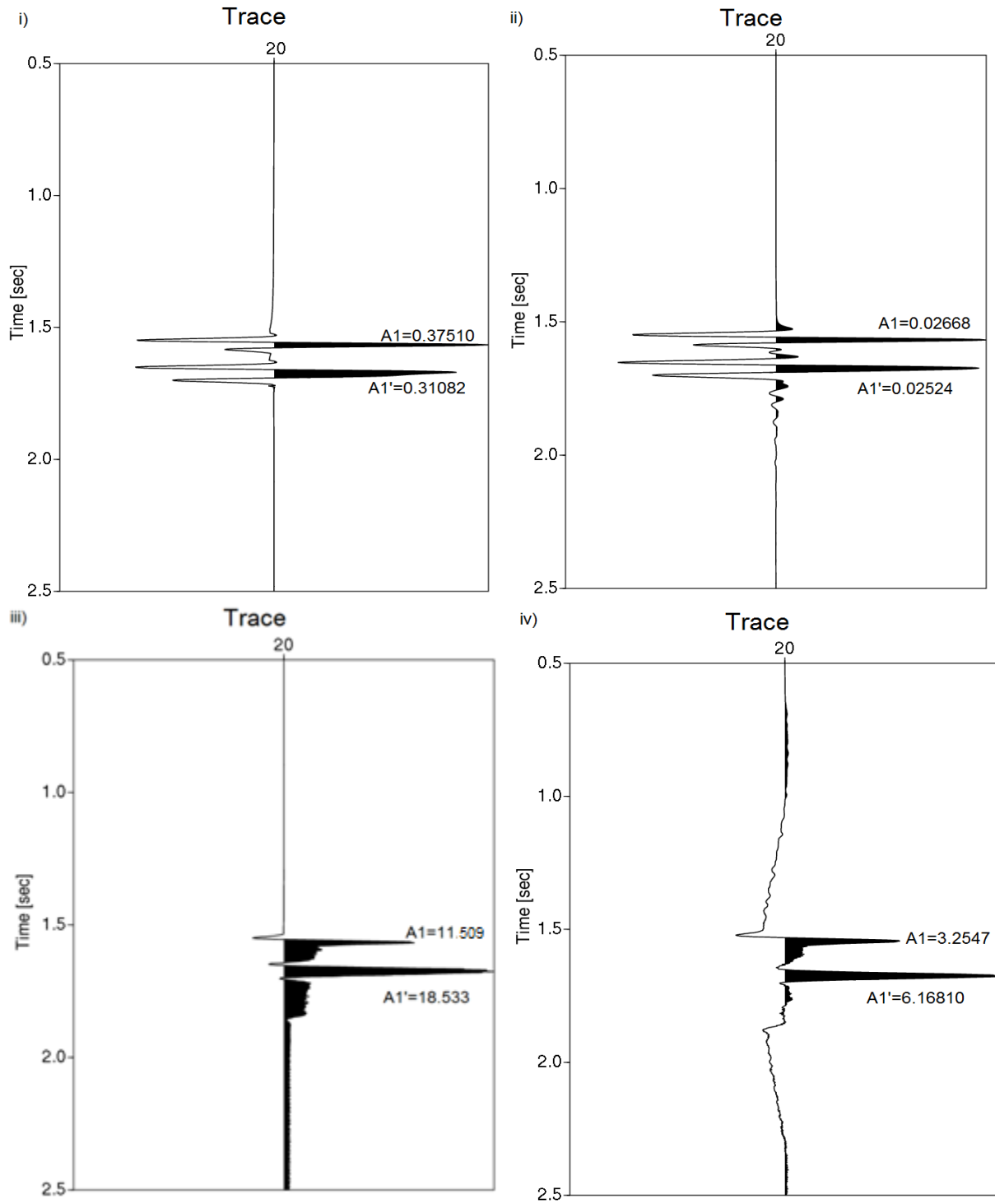


Figure 2.12b: Amplitude values for different modeling techniques at trace position 'b' for anticline. i) seismic trace ray tracing data, ii) seismic trace for Kirchhoff Helmholtz model, iii) seismic trace for modeling by demigration, and iv) seismic trace for modeling by demigration using SimPLI approach.

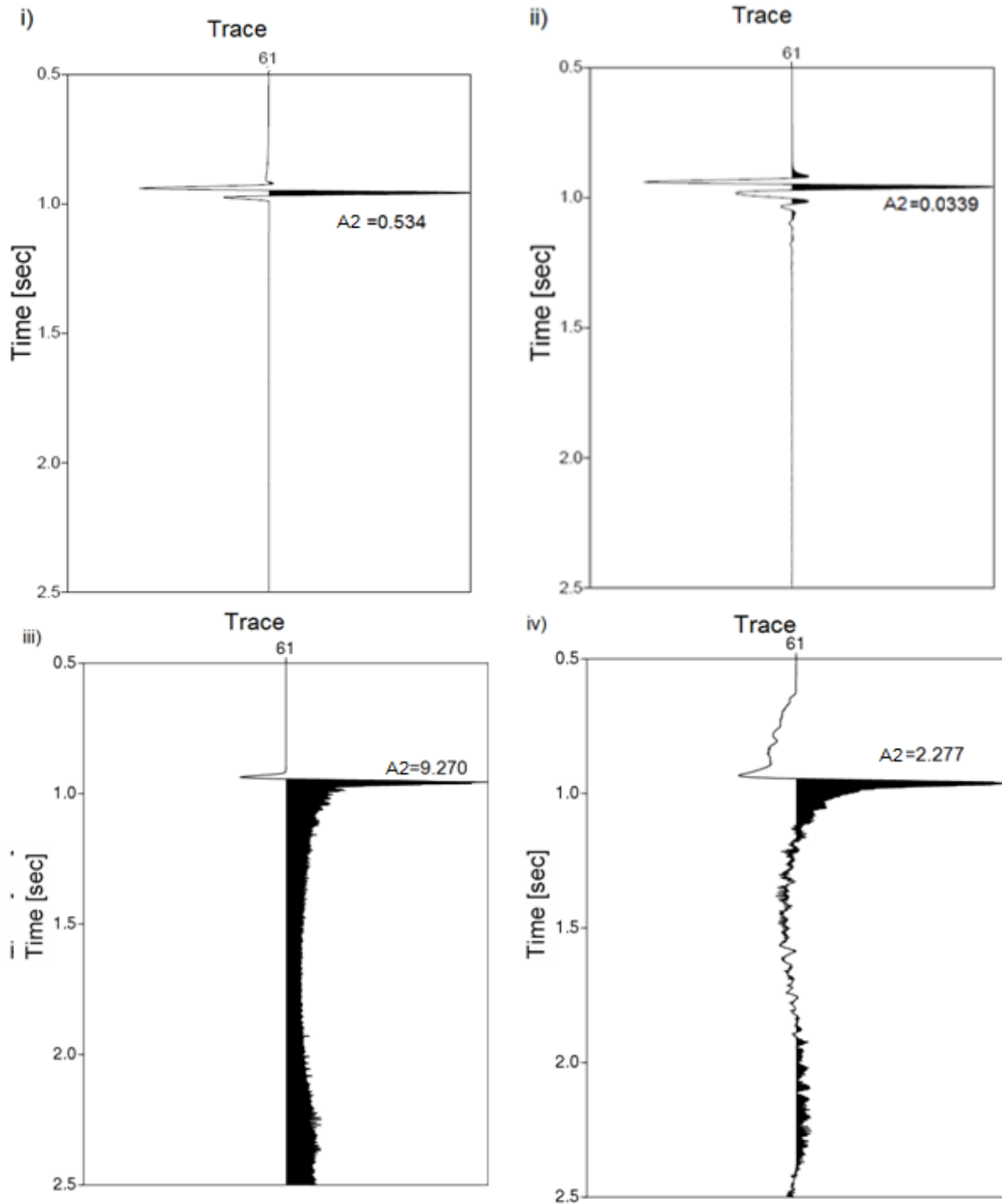


Figure 2.12c: Amplitude values for different modeling techniques at trace position 'c' for anticline. i) seismic trace ray tracing data, ii) seismic trace for Kirchhoff Helmholtz model, iii) seismic trace for modeling by demigration, and iv) seismic trace for modeling by demigration using SimPLI approach.

The trace location 'a' corresponds to the flank of the anticline structure (c.f. Figure 2.9). For trace location 'a' (c.f. Figure 2.12a) only the ray tracing data contains no later arrivals unlike the data obtained by the other modeling methods. For all other methods first arrivals possess larger amplitudes than the later arrivals. Although, both modeling by demigration results (conventional and the SimPLI approach) show later arrivals, the later arrivals exhibit only positive amplitudes. This can be due to the fact that the negative amplitudes are so weak that when the summation operation is performed these are dominated by the larger positive amplitudes. However, for the other two trace locations there are slight negative amplitudes for the later arrivals.

The location 'b' is located on the base of the anticline structure (c.f. Figure 2.9). For this trace location (c.f. Figure 2.12b) the picking is quite difficult due to the fact that different arrivals are merged together. In the Kirchhoff Helmholtz modeling the first arrival is stronger than the later arrival, similar with the ray tracing result. However, this is not the case for both modeling by demigration results.

For trace location 'c' (c.f. Figure 2.12c) located on top of the crest of the anticline there are no later arrivals.

Method	A1/A0	A2/A0	A1'/A0'
Ray Tracing	0,839018	1,200349	-
Kirchhoff Helmholtz Modeling	0,857106	1,089726	0,394216
Modeling by Demigration	0,695702	0,560358	0,448902
Modeling by Demigration (SimPLI)	0,734778	0,514054	0,573904

Table 2.3: Amplitude variations for different modeling methods at different time and trace location.

The ratio A1/A0 gives the correlation for the first arrivals between location 'b' and 'a'. All the methods have approximately the same ratio (0.69-0.86), which corresponds to small amplitude changes along the crest.

The ratio A2/A0 gives the correlation of amplitude variations from trace location 'c' to 'a'. The ratio for the ray tracing and Kirchhoff Helmholtz modeling method is more than 1.0 indicating higher amplitude values at the center than the flank of the anticline. The amplitudes become weaker towards the top of the anticline for modeling by demigration data, the ratio for both results is approximately 0.5.

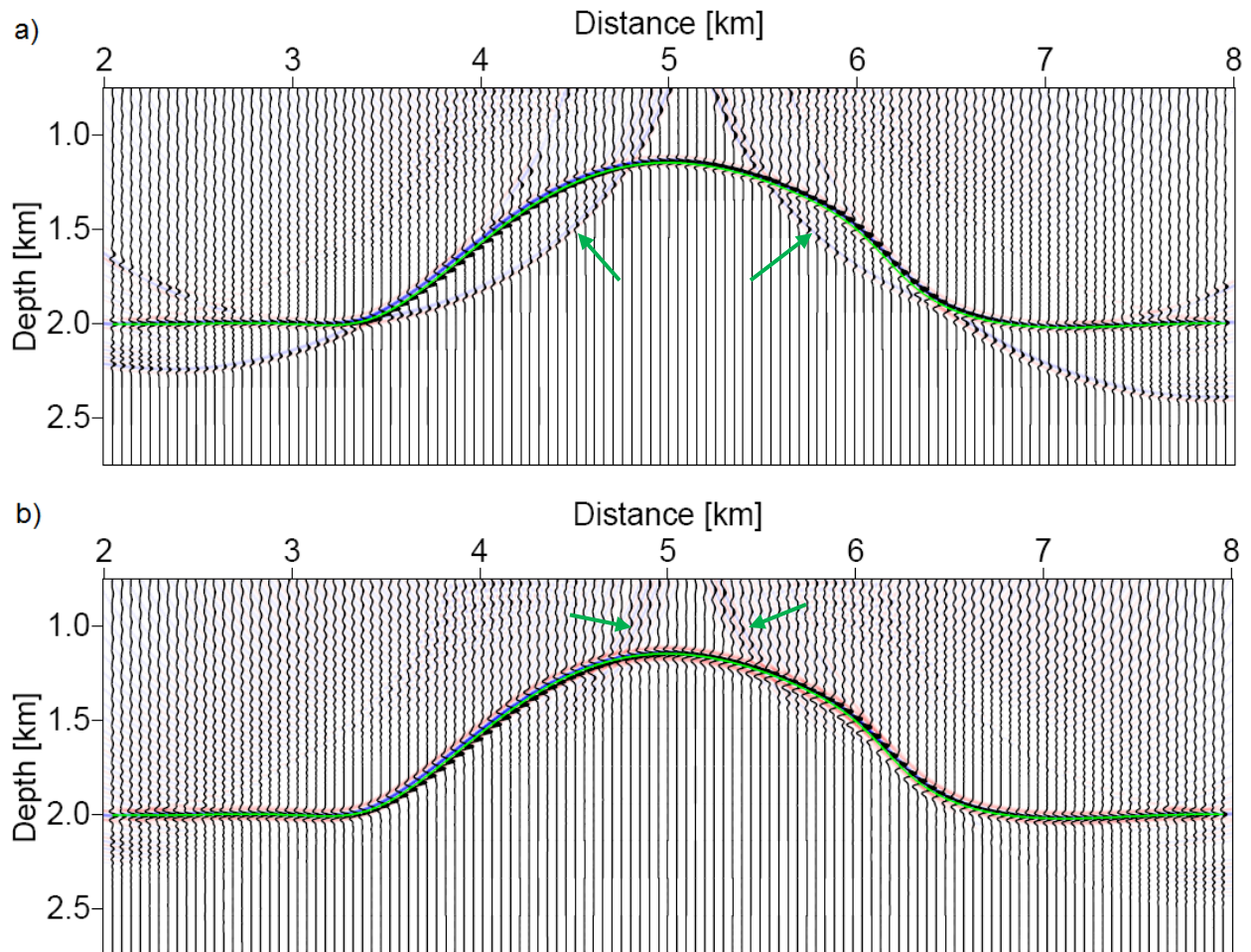
The ratio A1'/A0' gives the correlation of amplitude variations from trace 'b' to 'a' for the later arrivals. For the ray tracing there is no reference amplitude A0'. For all remaining modeling techniques the value of the ratio A1'/A0' ranges from 0.39 to 0.58. The ratio A1'/A0' for the modeling by demigration shows similar results as for the trace location 'c', this suggests that the amplitudes along the anticline limb get weaker towards the limb.

2.2.2.1 Migration Results

Using the ray tracing data as an input to migration, strong artifacts remain on the limb of the anticline, indicated by green arrows in Figure 2.13a. Although, the signal to noise ratio is slightly better for Kirchhoff Helmholtz data, still some residual noise can be observed on top of the crest of the anticline, indicated by green arrows in Figure 2.13b.

In the migrated images for modeling by demigration random noise can be seen on the flanks of the anticline structure. However, when compared to the Kirchhoff Helmholtz modeling the noise is slightly higher on the flanks of the anticline, indicated by green arrows in Figures 2.13c and 2.13d.

As the output from classical modeling by demigration contained some positive random noise on the flanks of the anticline, these are inherited in the migrated image. Similarly, for the SimPLI approach noise can be observed on the limb of the anticline. This is mainly due to the random negative noise on the modeled input data (c.f. Figure 2.11d).



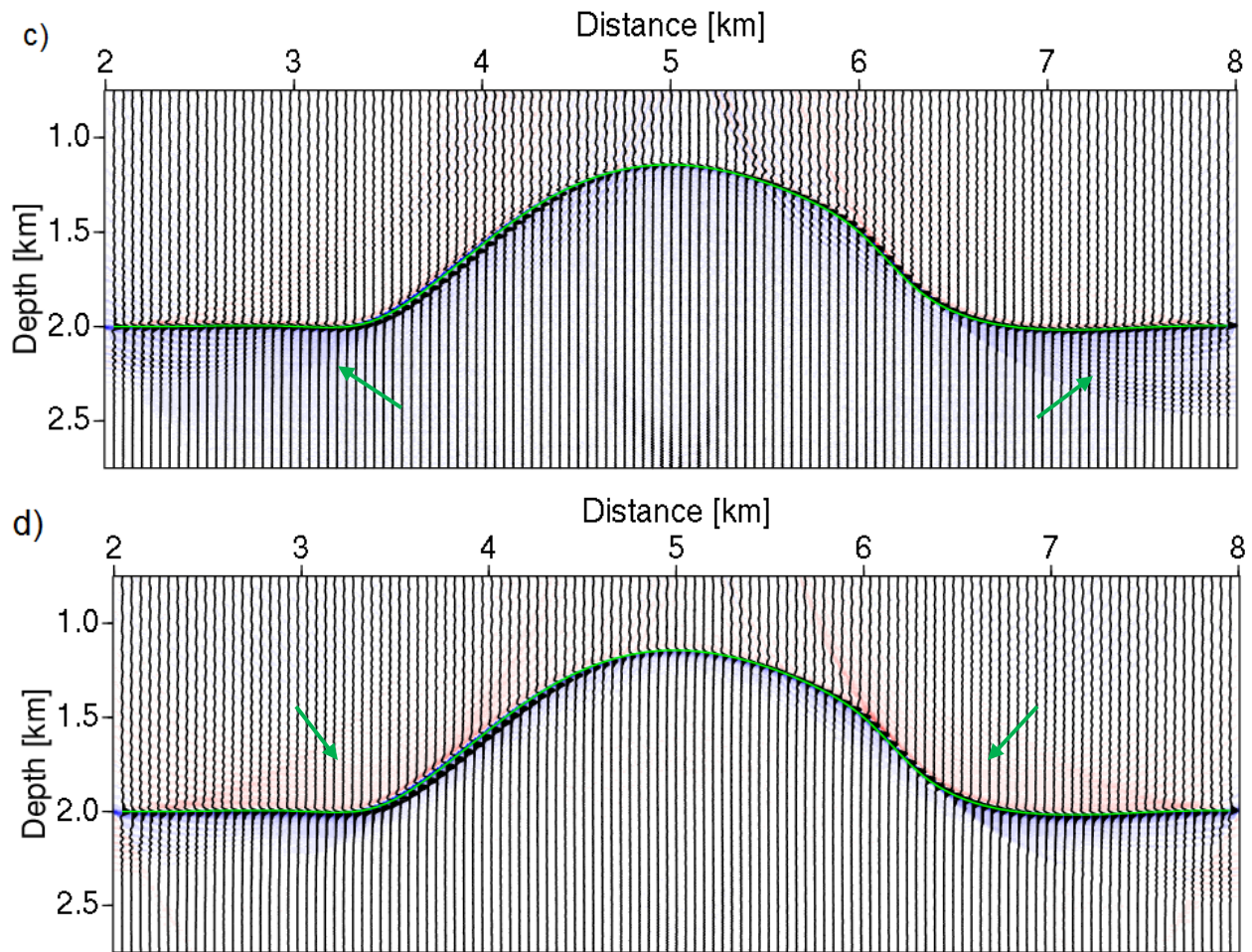


Figure 2.13: Migration result for different seismic modeling methods a) ray tracing, b) Kirchhoff Helmholtz model c) modeling by demigration, d) modeling by demigration using SimPLI approach. The green arrows represent the artifacts created by migration. Also shown is the anticline structure in green line.

2.3 Fault Model

In geology, a fault or fault line is a planar fracture in rock in which the rock on one side of the fracture has moved with respect to the rock on the other side. A model of a fault was created to observe the effects of diffractions from the fault edges. The model is a normal fault with a dip of 30° (c.f. Figure 2.14). In the case of this model the NIP tracer has been used which corresponds to a zero offset survey (exploding reflector type).

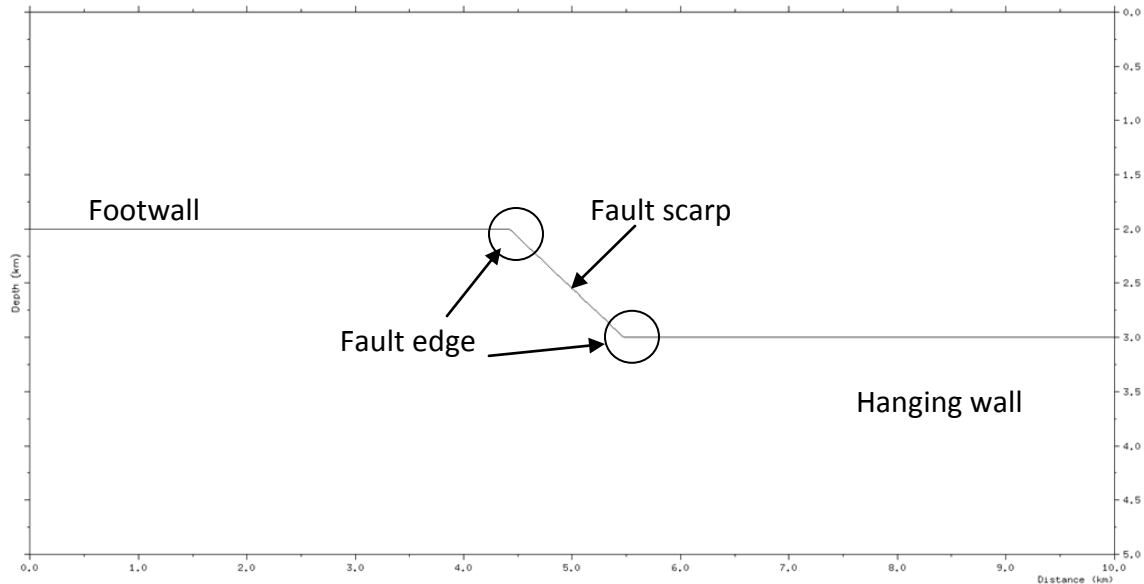


Figure 2.14: 2D view of the fault model also showing the encircled edge points where diffraction occurs. The different terminologies for the fault structure are also indicated.

2.3.1 Key Features

For a normal fault, an unmigrated section shows hyperbolic diffractions (c.f. Figure 2.15). These are produced due to the reflector terminations. The rock layers sharply terminating against a fault appear to cross with rock layers on the other side of the fault.

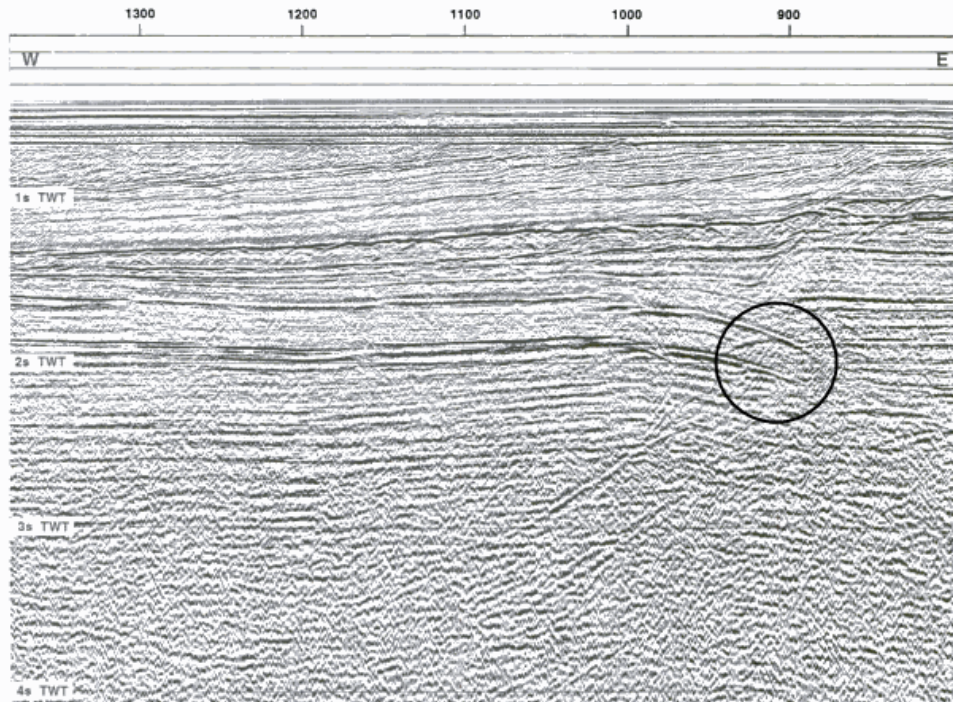


Figure 2.15: Unmigrated seismic section for fault, the key feature is circled (modified from Yielding et al., 2002).

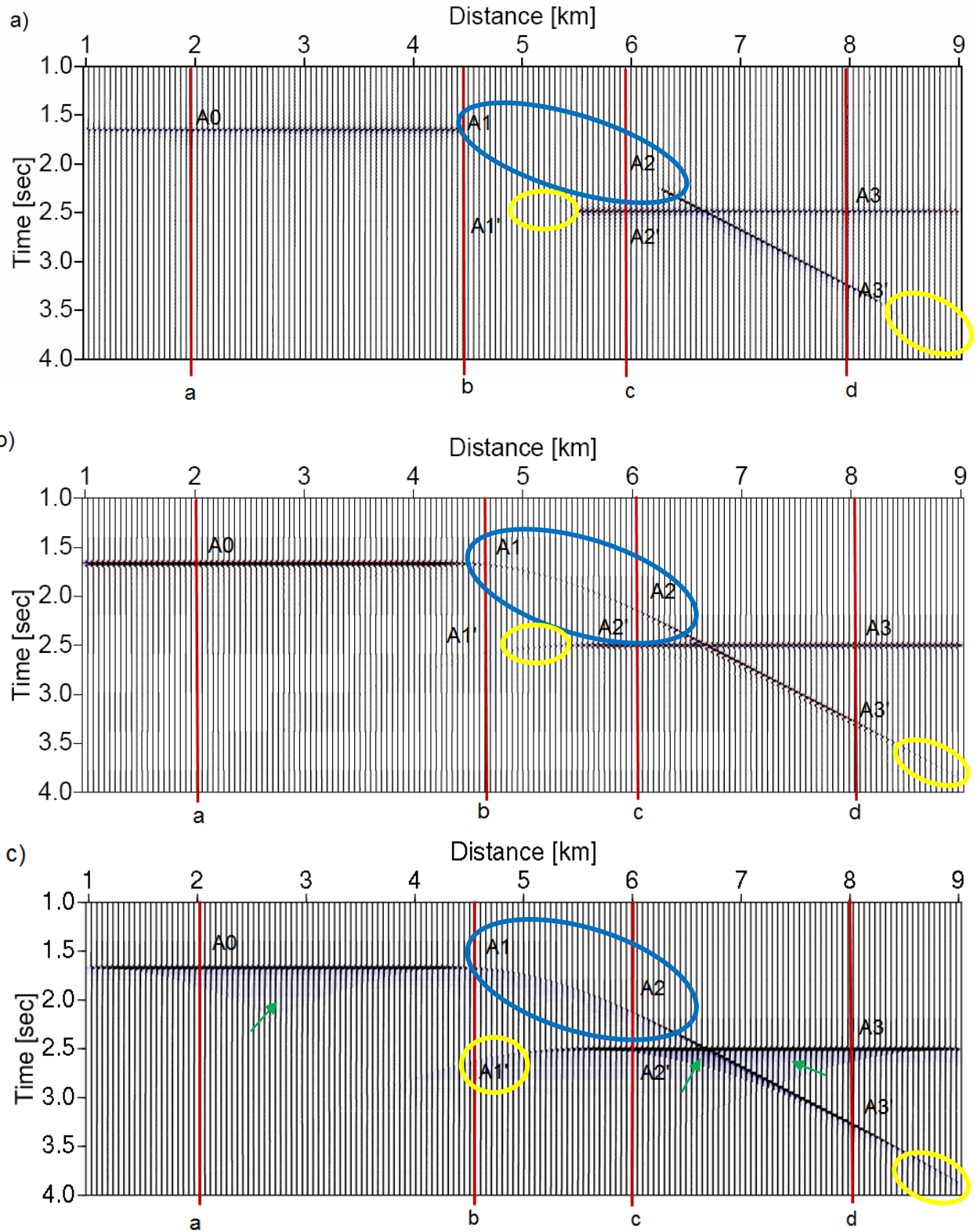
2.3.2 Seismic Modeling

In seismic modeling of the fault structure, the same procedure has been adopted as in the syncline and anticline structures. Figure 2.16 shows the results for the different modeling techniques. A visual inspection shows that all the seismic sections bear similar characteristics except for the ray tracing data.

The ray traced data will lack diffractions caused by the fault edges (indicated by blue circle in Figure 2.16a). By comparing diffraction effects with the other modeling methods it is clear that they resolve this in a better manner. The Kirchhoff Helmholtz modeling and both modeling by demigration approaches partially resolve the fault edge, although the amplitudes are very weak, indicated by blue circle in Figures 2.16b to 2.16d, respectively.

The tails of the fault structure are better resolved in the Kirchhoff Helmholtz modeling and modeling by demigration methods than the ray tracing method, which are in fact the fault scarp. This is indicated by the yellow circles in Figure 2.16b.

For both modeling by demigration results, the seismic section contains residual noise mainly due to the summation process (e.g. areas indicated by green arrows in Figures 2.16c and 2.16d). It can be observed as well that the noise associated with classical modeling by demigration has mainly positive amplitudes (blue color) on the lower side of the reflection. In comparison with the SimPLI type of modeling by demigration which has mainly negative amplitudes (red color) on the upper side of the reflection.



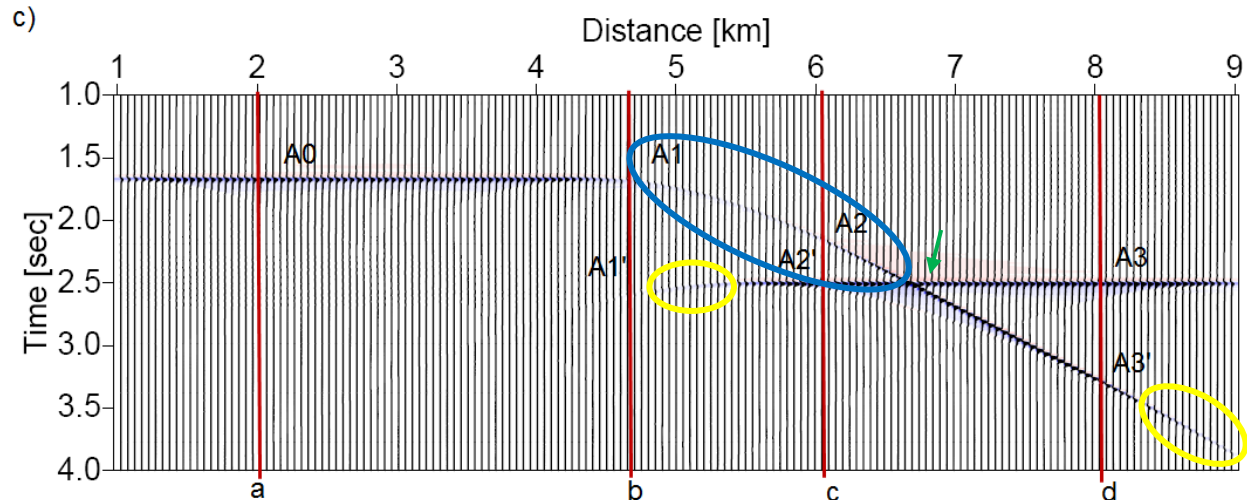


Figure 2.16: Synthetic data for fault model obtained by a) ray tracing with NIP tracer b) Kirchhoff Helmholtz modeling c) Modeling by demigration, d) demigration with input of migrated section obtained by SimPLI. Also shown is the location of the traces for amplitude picking in Figure 2.17.

For a detailed investigation on amplitude changes in the seismic data, I focused on four key locations marked by trace positions 'a', 'b', 'c', and 'd' in Figures 2.16a to 2.16d (indicated by red lines).

The modeling results for all trace locations are displayed in Figures 2.17a to 2.17d. On these, trace locations the maximum amplitude values were identified at selected locations along the four traces.

As already discussed, comparisons between absolute amplitude values are not feasible since the various prototype software are not well calibrated yet. Therefore, in this thesis only relative amplitudes at the key locations are considered, and summarized in Table 2.4.

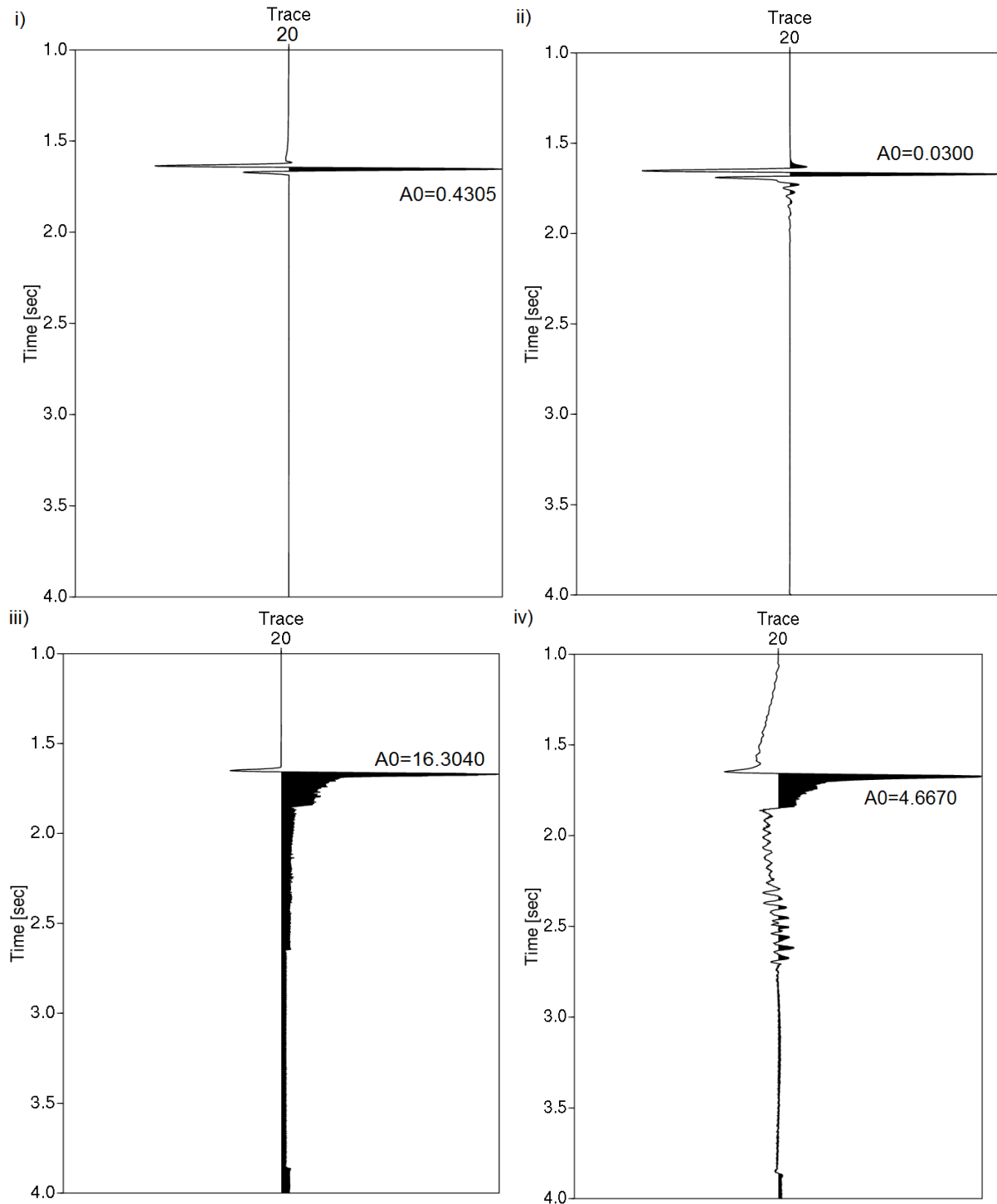


Figure 2.17a: Amplitude values for different modeling techniques at trace position 'a' for fault structure. i) seismic trace ray tracing data, ii) seismic trace for Kirchhoff Helmholtz model, iii) seismic trace for modeling by demigration, and iv) seismic trace for modeling by demigration using SimPLI approach.

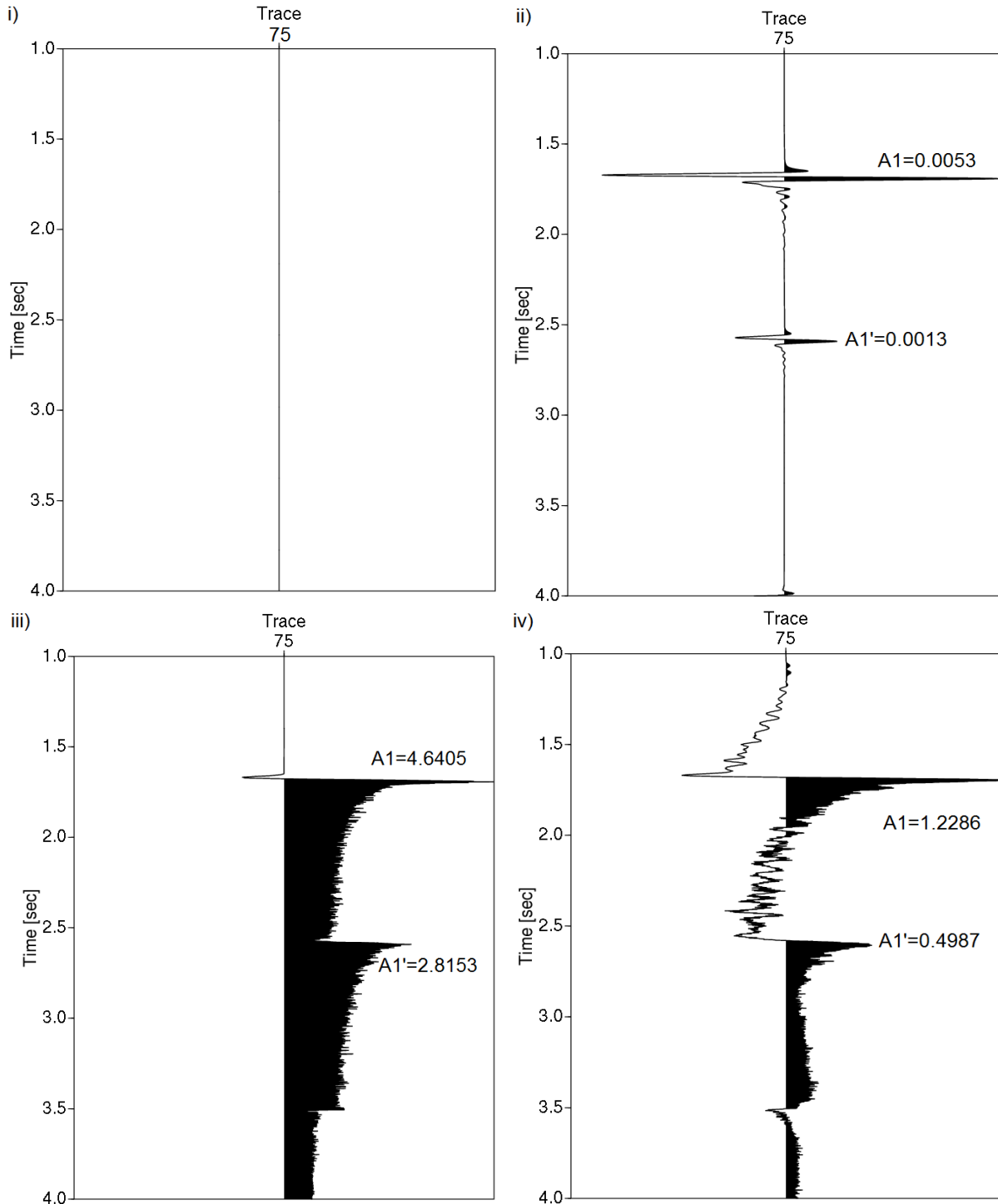


Figure 2.17b: Amplitude values for different modeling techniques at trace position 'b' for fault structure. i) seismic trace ray tracing data, ii) seismic trace for Kirchhoff Helmholtz model, iii) seismic trace for modeling by demigration, and iv) seismic trace for modeling by demigration using SimPLI approach.

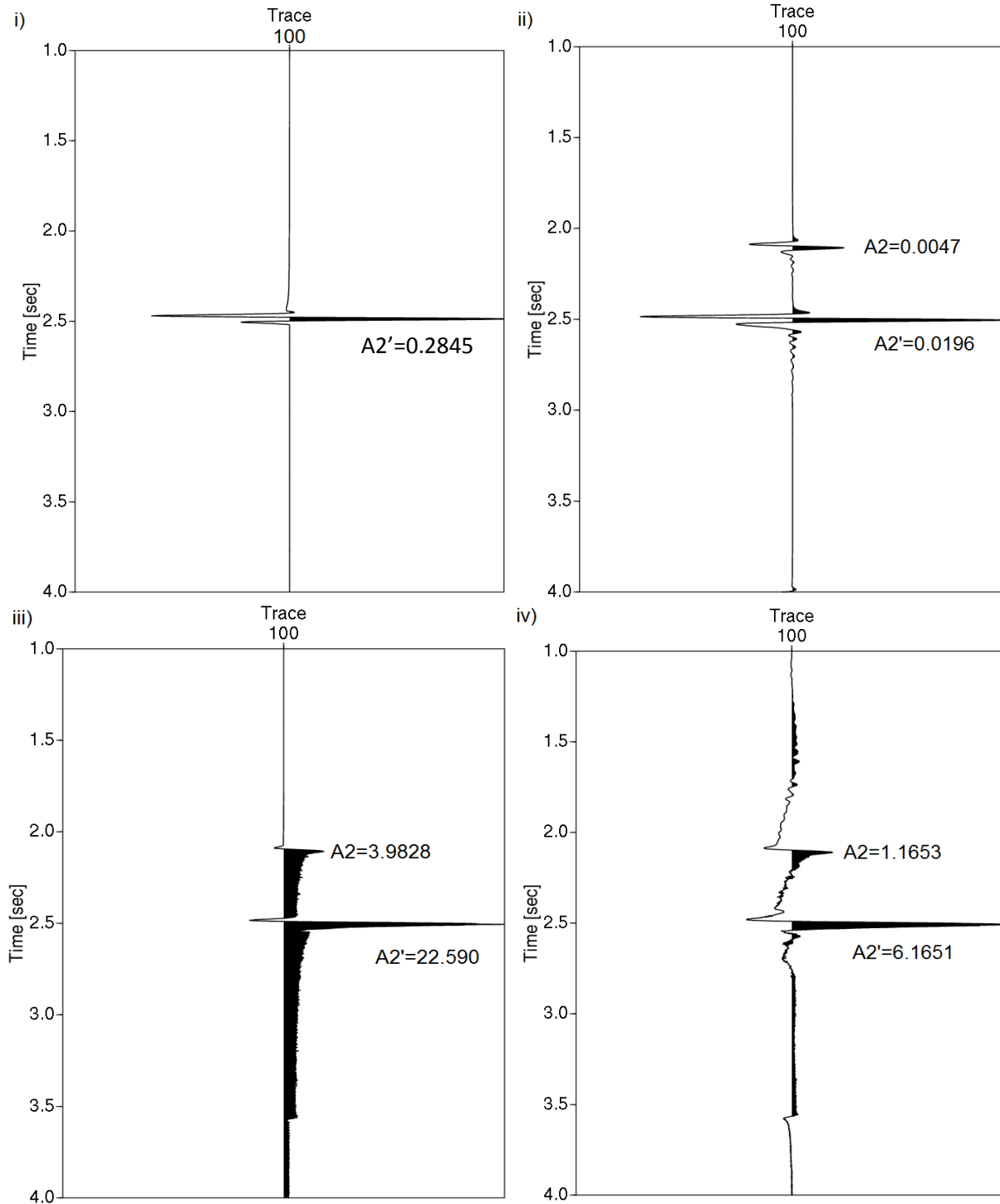


Figure 2.17c: Amplitude values for different modeling techniques at trace position 'c' for fault sstructure. i) seismic trace ray tracing data, ii) seismic trace for Kirchhoff Helmholtz model, iii) seismic trace for modeling by demigration, and iv) seismic trace for modeling by demigration using SimPLI approach.

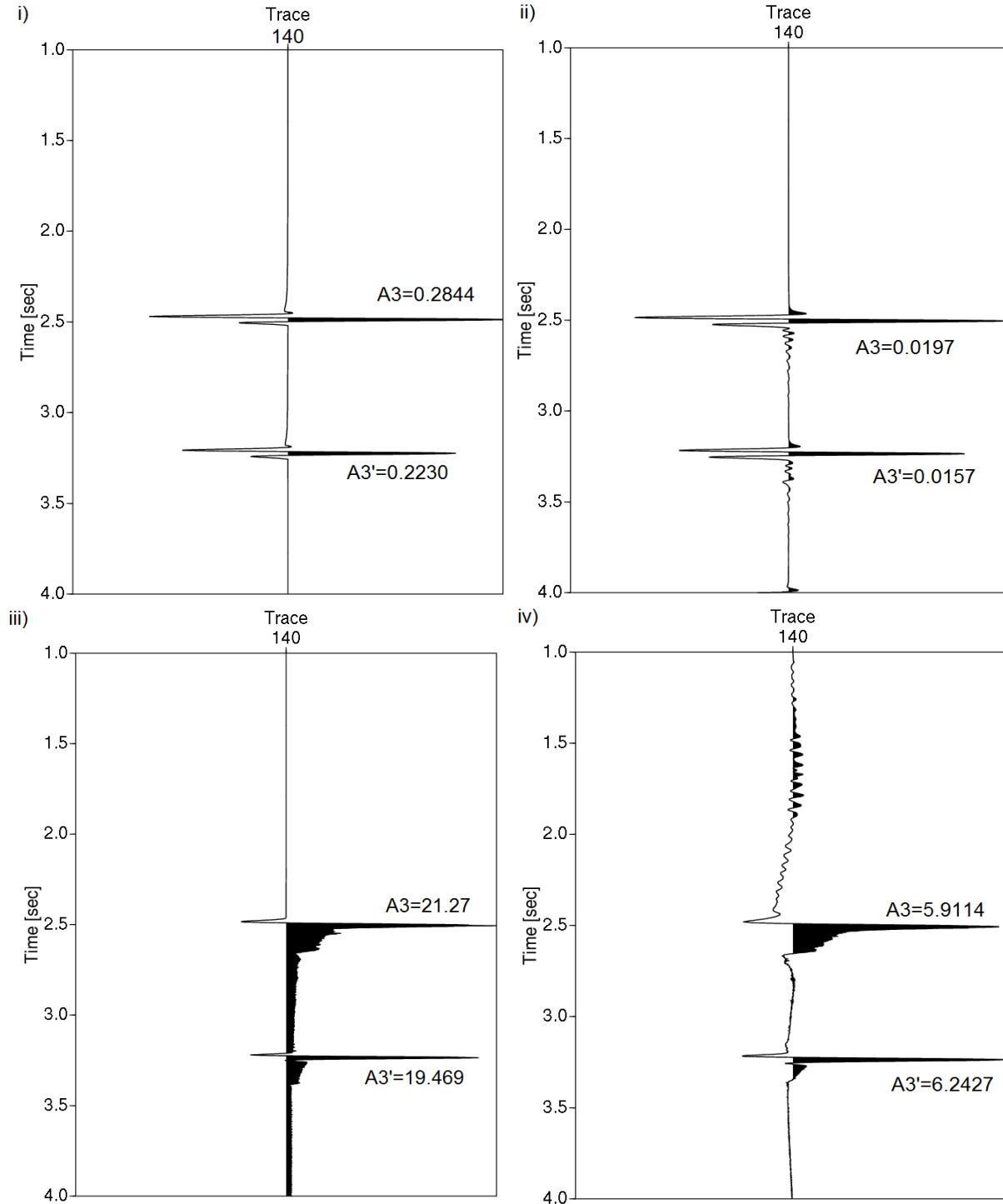


Figure 2.17d: Amplitude values for different modeling techniques at trace position 'd' for fault structure. i) seismic trace ray tracing data, ii) seismic trace for Kirchhoff Helmholtz model, iii) seismic trace for modeling by demigration, and iv) seismic trace for modeling by demigration using SimPLI approach.

For trace location ‘a’ (c.f. Figure 2. 17a), only first arrivals (A0) can be seen .This is because this location is present on the footwall of the fault (c.f. Figure 2.14). This area is represented by a flat layer resulting in only one peak response from the structure as expected.

In the case of location ‘b’ Figure 2.17b, the location is just on the fault edges (c.f. Figure 2.14). The response from the ray tracing method is as expected. However, for the Kirchhoff Helmholtz modeling and both modeling by demigration approaches a very dim response is seen. This indicates that they work somewhat better on the fault edge. It can also be seen that later arrivals are visible for both modeling techniques.

Figure 2.17c shows trace location ‘c’ located on the hanging wall of the fault (c.f. Figure 2.14). There are two main arrivals represented by A2 and A2’. As discussed earlier the ray tracing method cannot resolve the fault scarp, which causes no reflection to be seen at A2. The reflection from A2 can be seen in the Kirchhoff Helmholtz modeling and the modeling by demigration. The A2 arrival corresponds to the reflection from the fault scarp, the amplitude at this point is dim compared to the A2’ position.

The trace location ‘d’ (c.f. Figure 2.17d) refers to the location on the far part of the hanging wall. At this location, multiple arrivals can be seen. The first arrival A3 is larger in amplitude than the later arrival A3’. This is not true for the modeling by demigration using the SimPLI approach.

Method	A1/A0	A2/A0	A2’/A0	A3/A0	A3’/A0
Ray Tracing	-	-	0.660859	0.660627	0.518002
Kirchhoff Helmholtz Modeling	0.176667	0.156667	0.653333	0.656667	0.523333
Modeling by Demigration	0.284623	0.244284	1.40395	1.304588	1.194124
Modeling by Demigration (SimPLI)	0.263253	0.249689	1.320999	1.266638	1.337626

Table 2.4: Amplitude variations for different modeling methods at different time and trace location.

The ratio A1/A0 gives the correlation of amplitude variation from trace location ‘b’ to ‘a’. There is no such amplitude ratio for the ray tracing model. The ratio for the rest of the modeling methods is very low, which corresponds to large amplitude changes. In comparison with Kirchhoff Helmholtz modeling, the modeling by demigration shows better amplitude ratios indicating a more accurate result. The ratio A2/A0 is the correlation of amplitude variation from trace location ‘c’ to ‘a’. As for the A2/A0 ratio does not apply for ray tracing. For the other modeling methods it is similar to the ratio A1/A0, the reason being that the picked amplitude position lies under the fault scarp.

The amplitude ratio A2’/A0 is similar for ray tracing and Kirchhoff Helmholtz modeling with A2’ being less than the amplitude at the footwall of the fault. In case of modeling by demigration both cases show a high amplitude contrast, which corresponds to an increase in amplitudes toward the hanging wall. The ratio A3/A0 shows the same characteristics as A2’/A0 because both locations are on the hanging wall.

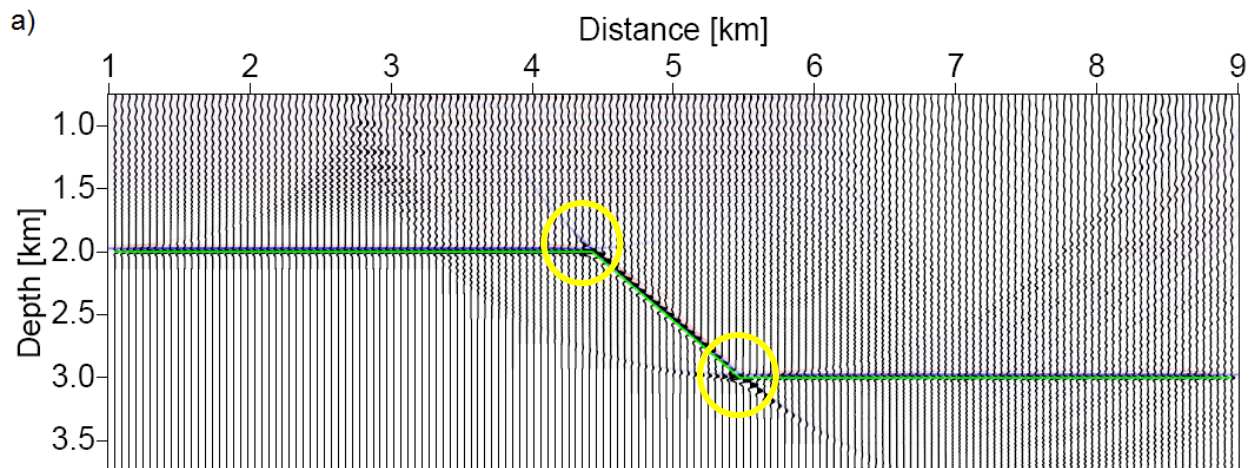
In case of the amplitude ratio A_3'/A_0 it shows decreasing amplitudes for Kirchhoff Helmholtz modeling. On the contrary, the values are higher in both modeling by demigration approaches, giving rise to the fact that the fault tail in Figures 2.16c and 2.16d have higher amplitude values than in Figures 2.16a and 2.16b.

2.2.1.1 Migration

The seismic results have been migrated using the IMAGING software (in house Kirchhoff PSDM software of NORSAR). The following discussion is mainly based on the visual inspection of the migrated images.

After migrating the ray traced data artifacts can be seen near the fault edges (shown by yellow circles in Figure 2.18a), which is due to the lack of proper diffractions in the input data. These artifacts are not visible on the Kirchhoff Helmholtz migrated image (c.f. Figure 2.18b).

Migration of modeling by demigration data shows similar characteristics as in case of Kirchhoff Helmholtz data. However, there are some artifacts seen on the lower fault edge (yellow circles in Figures 2.18c and 2.18d). Since the input data contained noise above and below the reflection, these contributions are mapped back as distortions using migration. The major noise contribution in classical modeling by demigration showed positive amplitudes and can be seen mapped on the corresponding migrated section on the lower part of the interface (indicated by green arrows in Figure 2.18c). In case of the SimPLI approach of modeling by demigration negative amplitude noise was observed (c.f. Figure 2.16d) and which is mapped along the fault scarp after migration (c.f. Figure 2.18d)



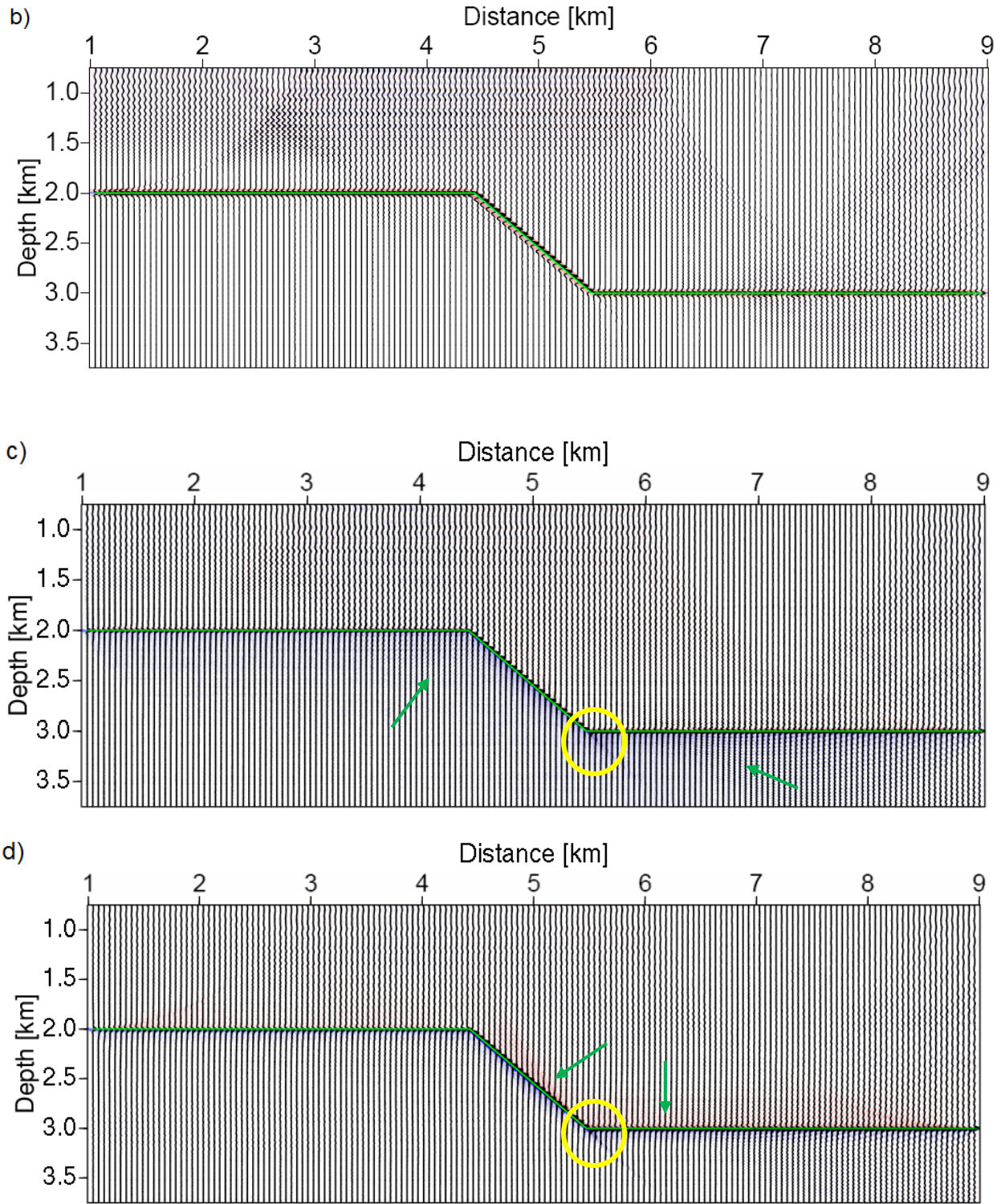


Figure 2.18: Migration result for different seismic modeling methods a) ray tracing, b) Kirchhoff Helmholtz model c) modeling by demigration, d) modeling by demigration using SimPLI approach. The green arrows represent the artifacts created by migration. Also shown is the fault structure in green line.

Chapter 3

Conclusions

Based on the simulations and discussion carried out in Chapter 2, some main conclusions can be stated:

- Standard ray tracing performed poorer when applied to complex structures as expected. This was noticeable at the steep limbs of the fold structures and at the fault edges, and was caused by the lack of diffracted and caustic energy.
- Kirchhoff Helmholtz (KH) modeling gave significantly better results than ray tracing, since this technique can handle complex curvatures associated with a given target horizon. The KH method was therefore used to benchmark modeling by demigration.
- Since modeling by demigration is based on the inverse integral of Kirchhoff, similar results as in case of KH are achieved. The results of this present study supported this main assumption, hence demonstrating the feasibility of this new modeling technique.
- Compared to the Kirchhoff Helmholtz technique, modeling by demigration is more efficient. KH modeling makes use of discretized versions of the interface(s), whereas modeling by demigration considers the complete geological structure as one volume when computing. The latter technique can be considered as a stacking process that smoothens the simulated reflection responses. Thus, there is no need to construct smooth reflectors.
- This study has investigated two possible implementations of modeling by demigration: the original version proposed in the literature and the one based on the SimPLI approach. SimPLI represents an efficient way of simulating PSDM images. It is demonstrated here that this new implementation of modeling by demigration shows promising results.

Due to the limited time frame of this study, proper calibrations of the different prototype software employed could not be included. This should be the topic of future work.

Appendix A

Workflow & Tools

This appendix gives an overview of the different software programs employed in this study, together with used workflows.

A.1 NORSAR-3D

NORSAR 3D Ray Modeling is a powerful tool to generate synthetic seismic data. The package can handle various types of realistic acquisition configurations; this can then be used to achieve optimal positions of seismic lines in data acquisitions (survey planning).

In the feasibility study of Modeling by Demigration NORSAR 3D was used both to create synthetic seismic data (using the ray tracing approach) as well as defining a set of controlled geological models. The workflow to create the models and data is shown in Figure A.1.

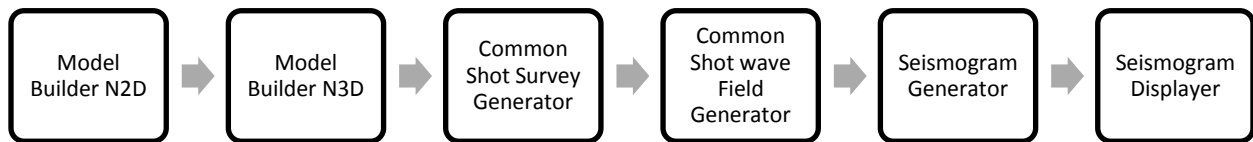


Figure A.1: NORSAR workflow from creating a 2D model to compute and display synthetic data.

Each step will be explained in more detail below.

A.1.1 Model Builder

With the Model Builder, a geological model could be created. First, the model geometry is constructed in NORSAR-2D. This is done by creating interfaces, either directly in converting depth, or by depth to time horizons. Interfaces the blocks of the model are defined. Next, geophysical parameters like P-velocity and density are assigned to each block (c.f. Figure A.2).

Figure A.2 shows a simple two-layer structure, separated by a syncline shaped interface. The chosen properties are represented by constant functions. P-wave velocity and density were directly specified, whereas the S-wave velocity was calculated from the constant ratio of $P/S=1.732$.

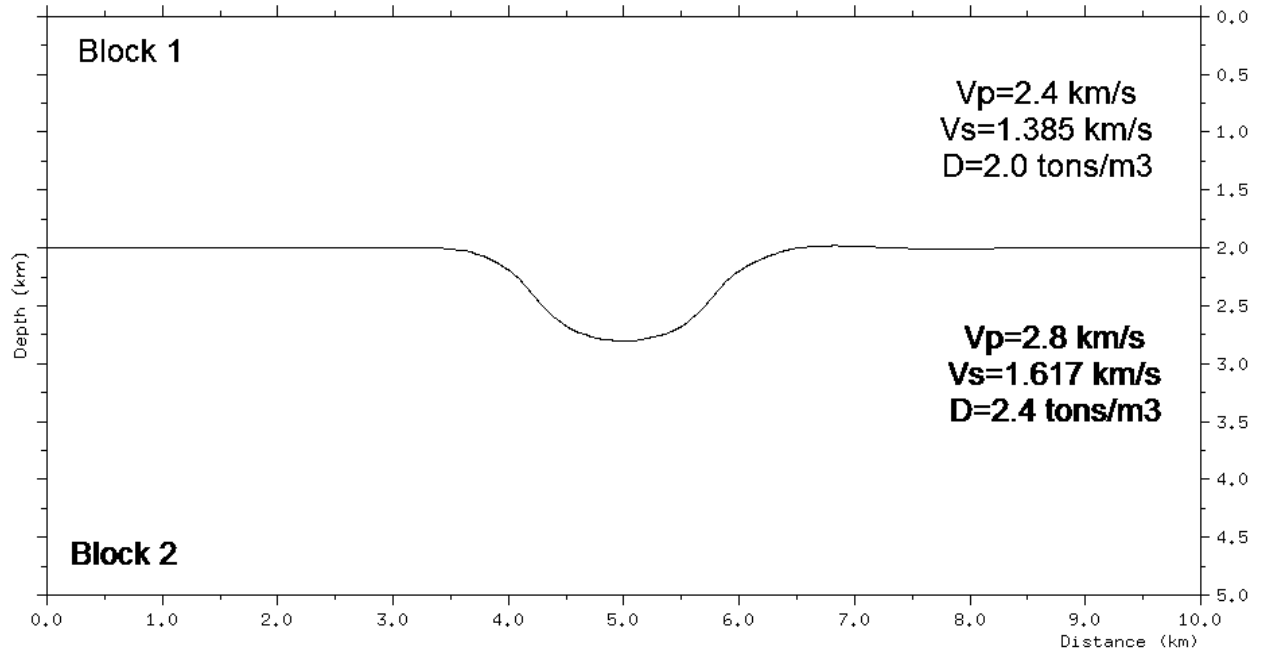


Figure A.2: Sketch of a simple syncline model along with the different material properties: P-wave velocity, S-wave velocity, and density.

A.1.2 Exporting and Importing a Model

The 2D model could then be exported using the SMIF utility in NORSAR-2D. In this way, a 2D model could be used to generate a 2.5D controlled model in NORSAR-3D, which later could be used in Kirchhoff Helmholtz modeling, and modeling by demigration.

A.1.3 Common Shot Survey

A zero offset survey was created using the Common Shot Survey. This option was used, because the Kirchhoff Helmholtz modeling software uses this survey geometry to create Green's functions. The survey was created using a sample interval of the shots of 50m. Figure A.3 shows the parameters used to create the survey. In Figure A.4, the actual zero offset rays are shown associated with this survey.

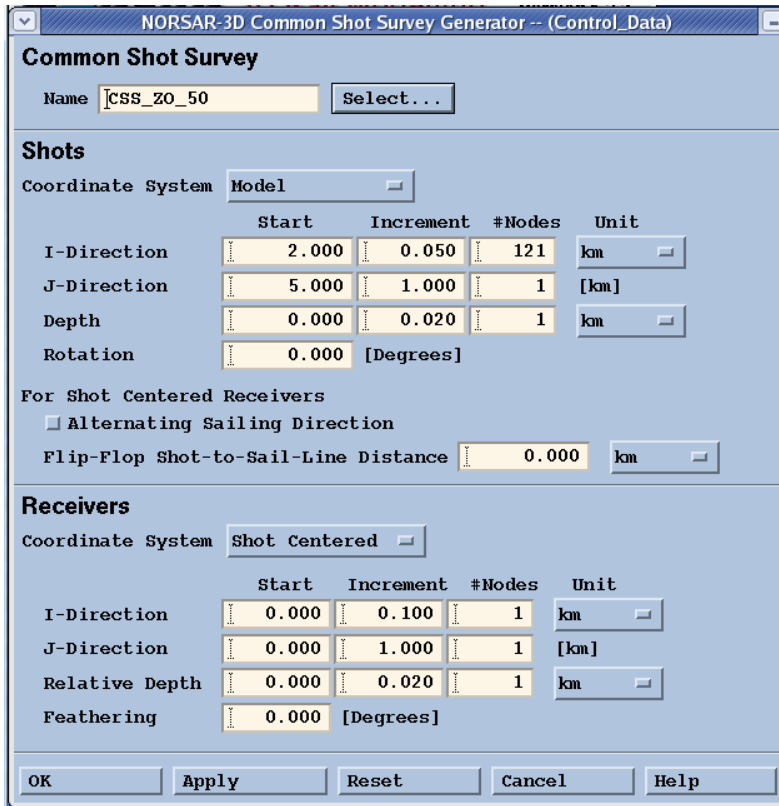


Figure A.3: Parameters used in creating a zero offset survey (shot point interval of 50m).

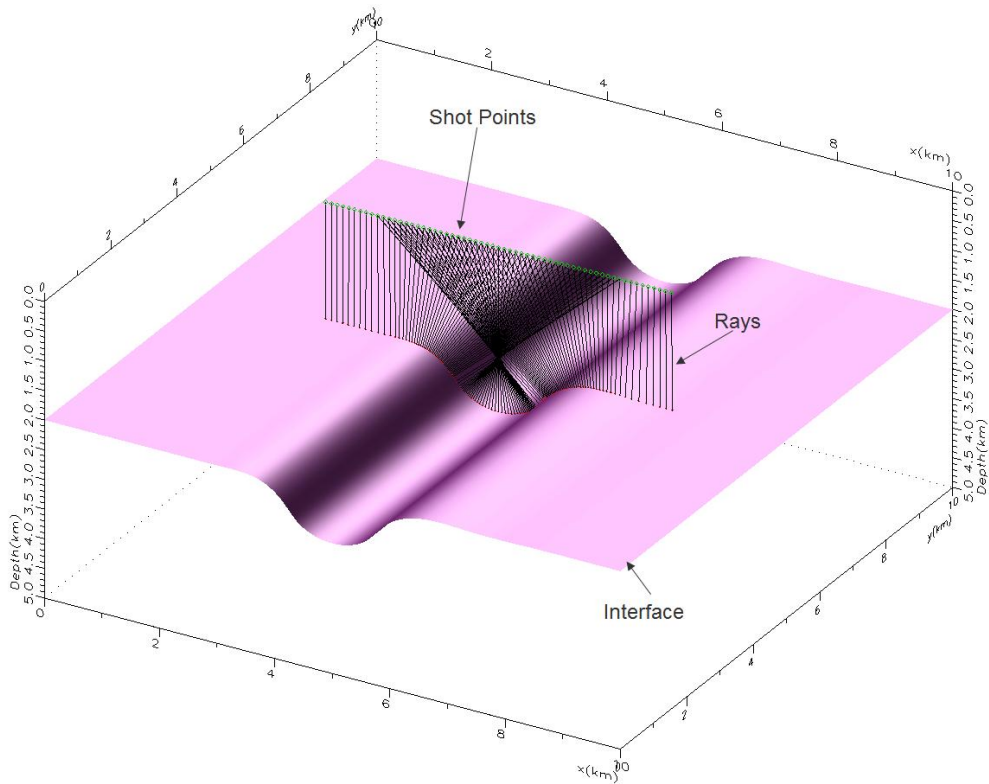


Figure A.4: A 3D view of rays for a zero offset acquisition.

A.1.4 Common Shot Wavefront Tracer

The discussion below is summarized from the NORSAR-3D, User's Guide 5.3, 2008.

The purpose of the Common Shot Wavefront Tracer is to simulate selected parts of the seismic wave-field from a number of shots to a number of receivers. The Common Shot Wavefront Tracer is an implementation of the Wavefront Construction concept developed at NORSAR. This is a modeling method based on ray tracing, but rather than tracing individual rays, the whole wave-field is propagated for the types of rays of interest. The restrictions with respect to the smoothness of the model and the frequencies of the source signal are the same for the Wavefront Tracer as for conventional ray tracing.

The Wavefront Construction method mimics true wave propagation in the sense that entire wavefronts are propagated time-step by time-step to create a 'moving surface' that passes through the model. A triangular mesh with a ray at each node is used to represent the wavefronts. Standard dynamic ray tracing is used in tracing rays from one wavefront to the next. The spatial sampling density of the wavefront is sustained by interpolation of rays in the network. Figure A.5 shows the wavefronts generated at time intervals of 0.4s, 1.0s and 1.8s from a source placed at the center of the survey (shot point 61).

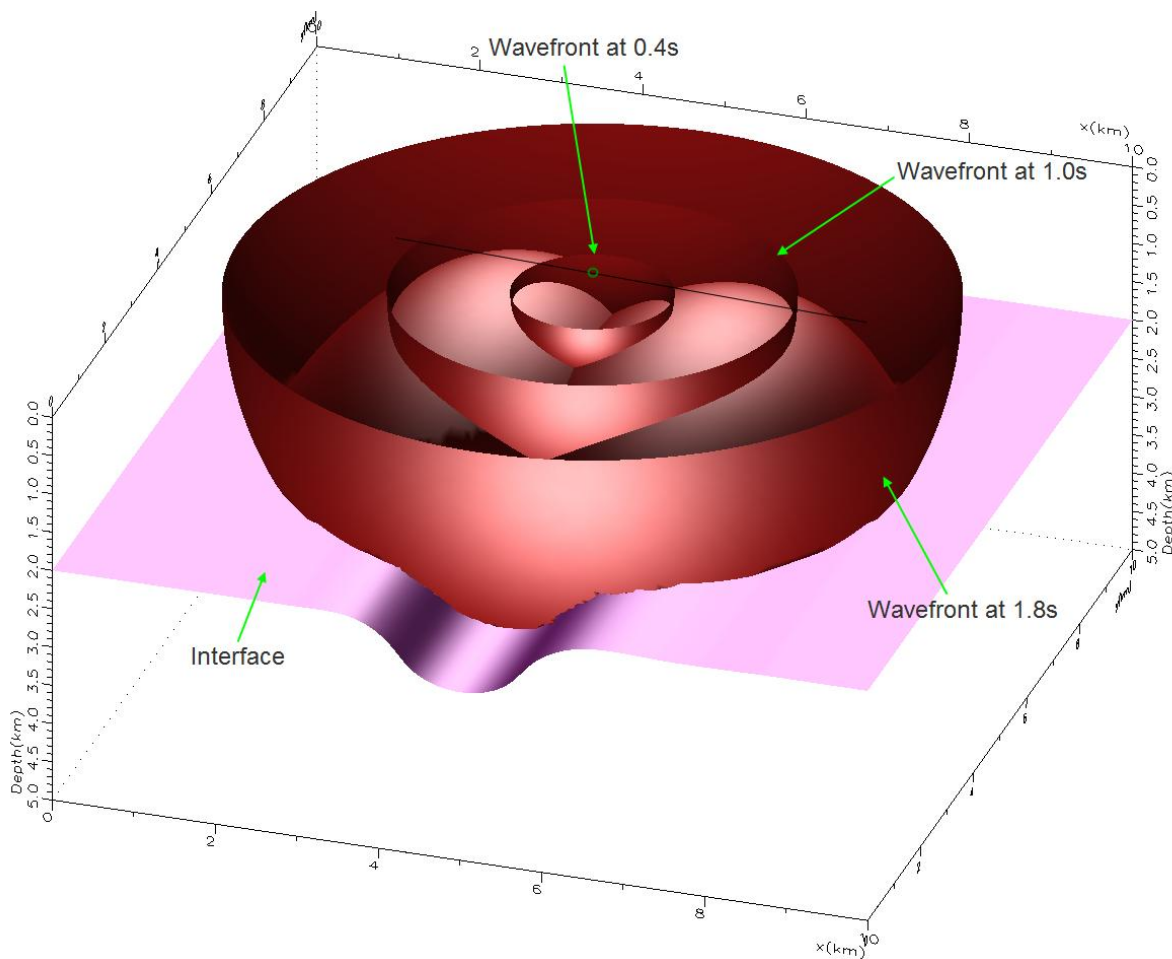


Figure A.5: Wavefront at different time intervals for the syncline model.

A.1.4.1 Input to the wavefront modeling

In order to do modeling, three data elements have to be defined within the Wavefront Tracer

1. Model
2. Survey
3. Ray Codes

Model

The model is made in the NORSAR-3D Model Builder. It consists of triangulated interfaces (TriMeshes) with smooth property (velocity and density) functions in-between. P-wave and S-wave velocity and density are required to do wavefront tracing.

Survey

The Survey is defined in the Survey Generator. Some survey parameters may be modified as the survey is loaded into the Wavefront Tracer, in particular the depth of shots and receivers may be changed to follow horizons in the model.

Ray codes

A Ray Code specifies in broad terms the paths for the rays through the model. Primary reflections, multiples, mode conversions (e.g. P- to S-wave) can be defined. The ray codes are defined in the User Interface and may be stored on a ray code file for later use.

Event set

The result of a modeling job in the Interactive or Batch Tracer is an Event Set. Event Set there consists of one Event File for each shot. An Event is an arrival from a shot to a receiver, corresponding to one particular ray. For each Event a number of parameters, called Event Attributes, are stored on the Event file.

The Event Attributes (traveltime, amplitude coefficients, etc.) for one or more arrivals at the receiver positions are found by interpolation from the wavefronts. When the wavefront encounters an interface in an open ray model, the material property functions on the departing side of the interface are used in the tracing to the next interface. The Wavefront Construction method is also used in the zero offset case (NIP, exploding reflector), where the interfaces in the model are 'exploded' and propagated to the surface as wavefronts.

Figure A.6 shows the complete workflow adopted in the common wavefront tracer.

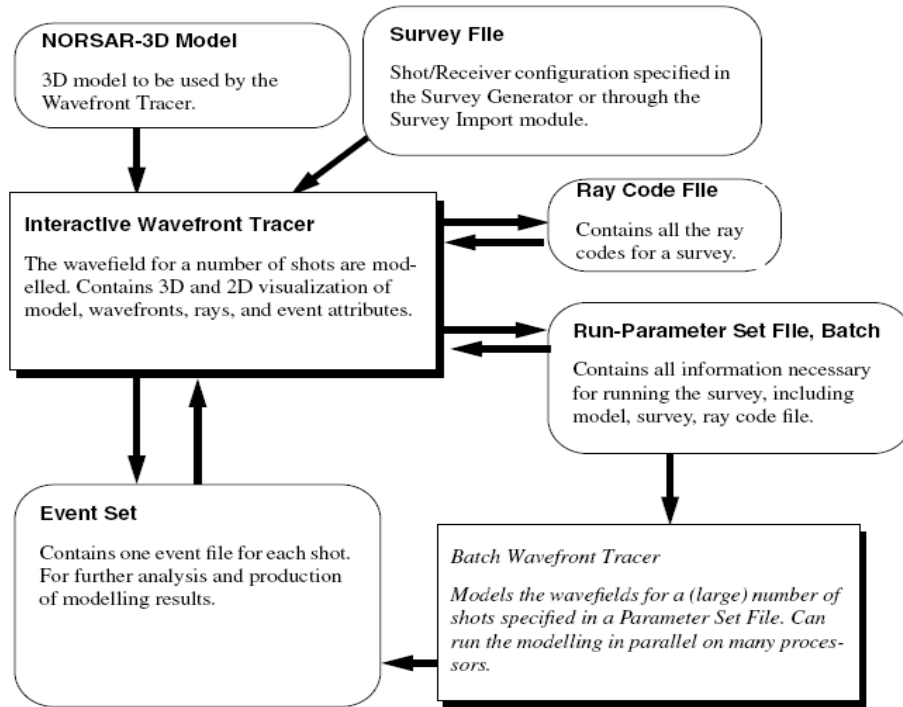


Figure A.6: Workflow adopted in Common Wave Front Tracer (NORSAR3D, User's Guide 5.3, 2008).

A.1.5 Seismogram Generator

The Seismogram Generator enables the user to create and plot synthetic seismograms. The unit consists of two modules -one for generating the seismograms and one for displaying them.

After creating the Event Trace by the ray tracer, the event file was used to create seismograms. The reflection coefficient obtained was convolved with the chosen wavelets, for example here a Ricker wavelet with a center frequency of 20Hz. The resulting seismogram for the syncline model was then plotted using Seismic Unix, 2008 (c.f. Figure A.7).

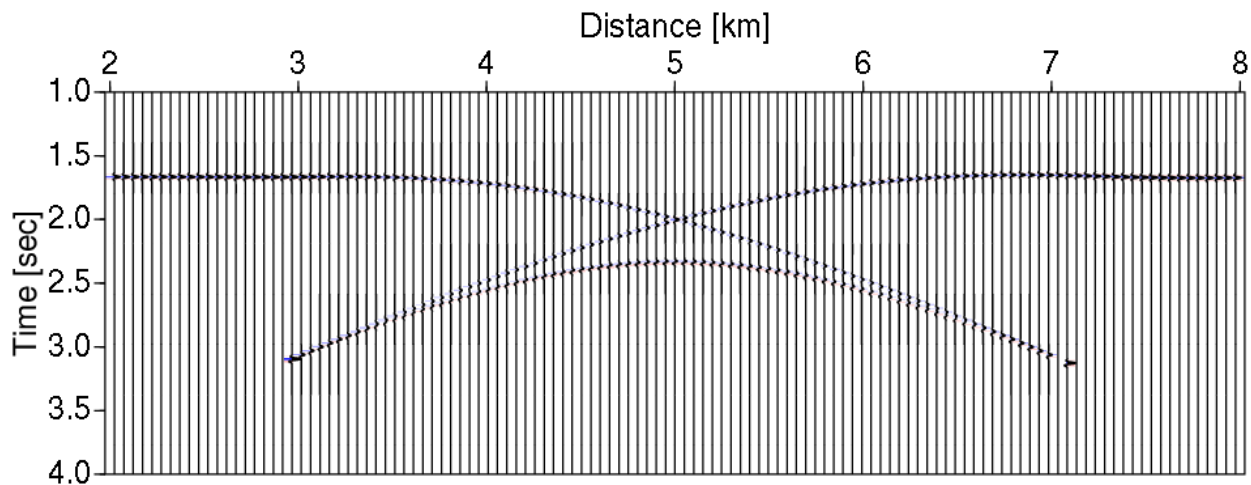


Figure A.7: Generation of synthetic seismogram using a Ricker zero-phase pulse with a center frequency of 20Hz.

A.2 Kirchhoff Helmholtz Modeling

The discussion below is summarized from the Kirchhoff Helmholtz, Basic theory and tutorial, 2007 and by hands on experience.

The Kirchhoff Helmholtz (KH) modeling technique is based on a numerical implementation of the Kirchhoff Integral. The Kirchhoff integral provides a robust method for implementing both seismic modeling and prestack depth migration, and can handle lateral velocity variations and turning waves. The modeling and migration algorithms require a smooth velocity function; therefore, a constant velocity is used in each layer.

The purpose of KH modeling is to obtain reflection seismograms that are more accurate/realistic than those obtained by classical ray tracing. Necessarily, the computational cost is higher, than but not as high as for the pure wave equation techniques based on finite difference.

Ray theory still forms the basis of the modeling, and hence many advantages are inherited, such as the selection of specific events. In order to model the reflection response of a chosen interface, rays are traced to that interface from both the sources (source field) and the receivers (receiver field) (i.e. computation of Green's functions).

The pre- and post-reflection ray paths in the overburden do not necessarily have to be direct waves (pure transmissions) but to make simple understanding of the results obtained direct P waves have been used here. Especial care has to be taken to make both source and receiver fields as complete and single valued as possible to reduce shadow zones. KH modeling is perfectly suited (and especially designed) to model caustics and diffractions caused by the shape of the reflector itself, this can be seen from the different cases considered in this thesis.

The workflow adopted in creating the seismogram is illustrated in Figure A.8.

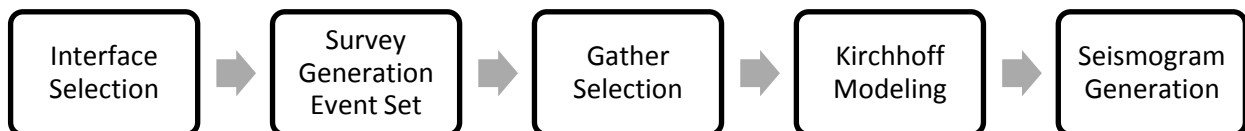


Figure A.8: Workflow used to create seismograms by Kirchhoff Helmholtz modeling.

A.2.1 Interface Selection

In the first step the Model is selected, this is the same NORSAR-3D model as used in ray tracing. Here, the syncline model will be employed for demonstration purpose. After selecting the desired model, the subsequent target horizon/interface to be modeled is selected (c.f. Figure A.9).

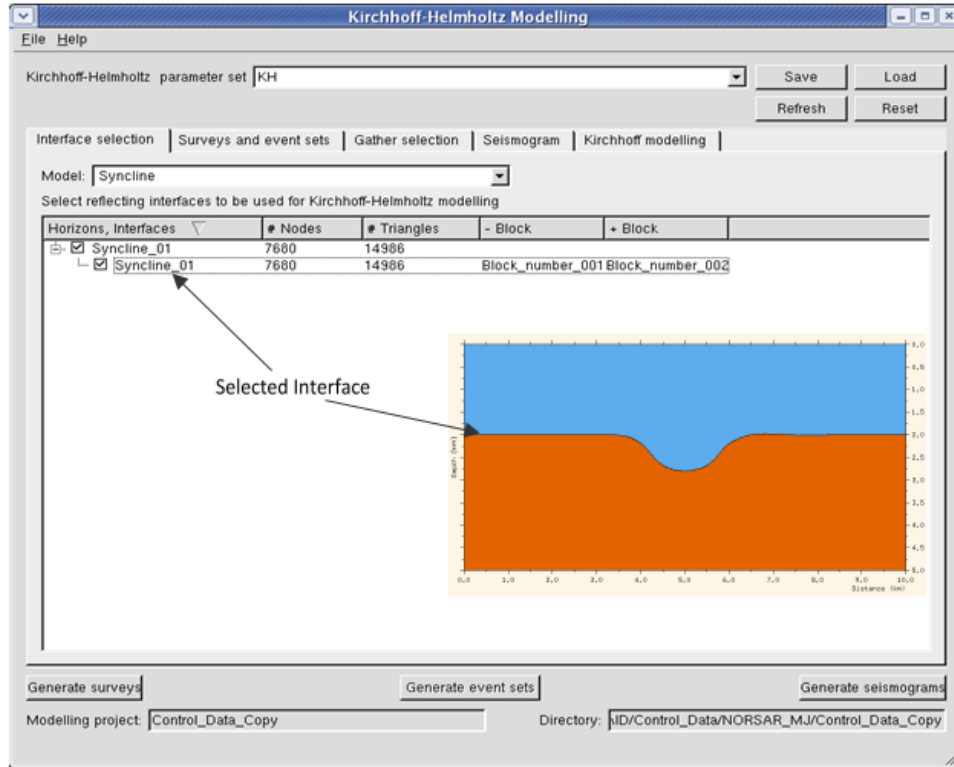


Figure A.9: Selection of Model and Interfaces in Kirchhoff modeling, also showing the selected interface.

A.2.2 Survey and event sets

The drop down box at the top is used to select a survey for the modeling project. Not all types of survey are allowed currently, and an error message is provided if an illegal choice is made. Special surveys were created using NORSAR-3D in which the Source/Receiver spacing was kept constant. For the calculation of the seismograms, it is necessary to evaluate the source and receiver wave fields along the desired interfaces (Green's function computations). These are calculated using the wavefront tracer and specific "virtual" surveys. The names of these surveys are set automatically and were named according to the Parameter Set saved "KH" (c.f. Figure A.10).

The events for both the source and receiver side were generated using NORSAR-3D common shot wavefront tracer.

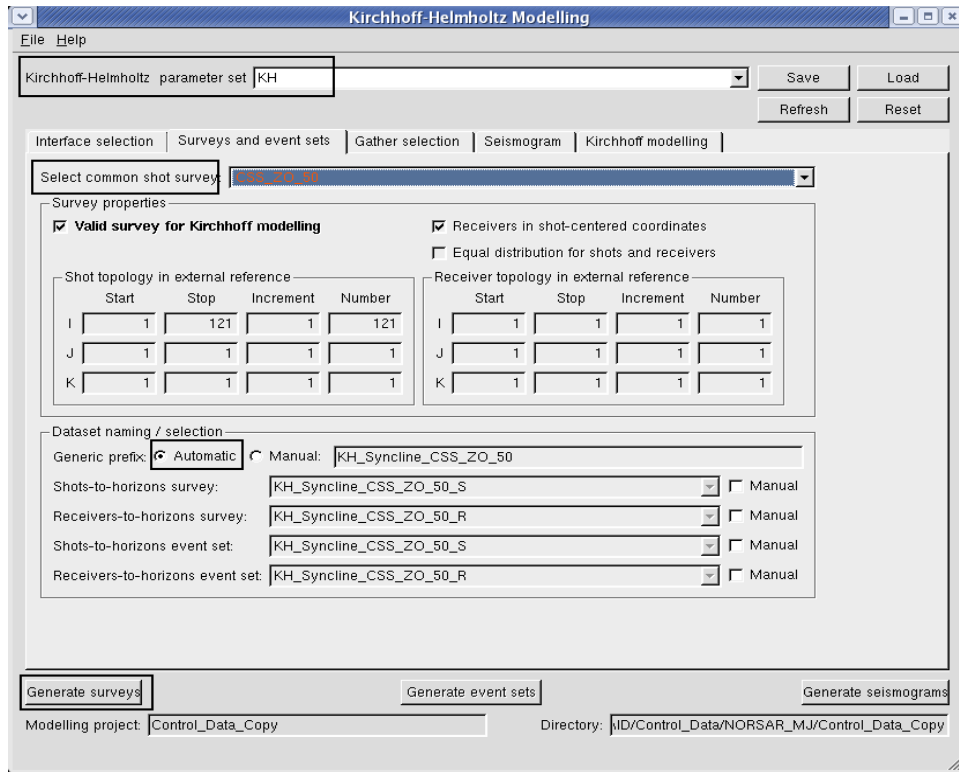


Figure A.10: Creation of virtual surveys for source and receiver and settings used for corresponding Events.

The survey design for the shots to Horizon survey is shown in Figure A.11. Crosses indicate the 121 shots (zero offset setting) and the rays generated for one fixed shot point are shown. The receivers in this case are placed along the chosen interface.

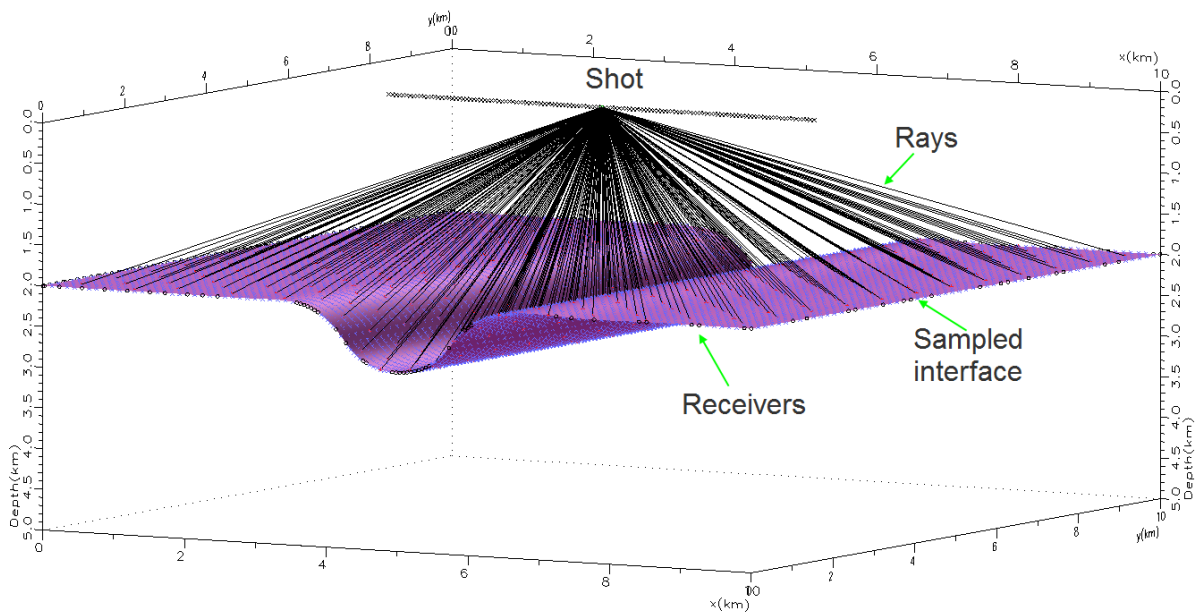


Figure A.11: Shot to Horizon virtual survey setting in NORSAR-3D, the blue cross represents the receivers; the pink is the sampled interface. The sampled rays correspond to one shot point position.

A.2.3 Gather Selection

In this step, the traces to be calculated are chosen. In all the cases the “Volume Gather” option has been used; with all Shots and Receivers selected (c.f. Figure A.12). Since the receiver distribution extends in three directions and the shot distribution extends in one direction, the total space defined by the traces is three-dimensional. The total number of traces in this example is 121.

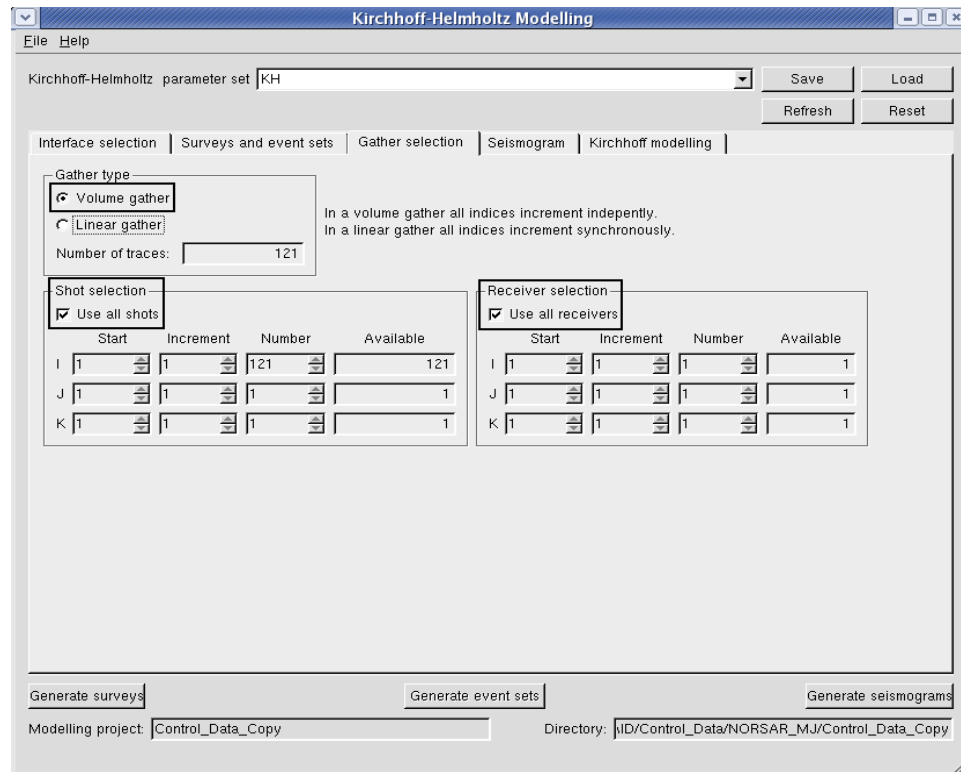


Figure A.12: Setting used in Gather Selection.

A.2.4 Seismograms

The sampling parameters of the desired traces are selected, as well as the output components desired. The source is assumed to be an impulse (explosive). The “pressure” component is currently simply the length of the displacement vector.

A Ricker wavelet with a center frequency of 20Hz is used to create the seismogram. The time sample interval is 2ms. The parameters used in the generation of the synthetic data are shown in Figure A.13. The saved file was displayed using different types of software e.g. Seismic Unix, 2008.

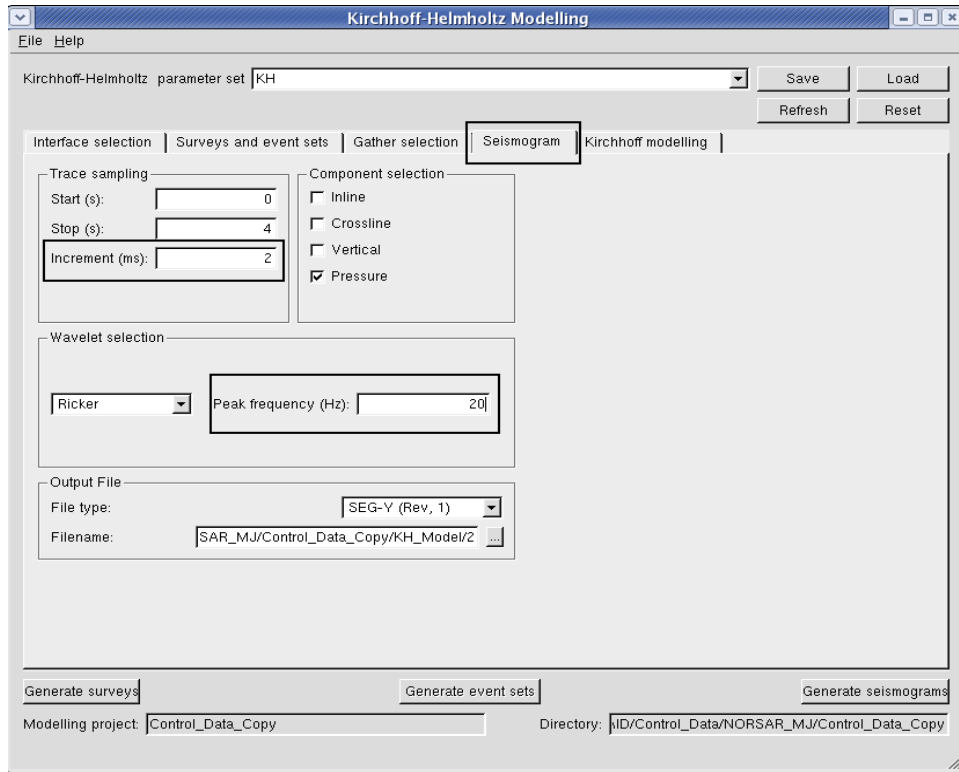


Figure A.13: Parameters used in the Seismogram generation.

A.2.5 Kirchhoff Modeling

This option allows the selection of a subset of the interfaces to be represented in the seismogram (Figure A.14). The multiplication factor can be used to scale or flip the traces. The model boundary taper is used to suppress artificial diffractions from the model boundary. The scattering model used is the “Linearized Isotropic”. After selecting the required parameters, the seismogram is generated. The parameters used are shown in Figure A.14. The resulting seismogram is shown in Figure A.15.

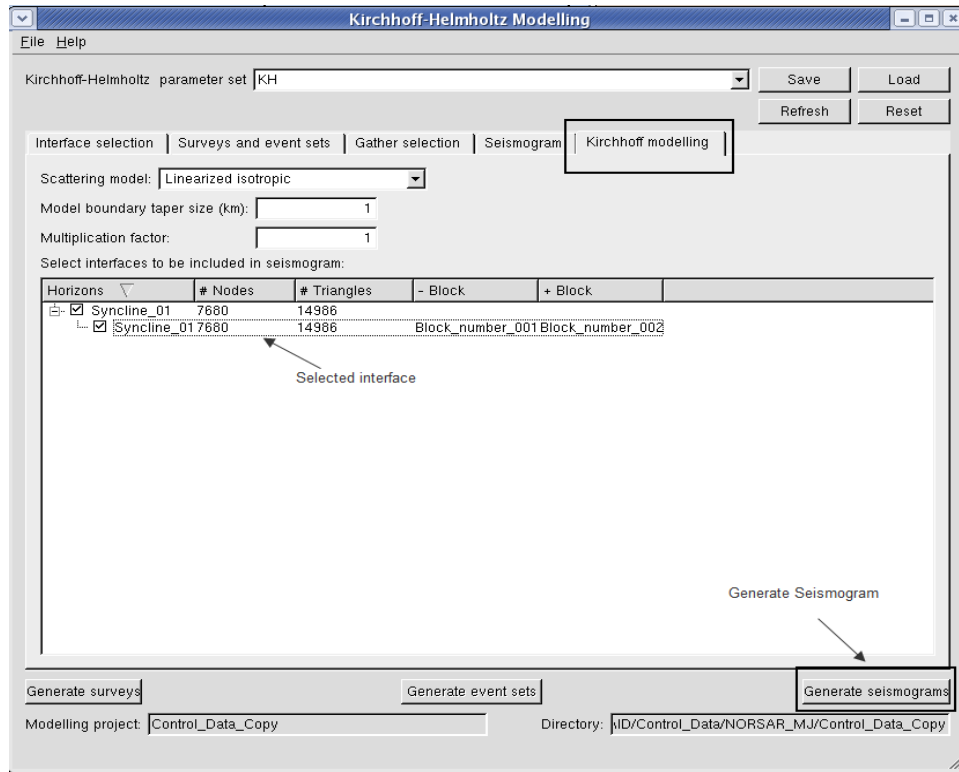


Figure A.14: Parameters used in Kirchhoff Modeling.

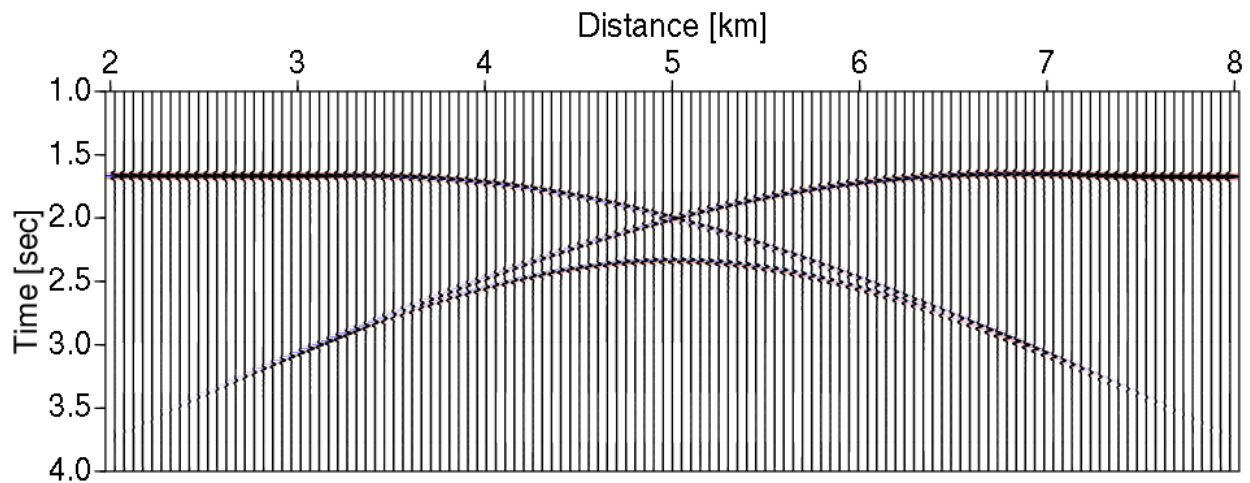


Figure A.15: Seismogram generated using Kirchhoff Helmoltz modeling technique with a Ricker pulse with center frequency of 20Hz.

A.3 Modeling by demigration

Two different implementations of this concept have been studied here;

1. Classical modeling by demigration,
2. Modeling by demigration SimPLI approach.

A.3.1 Classical modeling by demigration

The classical modeling by demigration has been implemented based on the principles given by Santo et al. in early 2000. The software although in its early stages of development uses the basic equations as described in chapter 1. The workflow for modeling by demigration is shown below;

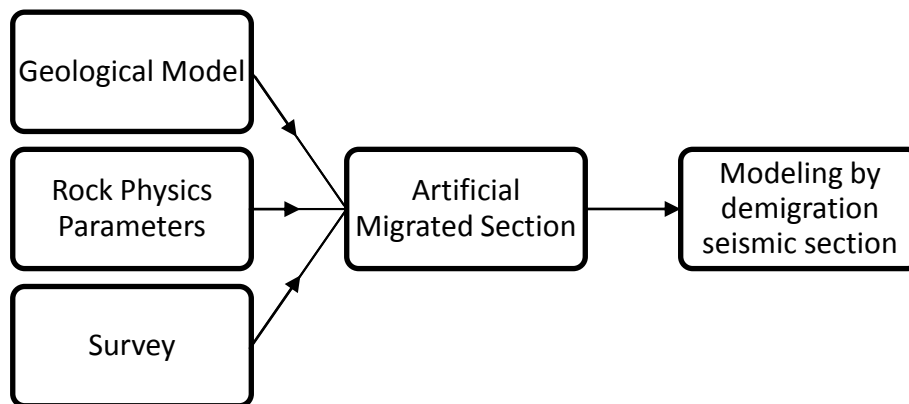


Figure A.16: Workflow for modeling by demigration

The inputs for modeling by demigration are explained in detail below:

Geological model

The interface created in NORSAR-3D was used as the geological model. The model was exported and then used as the input.

Rock physical properties

The rock physical properties like density and velocity for the layer above and below the interface were given. These are the same properties as used in the other modeling methods.

Survey

A zero offset survey has been used; this corresponds to the concepts explained in Chapter 1.

A.3.1.1 Artificial migrated section

An artificial migrated section has been created based on the input parameters. This represents an intermediate step in the modeling by demigration formulation (c.f. Figure A.17).

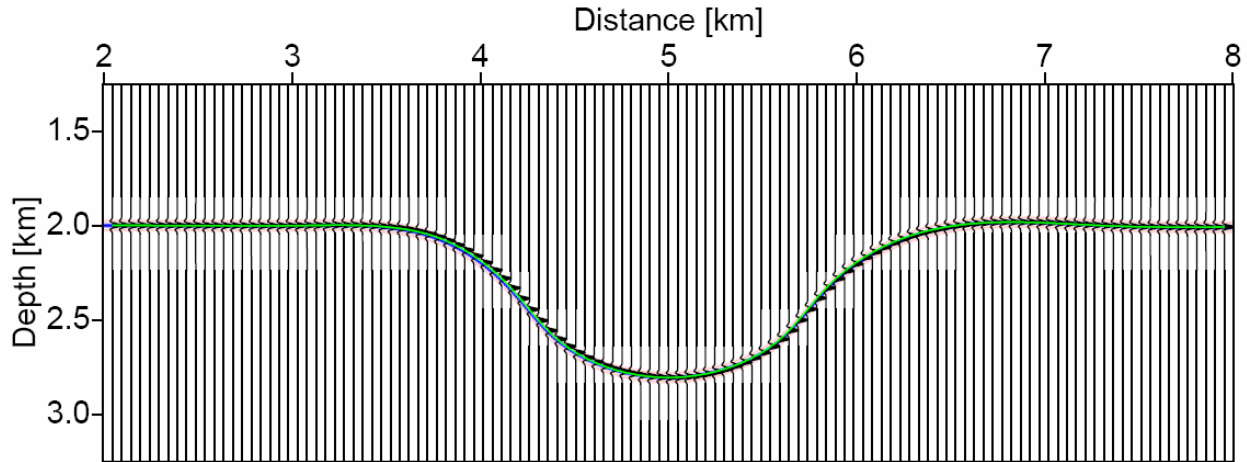


Figure A.17: Artificial migrated section.

A.3.1.2 Result

The result of modeling by demigration is a seismic section. The wavelet used in creating the section is a Ricker zero phase pulse with a center frequency of 20 Hz (c.f. Figure A.18).

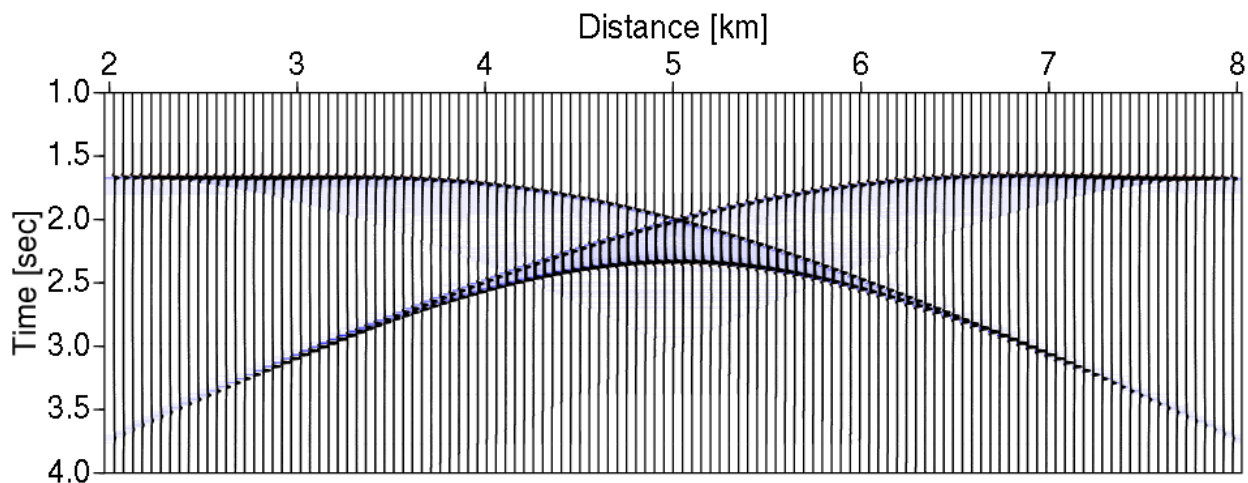


Figure A.18: Seismic section obtained by modeling by demigration.

A.3.2 Modeling by demigration SimPLI approach

This is the new concept, in which the artificial migration step computed from Eqs. (3) – (6) is replaced by the SimPLI migrated image.

A.3.2.1 Simulated Prestack Local Imaging (SimPLI)

The SimPLI “Simulated Prestack Local Imaging” concept efficiently estimates PSDM sections within a specific target without the need to calculate and process synthetic data. The SimPLI approach is a new concept for modeling the seismic response of hydrocarbon reservoirs. By deriving the SimPLI filters (which represent the total illumination and resolution effects of a survey/overburden combination) and combining these with the reflectivity output of the multi-domain model, a 2D/3D simulated seismic PSDM image of the structure in the local target can be obtained. This allows an interpreter to rapidly analyze the dynamic reservoir model in terms of seismic response, i.e. PSDM images. SimPLI considers a PSDM section as a filtered version of

the Earth's structure where the filter is locally described by the available wave number vectors. This removes the need to go through the classic process of combining synthetic-data generation and PSDM to get the migrated version of the structure (SeisRoX, User's Guide 1.2.4, 2008).

The workflow for the SimPLI is shown in Figure A.19.

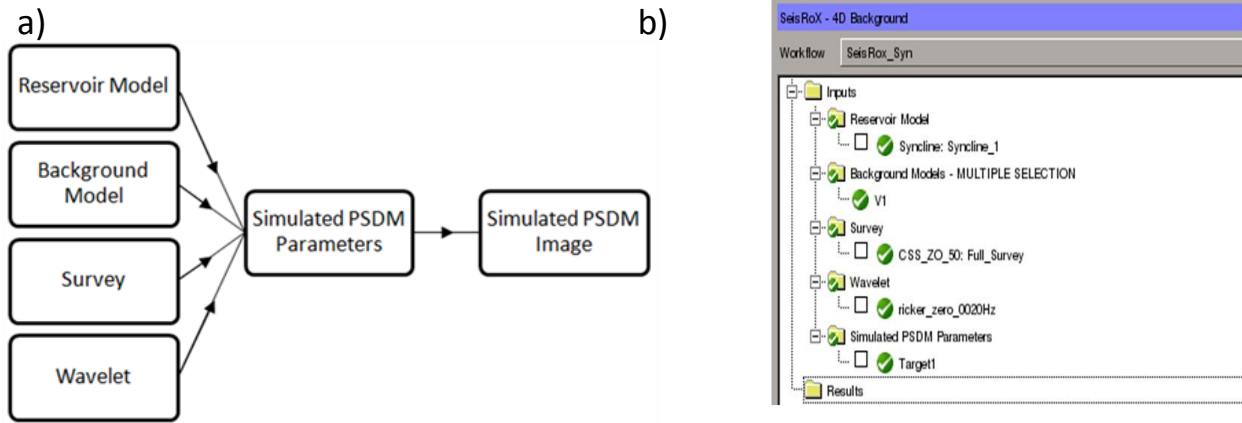


Figure A.19: a) Flow diagram for SimPLI, b) the Inputs required by the software (syncline case).

Reservoir Model

The input to SimPLI is the geological/reservoir model, which can be constructed in NORSAR-3D and then transferred to SeisRoX or made directly in SeisRoX. The syncline model will be used to demonstrate the SimPLI workflow. Figure A.20 shows the selection of the reservoir model.

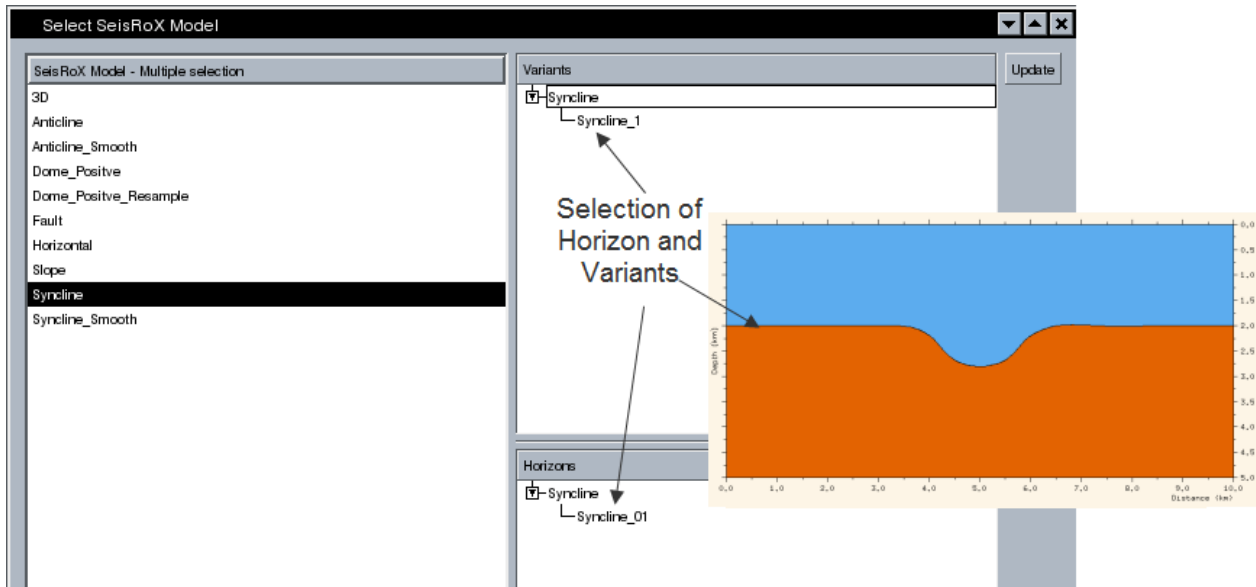


Figure A.20: Selection of Variant and Horizon for the Reservoir Model.

Background Model

In this study the background model is set to a constant velocity model (2.4 km/s).

Survey

The same zero-offset survey configuration as for the alternative methods was used.

Wavelet

A Ricker zero phase wavelet of 20Hz was used to create the simulated migrated seismic section.

Simulated PSDM Parameters

The parameters have been selected to keep the emphasis on the geological feature (c.f. Figure A.21).

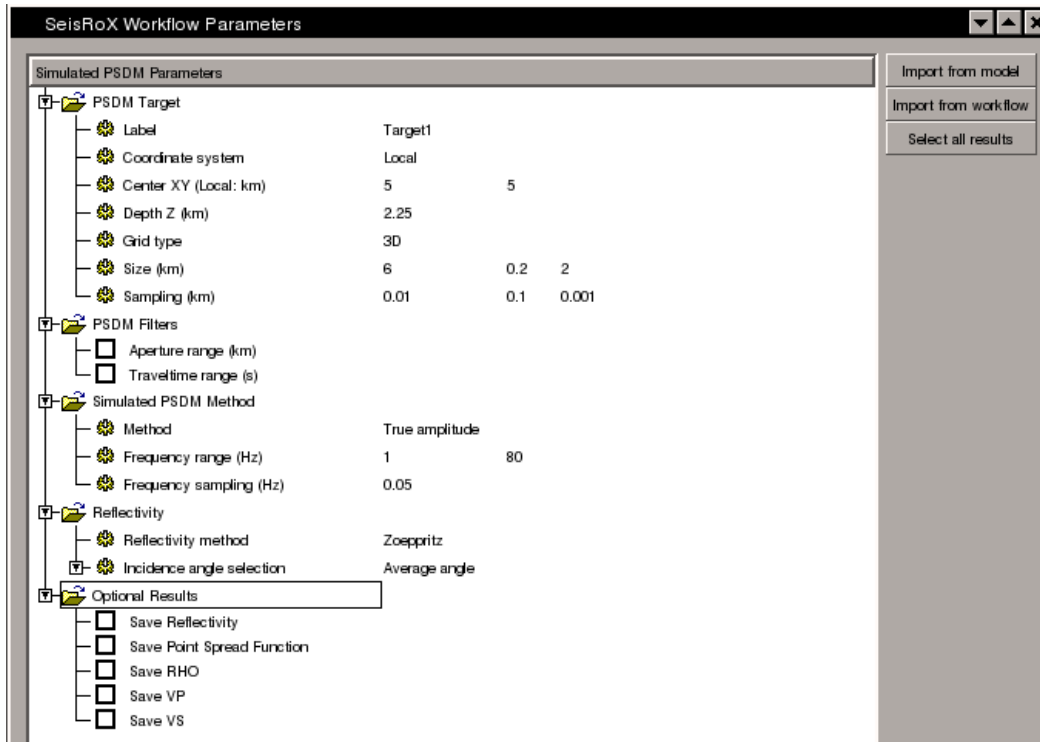


Figure A.21: Parameters used in the Simulated PSDM.

PSDM Target

The PSDM target cube is defined by giving its center, size and sampling. The coordinate system is defined as local for the center of the PSDM target. Since for now the Demigration software requires the data to be in 3D the option of grid type is chosen as 3D.

The target is kept small and local so that the SimPLI filter (or PSF) should not to change dramatically.

PSDM filters

By choosing one of the PSDM Filters (aperture or traveltime range c.f. Figure A.19), the corresponding effect will be calculated and can then be used to sub-select the illumination vectors. The aperture is defined as the horizontal distance between the CMP of the (source, receiver) couple attached to each illumination vector (survey dependent) and the target centre. It is highly recommended to filter on aperture, as also done in PSDM.

The traveltime is the sum of the traveltime between source and target center, and target centre and receiver (the so-called scattering traveltime), and hence, cannot be higher than the recording time of the real acquisition.

Simulated PSDM Method

The actual SeisRoX version allows simulation of an ideal, so-called "True Amplitude", PSDM. This means that all illumination vectors are considered to contribute uniformly when generating the SimPLI filters, assuming that all amplitude corrections (geometrical spreading, attenuation, transmission, etc) would have been applied to the real data. It is therefore important to use the aperture and travelttime filters mentioned above to restrict the set of illumination vectors. The resulting SimPLI filter in the wave number domain can be seen in Figure A.22 for the syncline case.

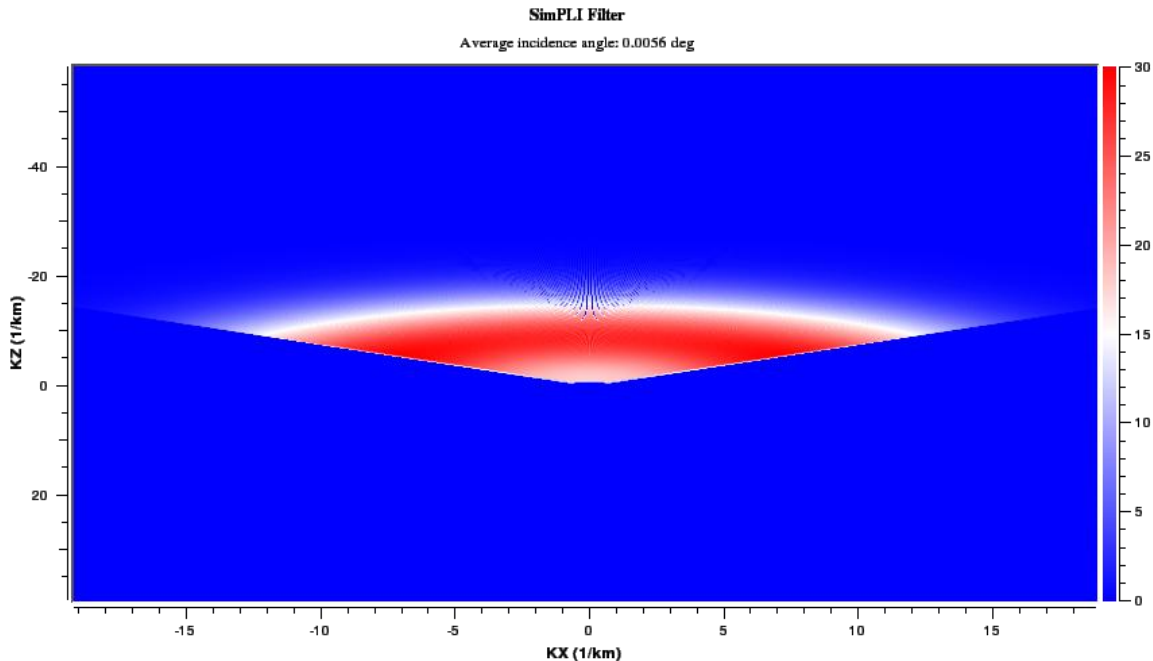


Figure A.22: SimPLI filter in the wave number domain, the sampling for the filter has been set to 0.05 with a frequency range of 0-80Hz.

Reflectivity

Reflectivity is a key parameter of the SimPLI method because it is used to generate the input cubes to be filtered with the SimPLI filter.

Reflectivity method: this parameter ensures that the Zoeppritz equations are used to calculate the input reflectivity cubes.

The Average angle option is used for creating the final reflectivity. The average angle of all incidence angles available within the illumination vectors are calculated and used to generate one reflectivity cube.

Result

The simulated PSDM cubes will be automatically stored as output, which will be used in the modeling by demigration workflow. The result obtained for the syncline example is shown in Figure A.24.

Note: The migrated horizon in Figure A.23 seems to be displaced from the actual target in a few places; this is due to a visual effect associated with the wiggle traces in Seismic Unix, 2008.

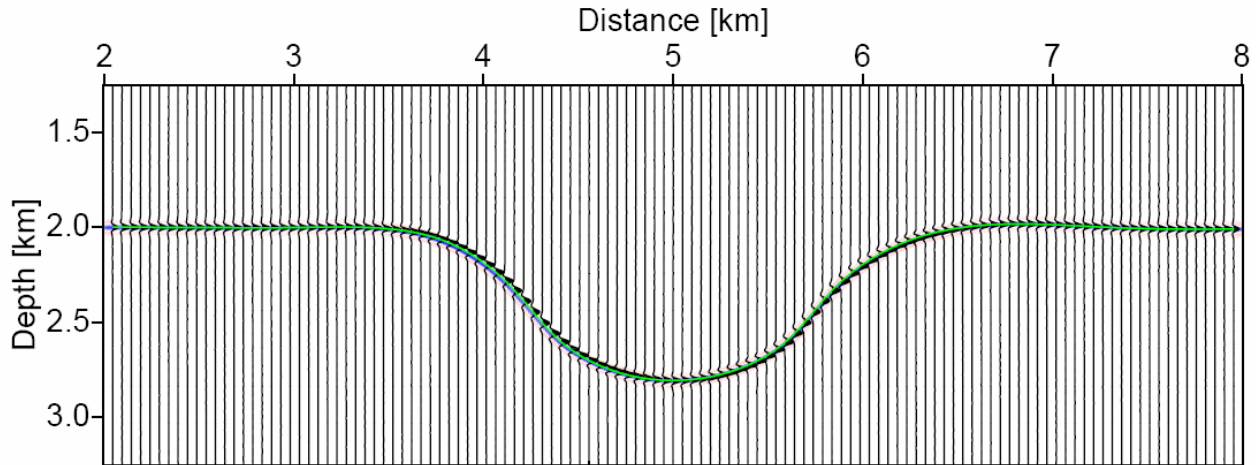


Figure A.23: SimPLI result for syncline, a migrated section similar to the input geological model.

By using the SimPLI approach to modeling by demigration the result is shown in Figure A.24.

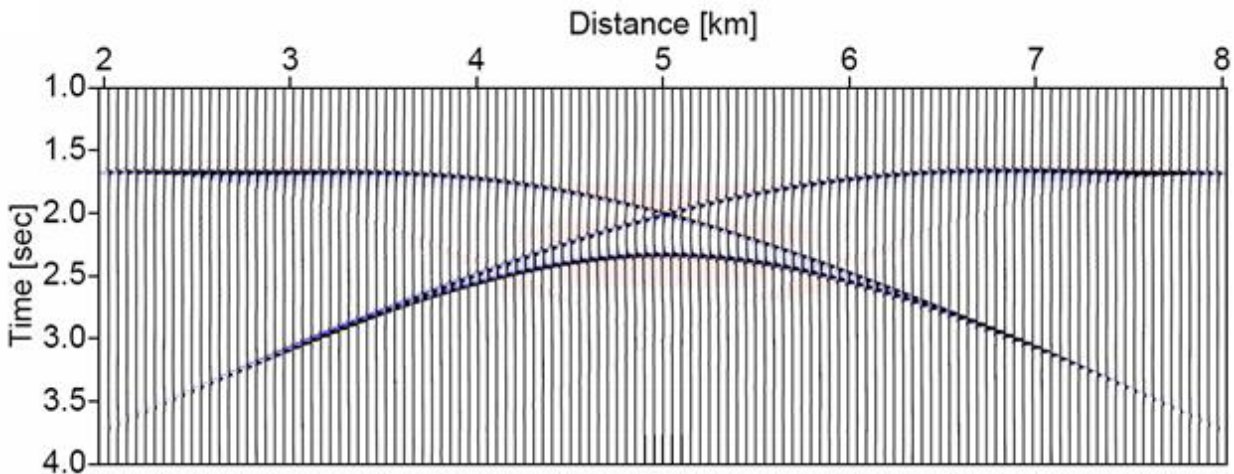


Figure A.24: Demigration input is migrated section obtained from SimPLI.

A.4 Kirchhoff PSDM migration

Migration is an inversion operation that involves rearrangement of seismic information so that reflections and diffractors are migrated to their true locations. Variable velocities and dipping horizons cause reflectors to be recorded at surface positions different from the subsurface positions which are then corrected by migration. Time migration produces a migrated time section and is valid for vertically varying velocity whereas depth migration produces a depth section and allows for horizontal variation of velocity as well. The results of both time and depth migration can be displayed in either time or depth. Migration was originally done on interpreted seismic data by hand but now it is a computer operation on uninterpreted data using some form of, or approximation to, the wave equation. It is also called imaging, which is the transformation of seismic data recorded as a function of arrival time into a scaled version of the true geometry of subsurface geological features that produced the recorded seismic energy. It involves focusing and positioning and depends on a specific earth model. "Focusing involves collapse of diffractors, maximizing amplitude, reproducing wavelet character, etc;

positioning involves locating events correctly, sharpening event terminations relative to faults, salt flanks, unconformities, etc” (Sheriff, 2002).

For the purpose of migration of the data the NORSAR prototype software IMAGING has been used. It represents a Kirchhoff type of Prestack Depth Migration (PSDM).

In the Kirchhoff PSDM migration (KPSDM) the input is the unmigrated seismic sections (here the synthetic data output from the different modeling techniques investigated).

The workflow for PSDM is shown in Figure A.25. Each of the inputs required are discussed below.

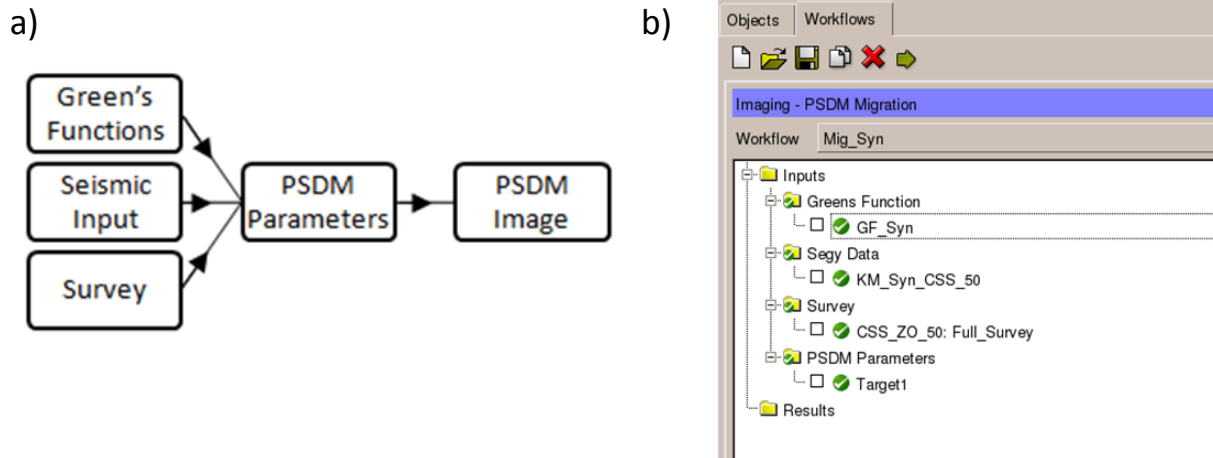


Figure A.25: a) Flow diagram for creating KPSDM section, b) the inputs required by the software in creating the PSDM section for syncline.

A.4.1.1 Generation of Green’s functions

Migration requires Green’s functions to be calculated. Figures A.26a and A.26b show respectively the workflow and typical parameters choices for GFs computations.

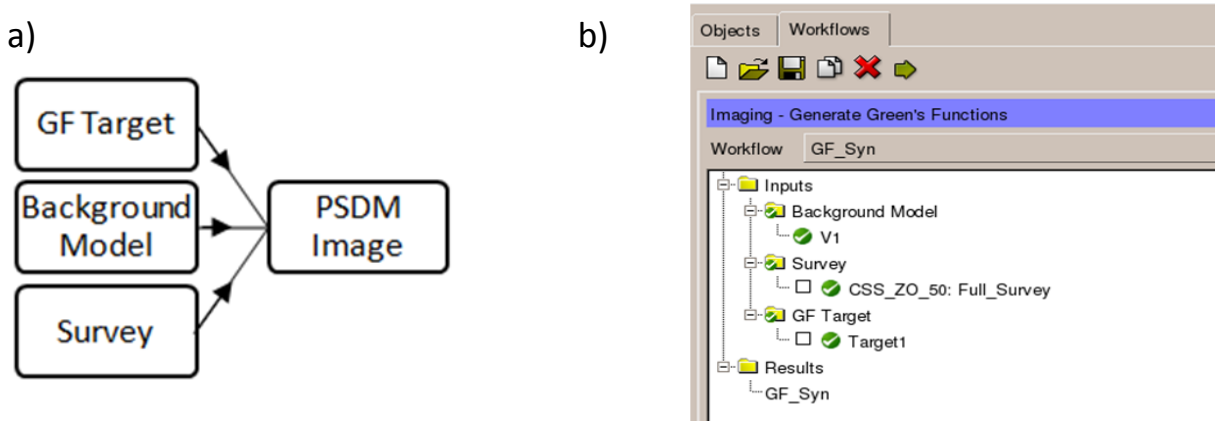
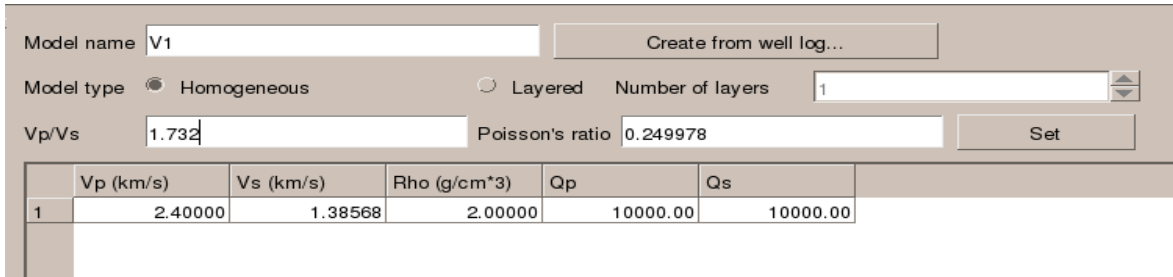


Figure A.26: a) Flow diagram for generating Green’s functions s, b) the Inputs required by the software in calculating the Green’s functions s for syncline example.

Background model

The background model defines the (smooth) velocities employed in migration. Due to the simplicity of the models considered in this thesis a constant velocity model was used (c.f. Figure A.27)



	Vp (km/s)	Vs (km/s)	Rho (g/cm ³)	Qp	Qs
1	2.40000	1.38568	2.00000	10000.00	10000.00

Figure A.27: Parameters used in creating the background model.

Survey

The survey contains the geometry of the survey used in generating the data. Hence, the same survey was selected as used in generating the data. The configuration of sources and receivers are stored in the survey file.

GF Target

Generation of Green's functions involves propagating waves (rays) from each shot and receiver position to each grid point of the target. A proper selection of the target zone is made as shown in Figure A.28. In this case the choice of target size is tailored 2.5 modeling.

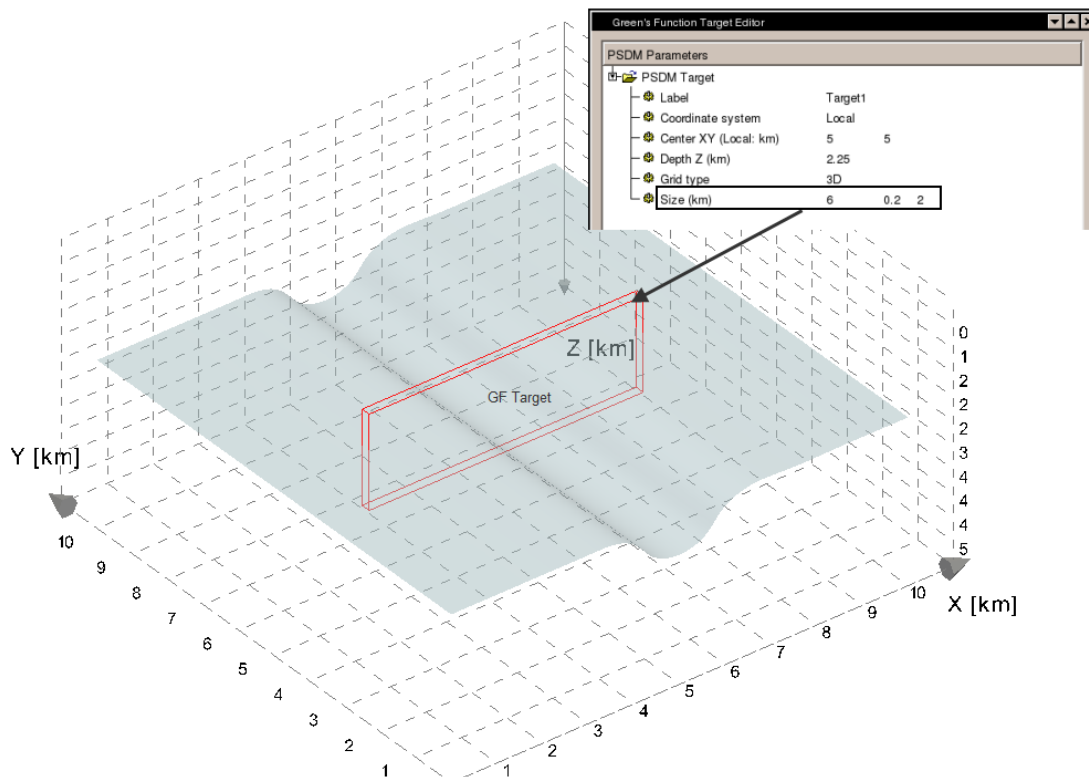


Figure A.28: GF Target zone shown in red along with its size parameters.

Figure A.32 gives an example of GF travel times computed for a homogenous model

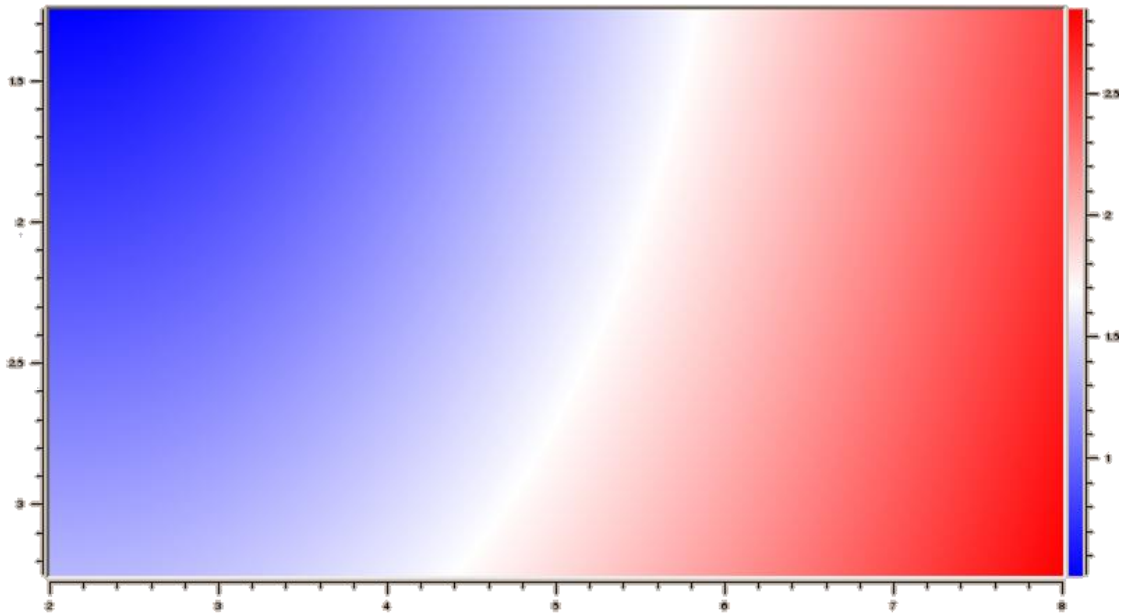


Figure A.29: GF traveltimes associated with a homogenous velocity model.

A.4.1.2 Seismic input and Survey

Corresponds to the unmigrated seismic sections output from the different modeling methods. The same survey layout has been used as in previous workflows.

A.4.1.3 PSDM Parameters

The parameters used in the migration of the seismic data are shown in Figure A.30. In order to obtain a properly migrated result the input data is filtered with a 2.5D filter honoring that the dataset is 3D but the survey is 2D (Yilmaz, 2001).

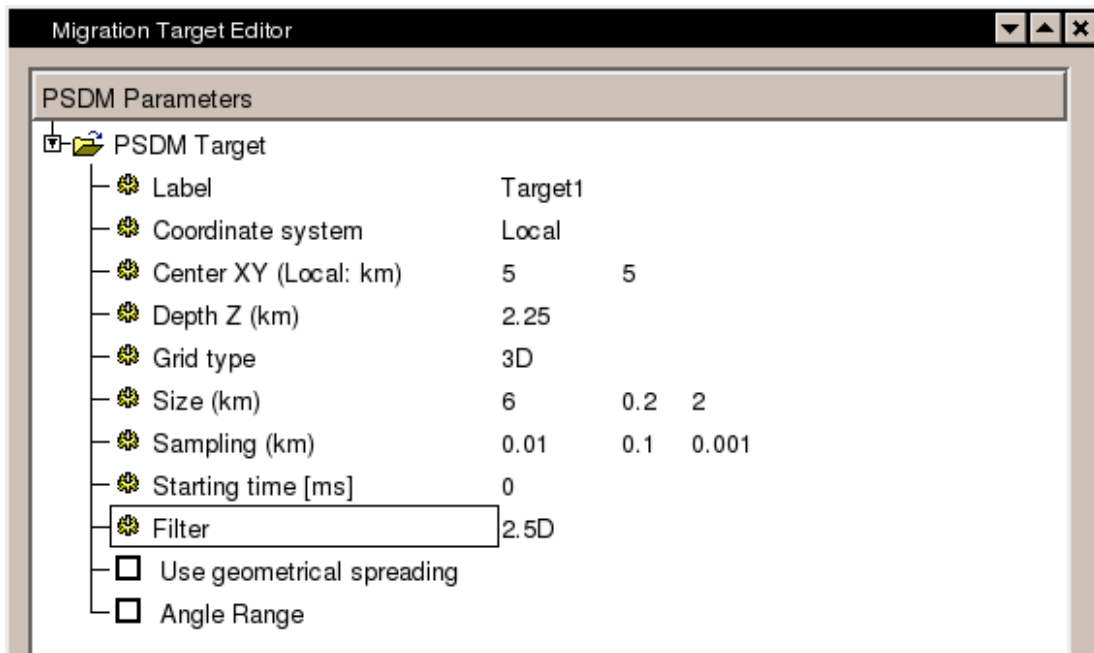
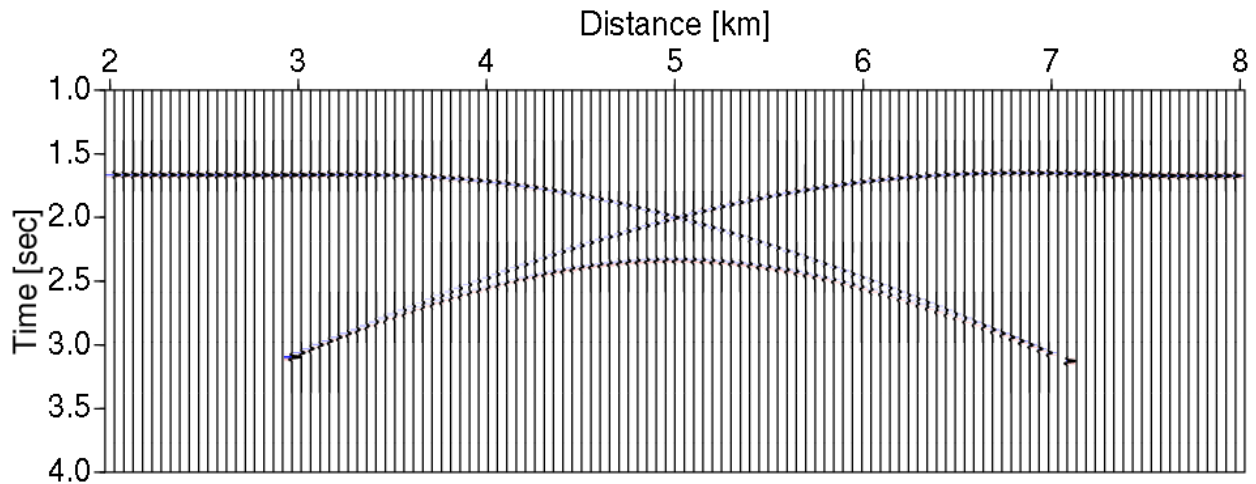
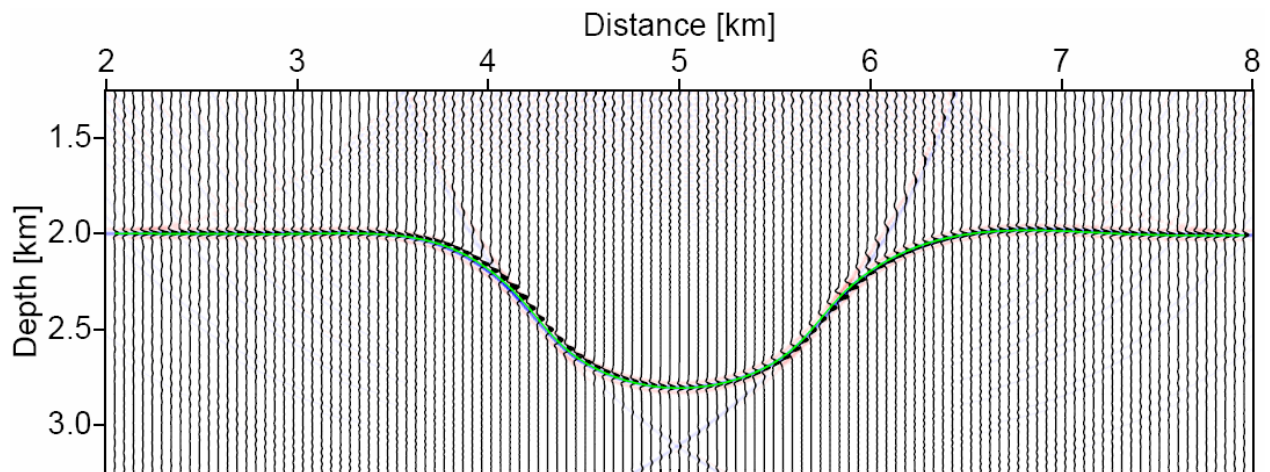


Figure A.30: Parameters used in PSDM migration.

In the example below, PSDM images based on input from either ray tracing, Kirchhoff Helmholtz modeling, or modeling by demigration are shown, along with the unmigrated sections (c.f. Figures A.31, A.32 and A.33).

Note: The migrated seismic horizon in Figures A.31b, A.32b, A.33b, and A.34b seems to be displaced from the actual target in a few places; this is due to a visual effect on displaying the wiggle traces in Seismic Unix, 2008.

**Figure A.31a: Unmigrated seismic section obtained from ray tracing.****Figure A.31b: Migrated seismic section based on ray traced data as input.**

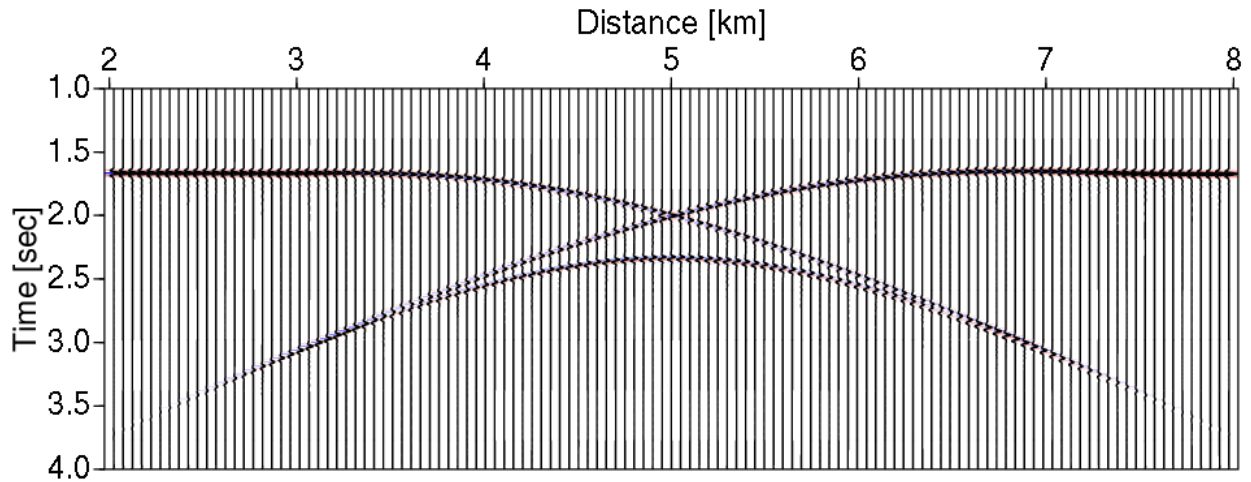


Figure A.32a: Unmigrated seismic section obtained from Kirchhoff Helmholz modeling.

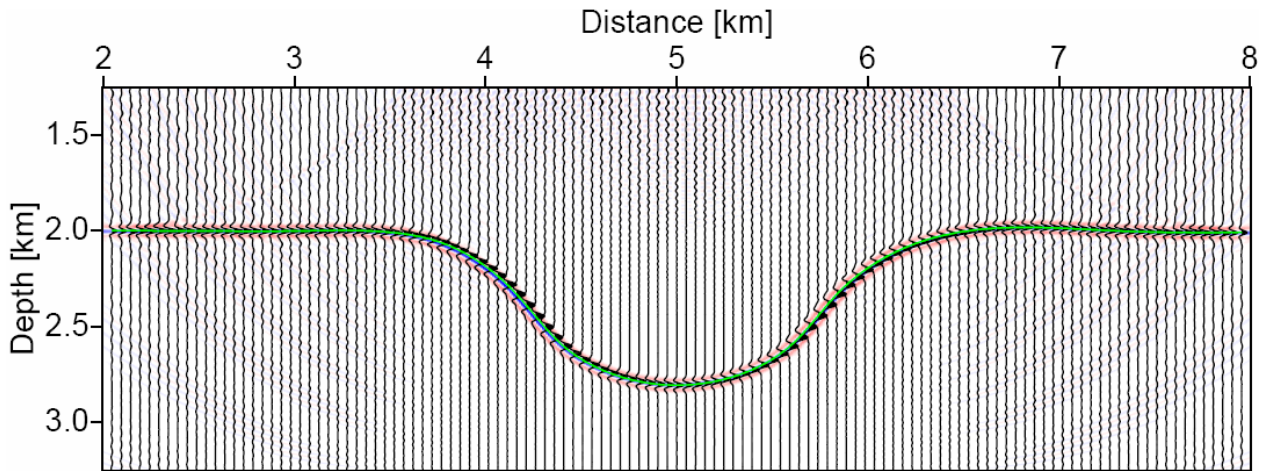


Figure A.32b: Migrated seismic section based on Kirchhoff Helmholz modeled input data.

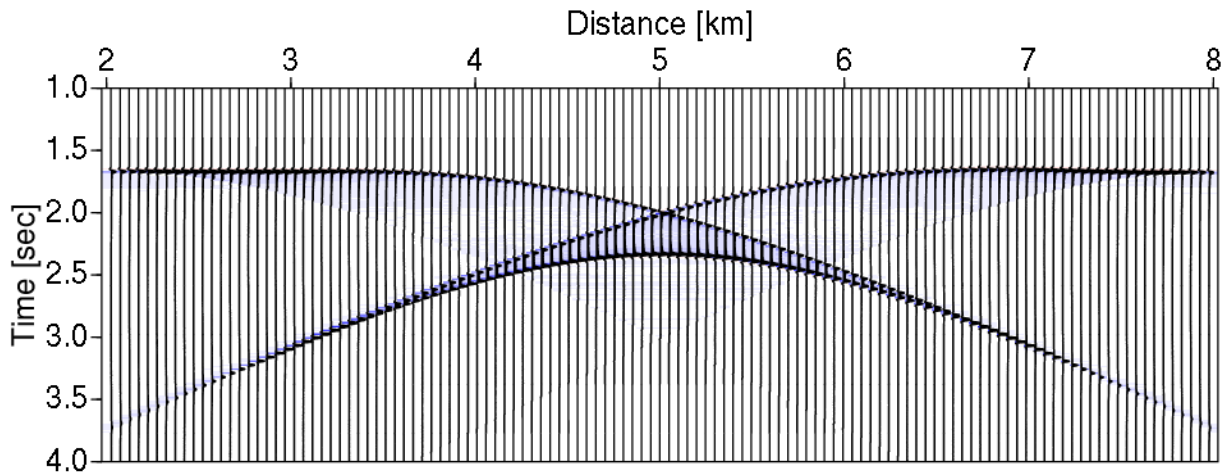


Figure A.33a: Seismic result using classical modeling by demigration.

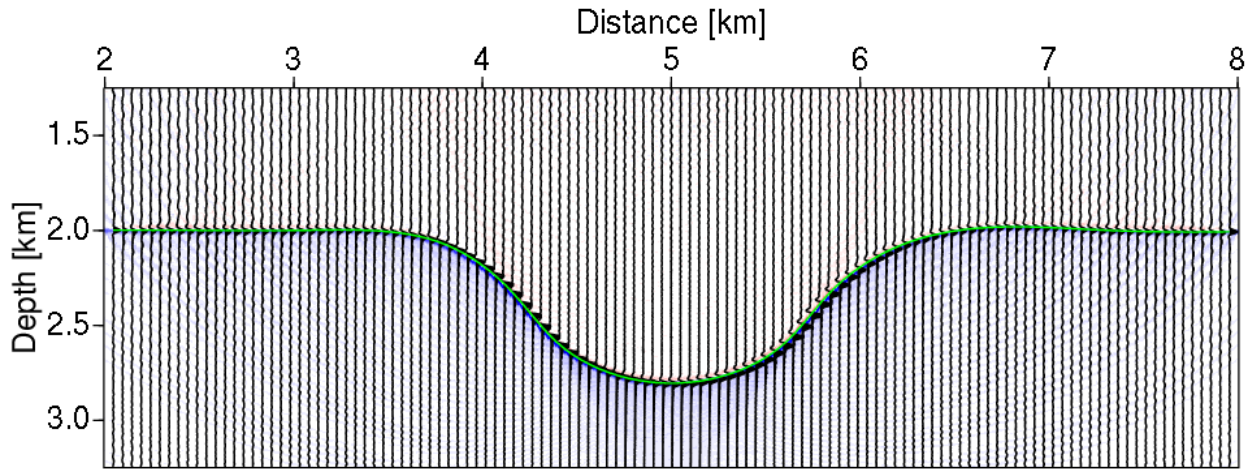


Figure A. 33b: migrated image for modeling by demigration using IMAGE software.

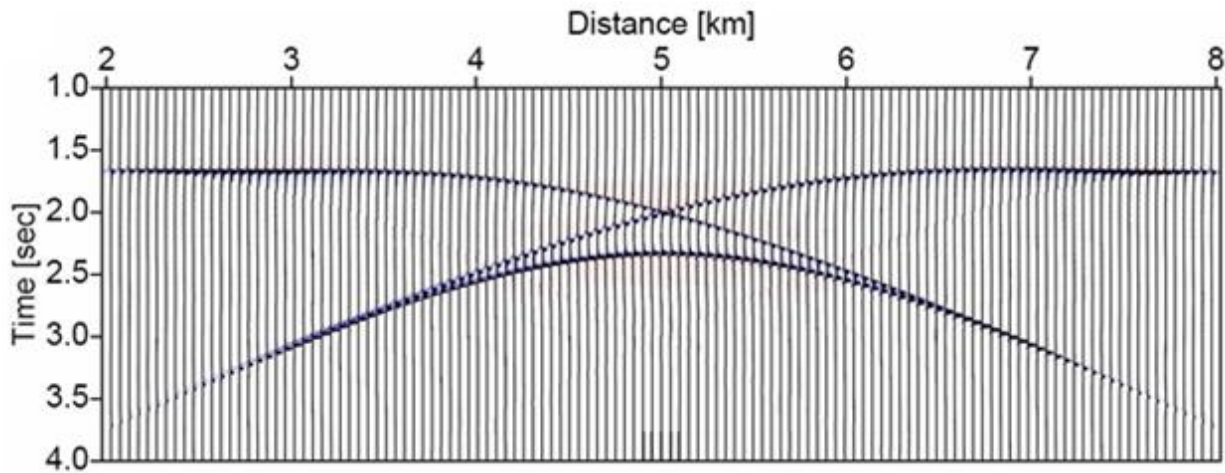


Figure A. 34: a) Unmigrated seismic section obtained from modeling by demigration using SimPLI approach.

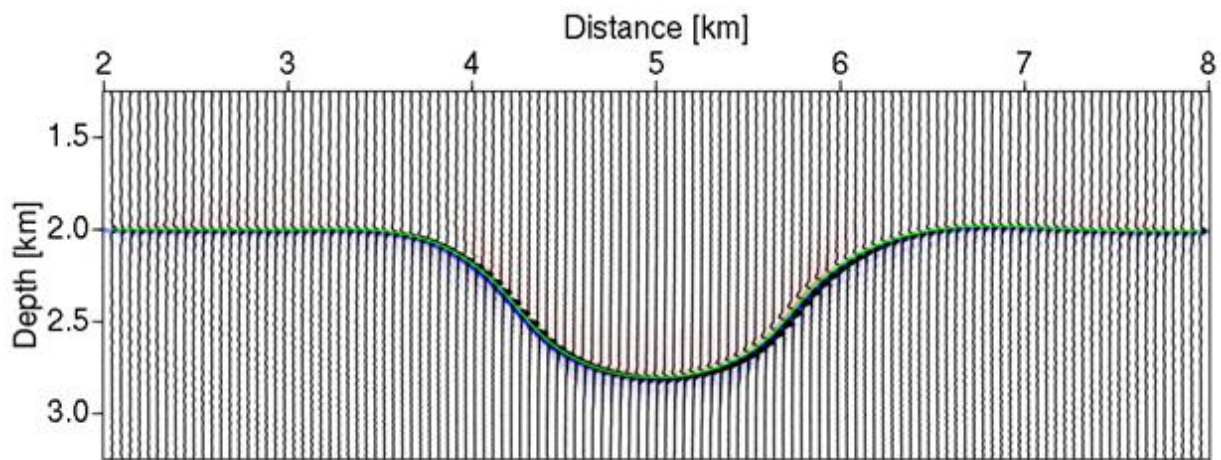


Figure A. 33b: Migrated seismic section based on SimPLI approach to modeling by demigration.

References

- Červený, V., 2001. *Seismic Ray Theory*. Cambridge University Press.
- Červený, V. & Hron, F., 1980. The ray series method and dynamic ray tracing system for three-dimensional inhomogeneous media. *Bulletin of the Seismological Society of America*, pp.47-77.
- Geilus, L. & Lecomte, I., 2000. The resolution in linearized Born and Krichhoff inversion. *Lecture Notes in Earth Sciences: Method and Applications of Inversion, Springer Verlag*, 92, pp.129-41.
- Gelius, L.-J., Lecomte, I. & Tabti, H., 2002. Analysis of the resolution function in seismic prestack depth imaging. *Geophysical Prospecting*, 5, pp.505-15.
- Gjøystdal, H., Drottning, Å., Lecomte, I. & Branston, M., 2007a. Advances in quantitative model-assisted seismic interpretation. *First Break*, 25, pp.95-102.
- Gjøystdal, H., Iversen, E., Lecomte, I. & Kaschwich, T., 2007b. Improved applicability of ray tracing in seismic acquisition, imaging, and interpretation. *Geophysics*, 72(5), pp.261-71.
- Guy, A., 2009. *Flexible and target-oriented Prestack Depth Migration tools: a ray-tracing approach*. Thesis Work, University Louis Pasteur.
- Hubral, P., Schleicher, J. & Tygel, M., 1996. A unified approach to 3-D seismic reflection imaging, Part I: Basic concepts. *Geophysics*, 61(3), pp.742-58.
- Kirchhoff Helmholtz, Basic theory and tutorial, 2007. NORSAR.
- Kraaijpoel, D., 2003. *Seismic ray fields and ray field maps: theory and algorithms*. PhD thesis, Faculty of Geosciences, Utrecht University.
- Lecomte, I., 2008. Method simulating local prestack depth migrated seismic images. *US patent # 7,376,539*.
- Lecomte, I. & Kaschwich, T., 2008. Closer to real earth in reservoir characterization: a 3D isotropic/anisotropic PSDM simulator. *Expanded Abstract, SEG 78th Annual Meeting*.
- Masaferroa, J., Bulnesb, M., Pobletb, J. & Eberlia, G., 2001. *Episodic folding inferred from syntectonic carbonate sedimentation: The Santaren anticline, Bahamas foreland*.
- Mussett, A., Khan, A. & Button, S., 2000. *Looking into the Earth: An introduction to geological geophysics*. Cambridge University Press.

NORSAR3D, User's Guide 5.3, 2008. NORSAR Innovation AS.

Santos, L.T., Jorg, S., Hubral, P. & Tygel, M., 2000a. Seismic modeling by demigration. *Geophysics*.

Santos, L.T., Jorg, S., Hubral, P. & Tygel, M., 2000b. Seismic modeling, migration and demigration. *The Leading Edge*.

Schlumberger, 2009. *The Oilfield Glossary*. [Online] Available at: <http://www.glossary.oilfield.slb.com/> [Accessed April 2009].

SEG/EAGE Salt Model, 2002.

Seismic Unix, 2008. Center for Wave Phenomena, Colorado School of Mines.

SeisRoX, User's Guide 1.2.4, 2008. NORSAR Innovation AS.

Sheriff, R.E., 1981. *Structural Interpretation of Seismic Data*. Tulsa, USA: SEG Publication.

Sheriff, R.E., 2002. *Encyclopadic dictionary of exploration geophysics*. Tulsa, USA: Society of Exploration Geophysics.

Tygel, M., Schleicher, J., Santos, L.T. & Hubral, P., 1999. The Krichhoff Helmboltz integral pair. *Journal of Computational Acoustics*, May.

Vinje, V., Iversen, E. & Gjøystdal, H., 1993. Traveltime and amplitude estimation using wavefront construction. *Geophysics*, pp.1153-67.

Yielding, G., Badley, M. & Freeman, B., 2002. Seismic reflections for normal faults in the Northern North Sea. In Robert E. Holdsworth, J.P.T. *Extensional tectonics*. Geological Society of London. pp.41-51.

Yilmaz, O., 2001. *Seismic Data Analysis*. Tulsa, USA: Society of Exploration Geophysics.